Christophe Ancey

Laboratoire hydraulique environnementale (LHE)

École Polytechnique Fédérale de Lausanne
Écublens

CH-1015 Lausanne

Notebook

Introduction to Fluid Rheology

version 1.0 of 4th July 2005

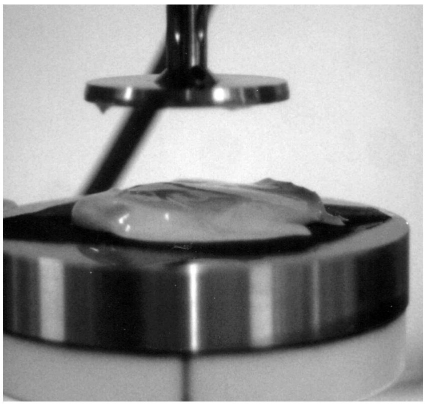

C. Ancey,
EPFL, ENAC/ICARE/LHE,
Ecublens, CH-1015 Lausanne, Suisse
christophe.ancey@epfl.ch, lhe.epfl.ch

Introduction to Fluid Rheology / C. Ancey

La gestion typographique a été réalisée à l'aide du package *french.sty* de Bernard Gaulle.

Remerciements : à Sébastien Wiederseiner et Martin Rentschler pour la relecture du manuscrit.

« Le physicien ne peut demander à l'analyste de lui révéler une vérité nouvelle ; tout au plus celui-ci pourrait-il l'aider à la pressentir. Il y a longtemps que personne ne songe plus à devancer l'expérience, ou à construire le monde de toutes pièces sur quelques hypothèses hâtives. De toutes ces constructions où l'on se complaisait encore naïvement il y a un siècle, il ne reste aujourd'hui plus que des ruines. Toutes les lois sont donc tirées de l'expérience, mais pour les énoncer, il faut une langue spéciale ; le langage ordinaire est trop pauvre, elle est d'ailleurs trop vague, pour exprimer des rapports si délicats, si riches et si précis. Voilà donc une première raison pour laquelle le physicien ne peut se passer des mathématiques ; elles lui fournissent la seule langue qu'il puisse parler.»

Henri POINCARÉ, in *La Valeur de la Science*

Table of contents

1 Rheometry **17**
1.1 How does a rheometer operate? 18
    1.1.1 A long history 18
    1.1.2 Anatomy of a modern rheometer 18
    1.1.3 Typical performance of modern lab rheometers 21
1.2 Principles of viscometry 22
    1.2.1 Fundamentals of rheometry 22
    1.2.2 Flow down an inclined channel 24
    1.2.3 Standard geometries 27
1.3 Inverse problems in rheometry 28
    1.3.1 A typical example: the Couette problem 28
    1.3.2 Earlier attempts at solving the Couette problem 28
    1.3.3 The wavelet-vaguelette decomposition 30
    1.3.4 Practical example 31
1.4 Rheometers and rheometrical procedures 33
    1.4.1 How to determine the flow curve? 33
    1.4.2 Stress/strain step 34
1.5 Typical rheological behaviors 37
    1.5.1 Outlining a flow curve 37
    1.5.2 Shear-thinning/thickening 37
    1.5.3 Yield stress 38
    1.5.4 Viscoelasticity 39
    1.5.5 Normal stress effects 45
    1.5.6 Thixotropy 46
1.6 Problems encountered in rheometry 51
    1.6.1 Problems with rheometers 51
    1.6.2 Limitations of the viscometric treatment 53
    1.6.3 Technical issues related to the derivation of the flow curve 54
    1.6.4 Problems related to sample preparation 55

1.7 Non-standard techniques: what can be done without a rheometer? 56
  1.7.1 Viscosity: free fall of a bead 56
  1.7.2 Yield stress: Slump test 56

2 Rheology and Continuum Mechanics 59
2.1 Why is continuum mechanics useful? An historical perspective 60
  2.1.1 Paradoxical experimental results? 60
  2.1.2 How to remove the paradox? 61
2.2 Fundamentals of Continuum Mechanics 63
  2.2.1 Kinematics 63
  2.2.2 Stress tensor 67
  2.2.3 Admissibility of a constitutive equations 69
  2.2.4 Specific properties of material 70
  2.2.5 Representation theorems 70
  2.2.6 Balance equations 72
  2.2.7 Conservation of energy 74
  2.2.8 Jump conditions 76
2.3 Phenomenological constitutive equations 79
  2.3.1 Newtonian behavior 79
  2.3.2 Viscoplastic behavior 79
  2.3.3 Viscoelasticity 81

3 Rheophysics 83
3.1 Fundamentals of rheophysics 84
  3.1.1 Movement of a single sphere and consequences on the flow regime 84
  3.1.2 From a single sphere to a bulk: averaging 90
  3.1.3 Averaged balance equations 92
  3.1.4 Passing from volume averages to ensemble averages 95
3.2 Dilute suspensions 99
  3.2.1 Dilute suspension in a Stokes regime: Stokesian theory 99
  3.2.2 Computations of the constitutive equation 104
3.3 Concentrated suspensions 105
  3.3.1 Constitutive equations for concentrated suspensions 105
  3.3.2 Regime diagram and computation of individual contributions 107

References 111

Foreword

Objective of the course

The objective of this course held in the framework of the doctoral school *Mechanics of Solids and Fluids* et EPFL is to provide the student with the modern tools needed to investigate the rheological behavior of complex fluids. Emphasis will be given to particle suspensions. The course will start with an introduction of experimental procedures. Phenomenological description of how matter flows will then be presented. The last part of the course will be devoted to the rheophysical approach to modelling the rheological behavior of particle suspensions.

This notebook will focus on materials encountered by geophysicists (mud, snow, magma, etc.) and in industrial or civil-engineering applications (concrete, slurries, etc.): in most cases we will consider only homogeneous and suspensions of particles within an interstitial fluid without loss of generality. Other complex fluids such as polymeric liquids are rarely encountered in geophysics and therefore they will not be addressed here.

Content of the notebook

The mere description of what the term rheology embraces in terms of scientific areas is not easy. Roughly speaking, rheology distinguishes different areas and offshoots such as the following: rheometry, formulation of constitutive equation, computational rheometry, microstructural analysis and interpretation of bulk rheological behavior, etc. Here we will focus on the following points[1]:

Rheometry. The term "rheometry" is usually used to refer to a group of experimental techniques for investigating the rheological behavior of materials. It is of great importance in determining the constitutive equation of a fluid or in assessing the relevance of any proposed constitutive law. Most of the textbooks on rheology deal with rheometry. The books by Coleman *et al.* (1966), Walters (1975), and by Bird *et al.* (1987) provide a complete introduction to the viscometric theory used in rheometry for inferring the constitutive equation. The book by Coussot & Ancey (1999*b*) gives practical information concerning rheometrical measurements with natural fluids. Though primarily devoted to food processing engineering, Steffe's book presents a detailed description of rheological measurements; a free sample is available on the web (Steffe, 1996).

In Chapter 1, we will review the different techniques that are suitable to studying various fluids. Emphasis is given both to describing the methods and the major experimental problems encountered with materials made up of particles and fluids.

---

[1] Other aspects of rheology, such as complex flow modelling and computational rheology, are not addressed in this introductory notebook.

Continuum mechanics. The formulation of constitutive equations is probably the early goal of rheology. At the beginning of the 20$^{\text{th}}$ century, the non-Newtonian character of many fluids of practical interest motivated Professor Bingham to coin the term *rheology* and to define it as the study of the deformation and flow of matter. The development of a convenient mathematical framework occupied the attention of rheologists for a long time after the Second World War. At that time, theoreticians such as Coleman, Markovitz, Noll, Oldroyd, Reiner, Toupin, Truesdell, etc. sought to express rheological behavior through equations relating suitable variables and parameters representing the deformation and stress states. This gave rise to a large number of studies on the foundations of continuum mechanics (Bird *et al.*, 1987). Nowadays the work of these pioneers is pursued through the examination of new problems such as the treatment of multiphase systems or the development of nonlocal field theories. For examples of current developments and applications to geophysics, the reader may consult papers by Hutter and coworkers on the thermodynamically consistent continuum treatment of soil-water systems (Wang & Hutter, 1999; Hutter *et al.*, 1999), the book by Vardoulakis & Sulem (1995) on soil mechanics, and the review by Bedford & Dumheller (1983) on suspensions. A cursory glance at the literature on theoretical rheology may give the reader the impression that all this literature is merely an overly sophisticated mathematical description of the matter with little practical interest. In fact, excessive refinements in the tensorial expression of constitutive equations lead to prohibitive detail and thus substantially limit their utility or predictive capabilities. This probably explains why there is currently little research on this topic. Such limitations should not prevent the reader (and especially the newcomer) from studying the textbooks in theoretical rheology, notably to acquire the basic principles involved in formulating constitutive equations.

Two simple problems related to these principles will be presented in Chapter 2 to illustrate the importance of an appropriate tensorial formulation of constitutive equations.

Rheophysics. For many complex fluids of practical importance, bulk behavior is not easily outlined using a continuum approach. It may be useful to first examine what happens at a microscopic scale and then infer the bulk properties using an appropriate averaging process. Kinetic theories give a common example for gases (Chapman & Cowling, 1970) or polymeric liquids (Bird *et al.*, 1987), which infer the constitutive equations by averaging all the pair interactions between particles. Such an approach is called *microrheology* or *rheophysics*. Here we prefer to use the latter term to emphasize that the formulation of constitutive equations is guided by a physical understanding of the origins of bulk behavior. Recent developments in geophysics are based on using kinetic theories to model bed load transport (Jenkins & Hanes, 1998), floating broken ice fields (Savage, 1994), and rockfall and granular debris flows (Savage, 1989). It is implicitly recognized that thoroughly modelling the microstructure would require prohibitive detail, especially for natural fluids. It follows that a compromise is generally sought between capturing the detailed physics at the particle level and providing applicable constitutive equations. Using dimensionless groups and approximating constitutive equations are commonly used operations for that purpose. In Chap. 3, we will consider suspensions of rigid particles within a Newtonian fluid to exemplify the different tools used in rheophysics. Typical examples of such fluids in a geophysical context include magma and mud.

Notations, formulas, & Conventions

The following notations and rules are used:

- Vectors, matrices, and tensors are in bold characters.
- For mathematical variables, I use slanted fonts.
- Functions, operators, and dimensionless numbers are typed using a Roman font.
- The symbol O (capital O) means "is of the order of" .
- The symbol o (lower case) means "is negligible relative to" .
- I do not use the notation D/Dt to refer to refer to the material derivative, but $\mathrm{d}/\mathrm{d}t$ (that must not be confused with ordinary time derivative). I believe that the context is mostly sufficient to determine the meaning of the differential operator.
- The symbol $\propto$ means "proportional to".
- The symbol $\sim$ or $\approx$ means "nearly equal to".
- I use units of the international system (IS): meter [m] for length, second [s] for time, and kilogram [kg] for mass. Units are specified by using square brackets.
- For the complex computations, I use $\Re$ to refer to the real part of a complex and $\imath$ is the imaginary number.
- The superscript ^{T} after a vector/tensor means the transpose of this vector/tensor.
- We use $\mathbf{1}$ to refer to the unit tensor (identity tensor/matrix).
- Einstein's convention means that when summing variables, we omit the symbol $\sum$ and we repeat the indice. For instance we have $\mathbf{a} \cdot \mathbf{b} = a_i b_i$.
- The gradient operator is denoted by the *nabla* symbol ∇. The divergence of any scalar or tensorial quantity f is denoted by $\nabla \cdot f$. For the Laplacian operator, I indifferently use ∇^2 or $\triangle$. The curl of any vector $\mathbf{v}$ is denoted by $\nabla \times \mathbf{v}$. We can use the following rule to check the consistency of an operator

Operation name	*Operator symbol*	*Order of result*
gradient	∇	$\Sigma + 1$
divergence or outer product	$\nabla\cdot$	$\Sigma - 1$
curl	$\nabla\times$	Σ
Laplacian	∇^2	$\Sigma - 2$

- The scalar product of two vectors $\mathbf{a}$ and $\mathbf{b}$ is denoted by $\mathbf{a} \cdot \mathbf{b}$. The dyadic or tensor product of $\mathbf{a}$ and $\mathbf{b}$ is denoted by $\mathbf{ab}$. The product between a tensor $\mathbf{A}$ and a vector $\mathbf{a}$ is denoted by $\mathbf{A} \cdot \mathbf{a}$. The cross product of two vectors $\mathbf{a}$ and $\mathbf{b}$ is denoted by $\mathbf{a} \times \mathbf{b}$. The inner product of two tensors is denoted by the double dot ":" (keep in mind that for second-order tensors $\mathbf{a}$ and $\mathbf{b}$ we have $\mathbf{a} : \mathbf{b} = \mathrm{tr}\, \mathbf{ab}$). We can use the following rule to check the consistency of a multiplication

Operation name	*Multiplication sign*	*Order of result*
dyadic or tensorial product	none	Σ
cross or outer product	$\times$	$\Sigma-1$
scalar or inner product	$\cdot$	$\Sigma-2$
scalar or inner product	$:$	$\Sigma-4$

Recall that the order of a scalar is 0, a vector is of order 1, and a tensor is of order at least 2. For instance, if $\mathbf{a}$ and $\mathbf{b}$ denotes vectors and $\mathbf{T}$ is a tensor, $\mathbf{T}\cdot\mathbf{a}$ is order $2+1-1=2$; $\mathbf{T}:\mathbf{a}$ is order $2+1-2=1$.

- The gradient of a vector $\mathbf{a}$ is a tensor $\nabla\mathbf{a}$, whose components in a Cartesian frame x_i are
$$\frac{\partial a_j}{\partial x_i}.$$
The divergence of a second-order tensor M_{ij} is a vector $\nabla\cdot\mathbf{M}$, whose jth component in a Cartesian frame x_i is
$$\frac{\partial M_{ij}}{\partial x_i}.$$
- The tensorial product of two vectors $\mathbf{a}$ and $\mathbf{b}$ provides a tensor $\mathbf{ab}$ such that for any vector $\mathbf{c}$, we have $(\mathbf{ab})\mathbf{c}=(\mathbf{b}\cdot\mathbf{c})\mathbf{a}$.
- A vector field such that $\nabla\cdot\mathbf{v}=\mathbf{0}$ is said to be *solenoidal.* A function f satisfying the Laplace equation $\nabla^2 f=0$ is said to be *harmonic.* A function f such that $\nabla^4 f=0$ is said to be *biharmonic.* A vectorial field $\mathbf{v}$ such $\nabla\times\mathbf{v}=0$ is said to be *irrotational.*
- An extensive use is made of the *Green-Ostrogradski* theorem (also called the *divergence* theorem):
$$\int_{\mathcal{V}}\nabla\cdot\ \mathbf{u}\,\mathrm{d}\mathcal{V}=\int_{\mathcal{S}}\mathbf{u}\cdot\mathbf{n}\,\mathrm{d}\mathcal{S},$$
where $\mathcal{S}$ is the surface bounding the volume $\mathcal{V}$ and $\mathbf{n}$ is the unit normal to the infinitesimal surface $\mathrm{d}\mathcal{S}$. A closely allied theorem for scalar quantities f is
$$\int_{\mathcal{V}}\nabla f\,\mathrm{d}\mathcal{V}=\int_{\mathcal{S}}f\mathbf{n}\,\mathrm{d}\mathcal{S}.$$
- For some algebraic computations, we need to use
  - Cartesian coordinates $(x,\,y,\,z)$,
  - or spherical coordinates $(x=r\cos\varphi\sin\theta)\,,\,y=r\sin\theta\sin\varphi,\,z=r\cos\theta)$ with $0\le\theta\le\pi$ and $-\pi\le\varphi\le\pi$, $\mathrm{d}S=r^2\sin\theta\mathrm{d}\theta\mathrm{d}\varphi$ on a sphere of radius r, $\mathrm{d}V=r^2\sin\theta\mathrm{d}r\mathrm{d}\theta\mathrm{d}\varphi$.
- Some useful formulas on vector and tensor products
$$\mathbf{N}:\mathbf{M}=\mathbf{M}:\mathbf{N},$$
$$\mathbf{a}\times(\mathbf{b}\times\mathbf{c})=(\mathbf{a}\cdot\mathbf{c})\mathbf{b}-(\mathbf{a}\cdot\mathbf{b})\mathbf{c},$$
$$(\mathbf{M}\cdot\mathbf{a})\cdot\mathbf{b}=\mathbf{M}:(\mathbf{ab})\ \text{ and }\ \mathbf{a}\cdot(\mathbf{b}\cdot\mathbf{M})=\mathbf{M}:(\mathbf{ab}),$$
$$\mathbf{ab}:\mathbf{cd}=\mathbf{a}\cdot(\mathbf{b}\cdot\mathbf{cd})=\mathbf{a}\cdot((\mathbf{b}\cdot\mathbf{c})\mathbf{d})=(\mathbf{a}\cdot\mathbf{b})(\mathbf{c}\cdot\mathbf{d})=\mathbf{ac}:\mathbf{bd}$$
$$\nabla(fg)=g\nabla f+f\nabla g,$$
$$\nabla\cdot(f\mathbf{a})=\mathbf{a}\cdot\nabla f+f\nabla\cdot\mathbf{a},$$
$$\nabla\cdot(\mathbf{a}\times\mathbf{b})=\mathbf{b}(\nabla\times\mathbf{a})-\mathbf{a}(\nabla\times\mathbf{b}),$$
$$\nabla\cdot\nabla\mathbf{a}=\frac{1}{2}\nabla(\mathbf{a}\cdot\mathbf{a})-\mathbf{a}\times(\nabla\times\mathbf{a}),$$
$$\nabla\cdot\mathbf{ab}=\mathbf{a}\nabla\mathbf{b}+\mathbf{b}\nabla\cdot\mathbf{a}$$
$$\mathbf{1}:\nabla\mathbf{a}=\nabla\cdot\mathbf{a},$$
$$\nabla\cdot(f\mathbf{1})=\nabla f,$$

- and on derivatives

  $$(\mathbf{a}\cdot\nabla)\mathbf{b} = \mathbf{a}\cdot(\nabla\mathbf{b})^T,$$

  $$\frac{\partial f(x)}{\partial \mathbf{x}} = \frac{\mathbf{x}}{x}\frac{\partial f(x)}{\partial x},$$

  $$\mathbf{ab} : (\nabla\mathbf{c}) = \mathbf{a}\cdot(\mathbf{b}\nabla)\,\mathbf{c},$$

  with $x = |\mathbf{x}|$.
- For some computations, we need the use the *Dirac function* $\int_{\mathbb{R}^3}\delta(\mathbf{x})\mathrm{d}\mathbf{x} = 1$, $\int_{\mathbb{R}^3}\delta(\mathbf{x}-\mathbf{x}_0)g(\mathbf{x})\mathrm{d}\mathbf{x} = g(\mathbf{x}_0)$, and $\delta(\mathbf{x}) = -\nabla^2(4\pi x)^{-1} = -\nabla^4 x(8\pi)^{-1}$, where $x = |\mathbf{x}|$. The last two expressions are derived by applying the Green formula to the function $1/x$ (see any textbook on distributions).
- The *Fourier transform* in an n-dimensional space is defined as

  $$\hat{f}(\boldsymbol{\xi}) = \int_{\mathbb{R}^n} f(\mathbf{x})e^{-\imath\boldsymbol{\xi}\cdot\mathbf{x}}\mathrm{d}\mathbf{x},$$

  for any continuous function. Conversely, the inverse Fourier transform is defined as

  $$f(\mathbf{x}) = \int_{\mathbb{R}^n} \hat{f}(\mathbf{x})e^{\imath\boldsymbol{\xi}\cdot\mathbf{x}}\mathrm{d}\boldsymbol{\xi}.$$

Further reading

This notebook gives an overview of the major current issues in rheology through a series of different problems of particular relevance to particle-suspension rheology. For each topic considered here, we will outline the key elements and point the student toward the most helpful references and authoritative works. The student is also referred to available books introducing rheology (Barnes, 1997; Tanner, 1988) for a more complete presentation; the tutorials written by Middleton & Wilcock (1994) on mechanical and rheological applications in geophysics and by Barnes (2000) provide a shorter introduction to rheology.

Continuum Mechanics, rheology

- K. Hutter and K. Jöhnk, *Continuum Methods of Physical Modeling* (Springer, Berlin, 2004) 635 p.
- H.A. Barnes, J.F. Hutton and K. Walters, *An introduction to rheology* (Elsevier, Amsterdam, 1997).
- H.A. Barnes, *A Handbook of Elementary Rheology* (University of Wales, Aberystwyth, 2000).
- K. Walters, *Rheometry* (Chapman and Hall, London, 1975).
- D.V. Boger and K. Walters, *Rheological Phenomena in Focus* (Elsevier, Amsterdam, 1993) 156 p.
- B.D. Coleman, H. Markowitz and W. Noll, *Viscometric flows of non-Newtonian fluids* (Springer-Verlag, Berlin, 1966) 130 p.
- C. Truesdell, *Rational Thermodynamics* (Springer Verlag, New York, 1984).
- C. Truesdell, The meaning of viscometry in fluid dynamics, *Annual Review of Fluid Mechanics*, **6** (1974) 111–147.

Fluid mechanics

- S.B. Pope, *Turbulent Flows* (Cambridge University Press, Cambridge, 2000) 771 p.
- W. Zdunkowski and A. Bott, *Dynamics of the Atmosphere* (Cambridge University Press, Cambridge, 2003) 719 p.
- C. Pozrikidis, *Boundary Integral and Singularity Methods for Linearized Viscous Flows* (Cambridge University Press, Cambridge, 1992) 259 p.
- G.K. Batchelor, *An introduction to fluid dynamics* (Cambridge University Press, 1967) 614 p.
- H. Lamb, *Hydrodynamics* (Cambridge University Press, Cambridge, 1932).

Polymeric fluid rheology

- R.B. Bird, R.C. Armstrong and O. Hassager, *Dynamics of Polymeric Liquids* (John Wiley & Sons, New York, 1987) 649 p.
- R.I. Tanner, *Engineering Rheology* (Clarendon Press, Oxford, 1988) 451 p.
- F.A. Morrison, *Understanding Rheology* (Oxford University Press, New York, 2001) 545 p.
- W.R. Schowalter, *Mechanics of non-Newtonian fluids* (Pergamon Press, Oxford, 1978) 300 p.

Suspensions and multi-phase materials

- W.B. Russel, D.A. Saville and W.R. Schowalter, *Colloidal dispersions* (Cambridge University Press, Cambridge, 1995) 525.
- P. Coussot and C. Ancey, *Rhéophysique des pâtes et des suspensions* (EDP Sciences, Les Ulis, 1999) 266.
- D.L. Koch and R.J. Hill, "Inertial effects in suspension and porous-media flows", *Annual Review of Fluid Mechanics*, **33** (2001) 619-647.
- R. Herczynski and I. Pienkowska, "Toward a statistical theory of suspension", *Annual Review of Fluid Mechanics*, **12** (1980) 237–269.
- S. Kim and S.J. Karrila, *Microhydrodynamics: Principles and Selected Applications* (Butterworth-Heinemann, Stoneham, 1991) 507 p.
- D.A. Drew and S.L. Passman, *Theory of Multicomponent Fluids* (Springer, New York, 1999) 308 p.
- Jean-Pierre Minier and Eric Peirano, "The pdf approach to turbulent polydispersed two-phase flows", *Physics Reports*, **352** (2001) 1–214.
- S. Dartevelle, "Numerical modeling of geophysical granular flows: 1. A comprehensive approach to granular rheologies and geophysical multiphase flows", *Geochemistry Geophysics Geosystems*, **5** (2004) 2003GC000636.
- D.A. Drew, "Mathematical modeling of two-phase flows", *Annual Review of Fluid Mechanics*, **15** (1983) 261–291.
- Y.A. Buyevich and I.N. Shchelchkova, "Flow of dense suspension", *Progress in Aerospace Science*, **18** (1978) 121–150.

Resources on the web

Proceedings of the Porquerolles summer school organized by the CNRS, look at

`http://www.lmgc.univ-montp2.fr/MIDI/`

Granular stuffs and geophysical flows, a site managed by Sébastien Dartevelle, Michigan Technology University

`http://www.granular.org`

The book on rheology (with emphasis on food rheology) is freely available at

`http://www.egr.msu.edu/~steffe/freebook/offer.html`

Of great interest is also the free-book distribution initiated by John Scaled and Martin Smith (School of Mines, Colorado, USA). Take a closer look at

`http//samizdat.mines.edu`,

where there are several books on continuum mechanics and inverse theory including the e-books by Jean Garrigues (in French) also available at

`http://esm2.imt-mrs.fr/gar/pagePerso.html`.

Of the same vein, but in French: `http://www.librecours.org`
together with: `http://www.sciences.ch`

Chapter 1

Rheometry

Prerequisites

- fluid mechanics: conservation law
- mathematics: differential analysis, tensorial analysis, algebra tools

Objectives

- to provide the mathematical basis underpinning viscometry theory
- to review the different techniques used in rheometry
- to deal with approximate methods for evaluating some rheological properties
- to introduce the readers with some techniques used for solving inverse problems in rheometry
- to pinpoint the commonly observed rheological behaviors (e;g., viscosity, viscoplasticity, viscoelasticity)

Content

Rheometry refers to a set of standard techniques that are used to experimentally determine rheological properties of materials (fluid or solid). The idea underpinning rheometry is to realize flows, where the stress and/or strain fields are known in advance, which makes it possible to deduce rheological properties from measurements of flow properties. A rheometer is usually an engine, which can exert a torque/force on a material and accurately measures its response with time (or conversely, it can impose a strain and measures the resulting torque). In this chapter, we start with a presentation of how a rheometer operates and how measurements can be used to infer the rheological properties of the material tested. Then, the experimental procedures and the typical behaviors observed are reviewed. Emphasis is also given to providing a general view on issues encountered in rheometry, either because of rheometer limitations or as a result of disturbing phenomena in the material tested.

1.1 How does a rheometer operate?

1.1.1 A long history

Originally, rheometers were based on an applied stress which was generated by a weights-and-pulleys arrangement, as shown for instance in Figure 1.1. These methods were then superseded by electrically driven motors; they were the first controlled-strain instruments. With logarithmic mechanical gear boxes, the most sophisticated rheometers (e.g. the Weissenberg Rheogoniometer) in the 1960's were able to span a shear-rate range typically from 10^{-4} to 10^{4} s^{-1}.

In the mid 1970s, a new generation of controlled-stress rheometers began to appear. The first had been developed by Deer and colleagues at the London School of Pharmacy, who used air bearings and an air-driven turbine to provide the torque.

Then around 1980, commercial versions of the new generation of electrically driven controlled-stress rheometers appeared, still based on air bearings that greatly reduced friction, but also using so-called drag-cup electrical motors that allowed controlled stresses to be more easily applied independently of rotation speed. Along with these features came new ways of measuring smaller and smaller rotation and rotation rates. The latest optical-disc technology now means that rotation rates as low as 10^{-8} rad s^{-1} (1 revolution in 20 years) can be measured! This has opened up a new range of previously unobtainable flow behaviour.

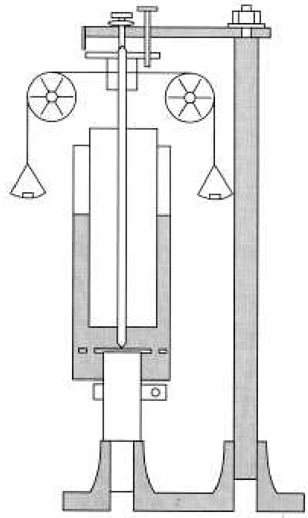

Figure 1.1 *A sketch of Searle's 1912 controlled-stress, concentric-cylinder viscometer. After (Barnes, 2000)*

1.1.2 Anatomy of a modern rheometer

At LHE, we use a CVOR 200 Bohlin rheometer. Figure 1.2 shows the heart of the rheometer when the engine hood is removed.

Figure 1.2 *Bohlin CVOR used at LHE.*

Most modern rheometers adopt the same architecture. As shown in Figure 1.3, there are several elements that are common in modern rheometers

1. Low inertia, contact-less, inductive motor assembly without any permanent magnets for accurate torque setting over a wide dynamic range and excellent transient response.
2. Precision air bearing with thrust and journal surfaces for frictionless support with high axial and radial stiffness.
3. Inductive, contact-less and multi-layer position sensor assembly for accurate measurement of speed and absolute position.
4. Precision collett-type chuck for attachment of upper measurement system with minimal axial run-out.
5. Leadscrew assembly with bespoke pre-tensioned nut and stepper motor for accurate control of measurement sensor position with no backlash.
6. Linear bearing to support and guide the air bearing and motor assembly.
7. Integral normal force sensors placed within the instrument mechanics
8. Temperature control unit (Peltier plate design shown)
9. Universal clamping arrangement designed to accept all available temperature control options.
10. Push button acrylic key pad incorporating all key gap setting and control functions with normal force and gap separation display.
11. Integral electronics and power supply incorporating microprocessor based control and measurement functions, including torque, speed, position and temperature. Data communication is to PC via a high speed serial link.
12. Composite outer covers to provide impervious barrier and protect instrument mechanics.

Figure 1.3 *Bohlin CVOR used at LHE.*

1.1.3 Typical performance of modern lab rheometers

Modern rheometer capabilities include

- control on sample temperature;
- quite a wide range of tools (parallel-plate, cone-plane, etc.);
- wide shear-rate range ($>$ 10 orders of magnitude);
- directional (including reverse flow) and oscillatory flow;
- high accuracy and resolution;
- direct monitoring via a PC.

Here are the typical features of modern high-performance rheometer (Bohlin CVOR) :

- Torque range $0.05 \times 10^{-6} 200 \times 10^{-3}$ mN.m
- Torque resolution 1×10^{-9} Nm
- Rotational-velocity range $1 \times 10^{-7} - 600$ rad/s
- Resolution in angular position 5×10^{-8} rad
- Frequency range $1 \times 10^{-5} - 150$ Hz
- Normal force range $1 \times 10^{-3} - 20$ N

1.2 Principles of viscometry

1.2.1 Fundamentals of rheometry

Rheometry and viscometry

At the very beginning, the term *rheometry* referred to a set of standard techniques for measuring shear viscosity. Then, with the rapid increase of interest in non-Newtonian fluids, other techniques for measuring the normal stresses and the elongational viscosity were developed. Viscometry is an important offshoot of rheometry, which applies to incompressible simple fluids. When the 'simple-fluid' approximation holds, it is possible to derive the flow curve and other rheological functions (e.g., normal stress differences) from the geometrical measurements: torque, rotational velocity, and thrust.

Nowadays, rheometry is usually understood as the area encompassing any technique that involves measuring mechanical or rheological properties of a material. This includes:

- visualization techniques (such as photoelasticimetry for displaying stress distribution within a sheared material);
- nonstandard methods (such as the slump test for evaluating the yield stress of a viscoplastic material).

In most cases for applications, shear viscosity is the primary variable characterizing the behavior of a fluid. Thus in the following, we will mainly address this issue, leaving aside all the problems related to the measurement of elongational viscosity.

The basic principle of rheometry is to perform simple experiments where the flow characteristics such as the shear stress distribution and the velocity profile are known in advance and can be imposed. Under these conditions, it is possible to infer the *flow curve*, that is, the variation of the shear stress as a function of the shear rate, from measurements of flow quantities such as torque and the rotational velocity for a rotational viscometer. In fact, despite its apparent simplicity, putting this principle into practice for natural or industrial fluids raises many issues that we will discuss below. Most rheometers rely on the achievement of *viscometric* flow (Coleman *et al.*, 1966).

The simplest curvilinear flow is the simple shear flow achieved by shearing a fluid between two plates in a way similar to Newton's experiment depicted in Chap. 2. However, in practice many problems (fluid recirculation, end effect, etc.) arise, which preclude using such a shearing box to obtain accurate measurements. Another simple configuration consists of an inclined plane or a parallel-plate rheometer.

For many fluids of practical interest, viscometry is then an indispensable theory that underpins rheometrical investigation by making a clear connection between bulk measurements and rheological data. We shall see later that an incompressible simple fluid is defined as follows:

1. only isochoric motions are permitted: bulk density is constant;
2. the stress tensor $\boldsymbol{\sigma}$ is determined, to within a pressure term, by the history of the relative deformation gradient[1] $\mathbf{F}$

   $$\mathbf{s} = \boldsymbol{\sigma} + p\mathbf{1} = \mathcal{F}(\mathbf{F}(t)),$$

   with $\mathbf{s}$ the extra-stress tensor, p the pressure, $\boldsymbol{\sigma}$ the stress tensor, and $\mathcal{F}$ a tensor-valued functional of $\mathbf{F}$. Time is denoted by t. This expression is called the *constitutive equation* or rheological law.

   Some specific material classes can be defined (see Chap. 2):

   - If the functional $\mathcal{F}$ involves the time derivative of $\mathbf{F}$ alone[2], the material is a fluid.

---

[1] See Chap. 2 for further information.

[2] i.e., the strain-rate tensor $\mathbf{d} = -\frac{1}{2}(\dot{\mathbf{F}} + \dot{\mathbf{F}}^T)$

  - If the functional $\mathcal{F}$ does not involve the time derivative of $\mathbf{F}$, the material is a solid.
  - If the functional $\mathcal{F}$ is a one-to-one function, then the fluid has no memory since the stress depends on the current state of deformation alone.
  - If $\mathcal{F}$ is an integral function, then the fluid behavior is characterized by memory effects: the stress state depends on the past states of deformation experienced by the material.

  More complicated behaviors can be imagined, but the important point here is to recall that a wide range of behavior can be described using this formulation. For instance, if $\mathcal{F}$ involves $\mathbf{F}$ and $\mathbf{d}$, the material is said to be *visco-elastic.*

Viscometric flows

On many occasions, it is possible to create flows that induces a relative deformation gradient that is linear with time, that is, the distance between two neighboring points varies linearly with time (this distance may be zero) at any time and any point of the material. In this case, it can be shown (Coleman *et al.*, 1966) that

- There is a tensor $\mathbf{M}$, which can be interpreted as the velocity gradient and the matrix representation of which takes the form

  $$\mathbf{M} = \begin{bmatrix} 0 & 0 & 0 \\ \dot{\gamma} & 0 & 0 \\ 0 & 0 & 0 \end{bmatrix},$$

  for some orthogonal basis $\mathcal{B}$ and such that the relative deformation gradient $\mathbf{F}$ is $\mathbf{F}(t) = \mathbf{R}(t) \cdot (\mathbf{1} - t\mathbf{M})$, where $\mathbf{R}$ is an arbitrary orthogonal tensor, which is a function of time and satisfies $\mathbf{R}(0) = \mathbf{1}$. In the basis $\mathcal{B}$, the strain-rate and stress tensors takes the form

  $$\mathbf{d} = \begin{bmatrix} 0 & \dot{\gamma} & 0 \\ \dot{\gamma} & 0 & 0 \\ 0 & 0 & 0 \end{bmatrix} \text{ and } \boldsymbol{\sigma} = \begin{bmatrix} \sigma_{11} & \sigma_{12} & 0 \\ \sigma_{21} & \sigma_{22} & 0 \\ 0 & 0 & \sigma_{33} \end{bmatrix}.$$

- In these expressions, $\dot{\gamma}$ is the shear rate and is assumed to a control parameter. If the fluid is a simple fluid, then there is a functional $\mathcal{F}$ such that

  $$\boldsymbol{\sigma} + p\mathbf{1} = \mathcal{F}(\mathbf{M}) = \mathcal{F}(\dot{\gamma}).$$

  To get rid of the pressure term (which can be determined only by solving the equations of motion, thus does not reflect any rheological property, but only isochoric constraint), we introduce
  - the shear-stress function $\tau(\dot{\gamma}) = \sigma_{21}$;
  - the first normal-stress difference $N_1 = \sigma_{11} - \sigma_{22}$;
  - the second normal-stress difference $N_2 = \sigma_{22} - \sigma_{33}$.

  These functions are called material functions since they reflect the rheological behavior of the material tested.

If a flow satisfies these conditions, it is called *viscometric.* Two subclasses are particularly important in practice:

- A *simple shear flow* is a particular case, where the shear rate is constant at any point and does vary with time. The Couette flow between two parallel, infinite, horizontal planes provides a typical example.
- More generally, curvilinear flows can be seen a generalized variant of simple-shear flows: the shear rate is permitted to vary with position, but the deformation field remains steady and two-dimensional for a certain basis.

Current geometries that allow realizing curvilinear flows are:

– simple shear flow: pressure-driven flow through parallel plates or gravity-driven flow down an inclined channel;
– vertical cylindrical tubes (Poiseuille flow): capillary rheometers;
– torsional flows: cone-and-plate and parallel-plate rheometers;
– helical flows such as flows between concentric cylinders (Couette flow): coaxial rheometers.

1.2.2 Flow down an inclined channel

To exemplify the viscometric approach, we will show how some flow properties such as the *discharge equation* (variation of the fluid discharge as a function of the flow depth) can be used to infer the constitutive equation. We consider a gravity-driven free-surface flow in a steady uniform regime down an inclined channel. The plane is tilted at an inclination θ to the horizontal. We use the Cartesian co-ordinate system of origin 0 and of basis $\mathbf{e}_x$, $\mathbf{e}_y$, $\mathbf{e}_z$ as depicted in Fig. 1.4.

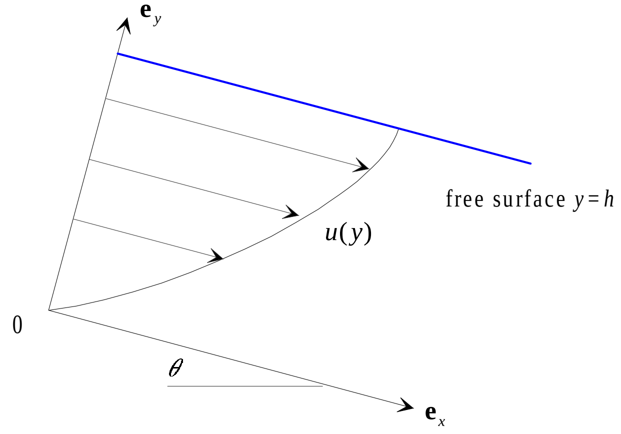

Figure 1.4 *Definition sketch for steady uniform flow*

The velocity field $\mathbf{u}$ only depends on the co-ordinate y and takes the following form: $u_x = u(y)$, $u_y = 0$, $u_z = 0$, where u is a function of y to be determined. Accordingly, the strain-rate tensor $\mathbf{d} = (\nabla\mathbf{u} + {}^t\nabla\mathbf{u})/2$ has the following components in the co-ordinate system:

$$\mathbf{d} = \frac{\dot{\gamma}}{2}\left[\begin{array}{ccc} 0 & 1 & 0 \\ 1 & 0 & 0 \\ 0 & 0 & 0 \end{array}\right], \tag{1.1}$$

where the shear rate $\dot{\gamma}$ is defined as a function of the co-ordinate y and implicitly of the inclination θ: $\dot{\gamma}(y) = (\partial u/\partial y)_\theta$.

The momentum balance can be written as:

$$\varrho\frac{\mathrm{d}\mathbf{u}}{\mathrm{d}t} = \varrho\mathbf{g} + \nabla\cdot\boldsymbol{\sigma}, \tag{1.2}$$

where ϱ and $\mathbf{g}$ respectively denote the local material density and gravitational acceleration. We assume that there is no slip at the bottom: $u(0) = 0$.

Furthermore, we assume that there is no interaction between the free surface and the ambient fluid above except the pressure exerted by the ambient fluid. Notably, we ignore surface tension effects on the free surface. Without restriction, the stress tensor can be written as the sum a pressure term p and a deviatoric term called the extra-stress tensor $\mathbf{s}$ (see also Chap. 2) (Tanner, 1988; Coleman *et al.*, 1966): $\boldsymbol{\sigma} = -p\mathbf{1} + \mathbf{s}$. For a homogeneous and isotropic simple fluid, the extra-stress tensor depends on the strain rate only: $\mathbf{s} = G(\mathbf{d})$, where G is a tensor-valued isotropic functional. In the present case, it is straightforward to show that the stress tensor must have the form

$$\boldsymbol{\sigma} = -p\mathbf{1} + \begin{bmatrix} s_{xx} & s_{xy} & 0 \\ s_{xy} & s_{yy} & 0 \\ 0 & 0 & s_{zz} \end{bmatrix}. \tag{1.3}$$

Thus, the stress tensor is fully characterized by three functions:

- the shear stress $\tau = \sigma_{xy} = s_{xy}$
- the normal stress differences: $N_1 = s_{xx} - s_{yy}$ and $N_2 = s_{yy} - s_{zz}$ called the first and second normal stress differences, respectively.

Since for steady flows acceleration vanishes and the components of $\mathbf{s}$ only depend on y, the equations of motion (1.2) reduce to

$$0 = \frac{\partial s_{xy}}{\partial y} - \frac{\partial p}{\partial x} + \varrho g \sin\theta, \tag{1.4}$$

$$0 = \frac{\partial s_{yy}}{\partial y} - \frac{\partial p}{\partial y} - \varrho g \cos\theta, \tag{1.5}$$

$$0 = \frac{\partial p}{\partial z}. \tag{1.6}$$

It follows from (1.6) that the pressure p is independent of z. Accordingly, integrating (1.5) between y and h imply that p must be written: $p(x,y) - p(x,h) = s_{yy}(y) - s_{yy}(h) + \varrho g(h-y)\cos\theta$. It is possible to express Eq. (1.4) in the following form:

$$\frac{\partial}{\partial y}\left(s_{xy} + \varrho g y \sin\theta\right) = \frac{\partial p(x,h)}{\partial x}. \tag{1.7}$$

This is possible only if both terms of this equation are equal to a function of z, which we denote $b(z)$. Moreover, Eq. (1.6) implies that $b(z)$ is actually independent of z; thus, in the following we will note: $b(z) = b$. The solutions to (1.7) are: $p\,(x,h) = bx + c$, where c is a constant, and $s_{xy}(h) - s_{xy}(y) + \varrho g(h-y)\sin\theta = b(h-y)$, which we will determine. To that end, let us consider the free surface. It is reasonable and usual to assume that the ambient fluid friction is negligible. The stress continuity at the interface implies that the ambient fluid pressure p_0 exerted on an elementary surface at $y = h$ (oriented by $\mathbf{e}_y$) must equal the stress exerted by the fluid. Henceforth, the boundary conditions at the free surface may be expressed as: $-p_0\mathbf{e}_y = \sigma\mathbf{e}_y$, which implies in turn that: $s_{xy}(h) = 0$ and $p_0 = p(x,h) - s_{yy}(h)$. Comparing these equations to former forms leads to $b = 0$ and $c = p_0 + s_{yy}(h)$. Accordingly, we obtain for the shear and normal stress distributions

$$\tau = \varrho g(h-y)\sin\theta, \tag{1.8}$$

$$\sigma_{yy} = s_{yy} - (p - p_0) = -\varrho g(h-y)\cos\theta. \tag{1.9}$$

The shear and normal stress profiles are determined regardless of the form of the constitutive equation. For simple fluids, the shear stress is a one-to-one function of the shear rate: $\tau = f(\dot\gamma)$. Using the shear stress distribution (1.8) and the inverse function f^{-1}, we find: $\dot\gamma = f^{-1}(\tau)$. A double integration leads to the flow rate (per unit width):

$$q = \int_0^h \int_0^y f^{-1}(\tau(\xi))d\xi = \int_0^h u(y)\mathrm{d}y. \tag{1.10}$$

An integration by parts leads to:

$$q(h,\,\theta) = [(y-h)u(y)]_0^h + \int_0^h (h-y)\left(\frac{\partial u}{\partial y}\right)_\theta \mathrm{d}y.$$

In this equation, the first expression of the right-hand term is hu_g if the slip condition at the bottom is relaxed. Making use of the shear stress equation leads to

$$q(h,\theta) = hu_g + \int_0^h (h-y)f\left(\varrho g\sin\theta(h-y)\right)\mathrm{d}y$$

By making the variable change: $\zeta = h - y$, we also obtain

$$q(h,\theta) = \int_0^h \zeta f\left(\varrho g\sin\theta v\right)\mathrm{d}\zeta + hu_g.$$

Thus the partial derivative of q with respect to h (at a given channel slope θ) is

$$\left(\frac{\partial q}{\partial h}\right)_\theta = hf(\varrho gh\sin\theta) + u_g + h\left(\frac{\partial u_g}{\partial h}\right)_\theta,$$

or equivalently

$$f(\tau_p) = \frac{1}{h}\left(\frac{\partial q}{\partial h}\right)_\theta - \frac{u_g}{h} - \left(\frac{\partial u_g}{\partial h}\right)_\theta.$$

where $\tau_p = \varrho g\sin\theta$ is the bottom shear shear. In the case (often encountered) of no-slip, this expression reduces to

$$\dot\gamma = f^{-1}(\tau(h)) = \frac{1}{h}\left(\frac{\partial q}{\partial h}\right)_\theta. \tag{1.11}$$

This relation allows us to directly use a channel as a rheometer.

The other normal components of the stress tensor cannot be easily measured. The curvature of the free surface of a channelled flow may give some indication of the first normal stress difference. Let us imagine the case where it is not equal to zero. Substituting the normal component s_{yy} by $s_{yy} = s_{xx} - N_1$ in (1.5), after integration we find:

$$s_{xx} = p + \varrho gy\cos\theta + N_1 + c, \tag{1.12}$$

where c is a constant. Imagine that a flow section is isolated from the rest of the flow and the adjacent parts are removed. In order to hold the free surface flat (it will be given by the equation $y = h$, $\forall z$), the normal component σ_{xx} must vary and balance the variations of N_1 due to the presence of the sidewalls (for a given depth, the shear rate is higher in the vicinity of the wall than in the center). But at the free surface, the boundary condition forces the normal stress σ_{xx} to vanish and the free surface to bulge out. To first order, the free surface equation is:

$$-\varrho gy\cos\theta = N_1 + c. \tag{1.13}$$

If the first normal stress difference vanishes, the boundary condition $-p_0\mathbf{e}_y = \sigma\mathbf{e}_y$ is automatically satisfied and the free surface is flat. In the case where the first normal stress difference does not depend on the shear rate, there is no curvature of the shear free surface. The observation of the free surface may be seen as a practical test to examine the existence and sign of the first normal stress difference and to quantify it by measuring both the velocity profile at the free surface and the free-surface equation.

1.2.3 Standard geometries

Computation of the shear-stress function and normal stress differences is very similar for other types of viscometers. Figure 1.5 reports the corresponding functions for the most common viscometers. All these techniques are robust and provide accurate measurements for classic fluids, with uncertainty usually less than 2%.

Rheometer type	Sketch	Viscometric function
Capillary tube (Poiseuille flow)	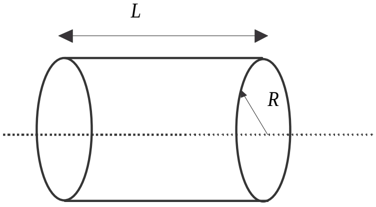	$\dot{\gamma}=\lambda\left(\frac{\Delta p_g}{L}\frac{R}{2}\right)=\frac{1}{\pi\alpha^2R^3}\frac{\partial\left(q\alpha^3\right)}{\partial\alpha}$ $\alpha=\frac{\Delta p_g}{L}$ (pressure variation per unit length) q: flow rate, Δp_g: applied pressure gradient
Concentric cylinder (Couette flow)	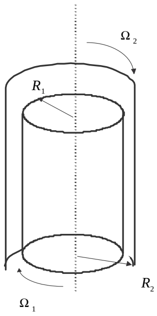	$\Delta\Omega=\Omega_2-\Omega_1=\frac{1}{2}\int_{C/(2\pi R_1^2)}^{C/(2\pi R_2^2)}\dot{\gamma}(\tau)d\ln\tau$ $\tau=\frac{C}{2\pi R_1^2}$ R_1: inner radius; R_2: outer radius C : torque (per unit height)
Parallel-plate	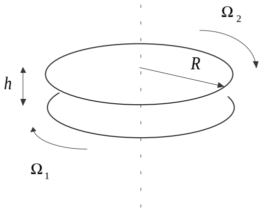	$\dot{\gamma}\approx R\frac{\Delta\Omega}{h}$, $C=\frac{M}{2\pi R^3}$, $\Delta\Omega=\Omega_2-\Omega_1$ $\tau=C\left(3+\frac{\partial\ln C}{\partial\ln\dot{\gamma}}\right)$ M : measured torque
Inclined plane	See Fig. 1	$\tau=\rho gh\sin\theta$ $\dot{\gamma}=\frac{1}{h}\left(\frac{\partial q}{\partial h}\right)$

Figure 1.5 *Chief geometries used in rheometry*

1.3 Inverse problems in rheometry

1.3.1 A typical example: the Couette problem

A longstanding problem in rheometry is the so-called Couette inverse problem, in which one tries to derive the flow curve $\tau(\dot\gamma)$ from the torque measurements $M(\omega)$ in a coaxial cylinder (Couette) rheometer, where τ is the shear stress, $\dot\gamma$ denotes the shear rate, ω is the rotational velocity of the inner cylinder, and M represents the torque per unit height (Coleman *et al.*, 1966). The shear stress τ exerted on the inner cylinder of radius R_1 can be directly related to the measured torque M by $\tau = \alpha_1 M$, with $\alpha_1 = 1/(2\pi R_1^2)$, independently of the form of the constitutive equation. The shear rate is related to the rotational velocity ω by

$$\omega = \int_{R_1}^{R_2} \frac{\dot\gamma(r)}{r} dr, \tag{1.14}$$

where R_2 denotes the outer-cylinder radius and it is assumed that (i) the rotational velocity of the outer cylinder is zero and (ii) there is no slip between the inner cylinder and the sheared material at $r = R_1$. In order to recover the flow curve from measurements of the rotational velocity $\omega(M)$, one must be able to

(i) relate the function $\dot\gamma(r)$ to $\tau(r)$,

(ii) find out a means of inverting the integral relationship (1.14),

(iii) estimate the continuous function $\dot\gamma(\tau)$ from a set of discrete values (ω_i, M_i).

For a broad class of fluids (simple fluids), the first step is systematically achieved since there is a one-to-one relation between the shear stress and the shear rate for steady viscometric flows: $\dot\gamma = \dot\gamma(\tau)$. Moreover, the momentum equations imply that the shear stress distribution across the gap is given by $S(r) = M/(2\pi r^2) = \tau(R_1/r)^2$, where r denotes the distance from the vertical rotation axis of the cylinders. Under these conditions, which are not too stringent, it is possible to make the variable change $r = R_1\sqrt{\tau/S}$ in the integral above; we then derive the well-known equation (Krieger & Elrod, 1953; Coleman *et al.*, 1966)

$$\omega(\tau) = \frac{1}{2}\int_{\beta\tau}^{\tau} \frac{\dot\gamma(S)}{S} dS, \tag{1.15}$$

where $\beta = (R_1/R_2)^2$. The next step is to recover $\dot\gamma$ from $\omega(\tau)$.

1.3.2 Earlier attempts at solving the Couette problem

Scientific statement and mathematical strategies

In the Couette inverse problem, Eq. (1.15) can be represented in the generic form: $\omega(\tau) = (K\dot\gamma)(\tau)$, where K is the integral operator

$$(Kf)(z) = \int_{\beta z}^{z} \frac{f(x)}{x} dx, \tag{1.16}$$

with β a constant parameter ($\beta < 1$). A considerable body of literature has been published over the last three decades on ill-posed inverse problems in this form (Bertero *et al.*, 1985, 1988; O'Sullivan, 1986; Tenorio, 2001). Schematically, we can split the various methods for solving

Couette-like problems into three main categories[3].

- *Least-square approach*: instead of solving $\omega = K\dot{\gamma}$, an attempt is made to minimize the residual $||\omega - K\dot{\gamma}||$, usually with an additional constraint on the norm of $||f||$ or its derivative(s), to control the smoothness of the solution. Tikhonov's regularization method used by Yeow *et al.* (2000) and Landweber's iterative procedure used by Tanner & Williams (1970) come within this category. The advantages of this method are its robustness against computation inaccuracies and measurement errors, its versatility, its fast convergence when the function to be recovered behaves reasonably well, and the relative facility of its implementation. The drawbacks are that it relies on an arbitrary selection of the regularization operator (even though specific procedures have been established) and its limited capacity to retrieve irregular functions.
- *Projection approach*: the idea here is to discretize the problem by projecting the function over a finite space spanned by a family of functions enjoying specific properties (such as orthogonality) u_i. Equation (1.15) is then replaced by the finite set of equations $\langle K\dot{\gamma},\, u_i\rangle = \langle \omega,\, u_i\rangle$ for $1 \leq i \leq p$, where $\langle f,\, g\rangle = \int_{\mathbb{R}} f(x)g(x)dx$ denotes the inner product in the function space (Dicken & Maass, 1996; Louis *et al.*, 1997; Rieder, 1997). Galerkin's method, used by Macsporran (1989) with spline functions, provides a typical example for Couette rheometry. Irregular functions can be recovered by these methods provided appropriate projection functions are chosen in advance.
- *Adjoint operator approach*: for many reasons, it is usually either not possible or not advantageous to compute the inverse operator K^{-1}. In some cases, however, it is possible to provide a weak inverse formulation, in which the function $\dot{\gamma}$ is expressed as

$$\dot{\gamma} = \sum_{i\in J} \langle K\dot{\gamma},\, u_i\rangle \Psi_i,$$

where the summation is made over a set J, Ψ_i is an orthonormal basis of functions, and u_i denotes a family of function solutions of the adjoint problem $K^* u_i = \Psi_i$, where K^* is the adjoint operator of K (Golberg, 1979). Typical examples include *singular-value decomposition* (Bertero *et al.*, 1985, 1988), a generalized formulation based on *reconstruction kernels* (Louis, 1999), *wavelet-vaguelette decomposition* (Donoho, 1995), and *vaguelette-wavelet decomposition* (Abramovich & Silverman, 1998). The solution to the inverse problem is found by replacing $K\dot{\gamma}$ with ω in the equation above and filtering or smoothing the inner products $\langle K\dot{\gamma},\, u_i\rangle$ and/or truncating the sum.

Mooney's and Krieger's approximation

Although the Couette problem admits an analytical theoretical solution in the form of an infinite series (Coleman *et al.*, 1966), deriving the shear rate remains a difficult task in practice because the derivation enters the class of ill-posed problems (Friedrich *et al.*, 1996). In rheometry, the first attempt at solving Eq. (1.15) can be attributed to Mooney (1931), Krieger & Maron (1952), and Krieger & Elrod (1953). When β is close to unity, it is possible to directly approximate the integral to the first order by

$$\omega(\tau) = \frac{1-\beta}{2}\dot{\gamma}(\tau) + o(\beta\dot{\gamma}).$$

---

[3] This partitioning is a bit arbitrary because there are interconnections between the three categories [e.g., Tikhonov's regularization can be viewed as a special case of singular-value decomposition (Bertero *et al.*, 1988)]. This is, however, sufficient in the present paper to outline the main approaches used so far and to situate the previous attempts at solving the Couette problem. Alternative methods, e.g., stochastic methods (Gamboa & Gassiat, 1997; Mosegaard & Sambridge, 2002), are also possible, but have never been used in rheometry as far as we know.

When β moves away from unity, further terms are needed in the expansion of the integral into a β series. One of the most common approximations is attributed to Krieger who proposed for Newtonian and power-law fluids (Yang & Krieger, 1978; Krieger, 1968):

$$\dot{\gamma} = \frac{2\Omega(1+\alpha)}{1-\beta^f} f, \tag{1.17}$$

with

$$f = \frac{\mathrm{d}\ln\Omega}{\mathrm{d}\ln C},\ \alpha = \frac{f'}{f^2}\chi_1(-f\log\beta),\ \text{and}\ \chi_1(x) = \frac{x}{2}(xe^x - 2e^x + x + 2)(e^x - 1)^{-2}.$$

However, this method can give poor results with yield stress fluids, especially if it is partially sheared within the gap. In this case, Nguyen & Boger (1992) have proposed using

$$\dot{\gamma} = 2\Omega \frac{\mathrm{d}\ln\Omega}{\mathrm{d}\ln C}.$$

A few rheologists used an alternative consisting of an expansion into a power series of (1.15). They obtained:

$$\dot{\gamma} = 2\Omega \sum\nolimits_{n=0}^{\infty} f\left(\beta^n C/(2\pi R_1^2)\right).$$

Although refined to achieve higher accuracy (Yang & Krieger, 1978), Krieger's approach was unable to provide reliable results for viscoplastic flows (Darby, 1985; Nguyen & Boger, 1992) or for data contaminated by noise (Borgia & Spera, 1990).

Tikhonov's regularization technique

Alternative methods have been proposed: Tanner & Williams (1970) developed an iterative procedure, whereas Macsporran (1989), Yeow *et al.* (2000), and Leong & Yeow (2003) used a regularized least-square approach, which involves discretizing the integral term and regularizing it.

These methods are very efficient for a wide range of well-behaved rheological equations. However, when the rheological behavior exhibits singularities such as a yield stress or a rapid shear-thickening, the regularization procedure can lead to unrealistic results by smoothing out the singularities or to complicated trial-and-error loops. For instance, when testing Tikhonov's method with viscoplastic flows, Yeow *et al.* (2000) had to evaluate the yield stress iteratively, which may involve a large number of computations and slow convergence. This undesired behavior is to a large extent the result of attempting to evaluate a continuous function ($\dot{\gamma}(\tau)$) from a finite set of discrete values representing measurements of bulk quantities. This task is more delicate than believed, especially when data are noisy. For a well-behaved rheological equation, imposing a certain degree of smoothness in the regularization procedures does not entail many problems. On the contrary, for complex rheological responses, it becomes increasingly difficult to discern genuine rheological properties, noise effects, and discretization errors.

1.3.3 The wavelet-vaguelette decomposition

We will begin by exposing the principle in a very simple manner. A more rigorous mathematical derivation follows in the Appendix. Let us assume that we can approximate any shear rate function $\dot{\gamma}(\tau)$ with a finite series of terms

$$\dot{\gamma}(\tau) \approx \sum_k a_k \Psi_k(\tau),$$

where Ψ_k denotes the k^{th} member of a family of orthogonal functions, i.e., $\int \Psi_k(\tau)\Psi_i(\tau)d\tau = \delta_{ik}$; making use of this property, we could compute the coefficients a_k as $a_k = \int \dot{\gamma}(\tau)\Psi_i(\tau)d\tau$ if the function $\dot{\gamma}(\tau)$ were known.

Using the linearity of the integral operator K, we have

$$\omega(\tau) = (K\dot{\gamma})(\tau) \approx \sum_k a_k\,(K\Psi_k)(\tau).$$

Note that the function $\omega(\tau)$ shares the same coefficients a_k as the shear-rate function, implying that if we were able to expand $\omega(\tau)$ into a $(K\Psi_k)$ series, we could determine the coefficients a_k, then find an approximation of $\dot{\gamma}(\tau)$.

Unfortunately, the functions $(K\Psi_k)(\tau)$ are not orthogonal, making it difficult to numerically compute a_k. Specific procedures such as the Schmidt orthogonalization procedure could be used to derive an orthogonal family of functions from $(K\Psi_k)(\tau)$, but here this involves overly complicated computations. We will envisage another technique based on dual bases. A dual basis of the function basis Ψ_k is a set of functions u_i such that $\int u_i(\tau)(K\Psi_k)(\tau)d\tau = \delta_{ik}$, implying that $a_k = \int \omega(\tau)u_k(\tau)d\tau$. Therefore the crux of the issue lies in the derivation of the dual basis u_k. In the following, we will show that the functions u_k can be built from the functions Ψ_i.

1.3.4 Practical example

Baudez *et al.* (2004) investigated the rheological properties of a polymeric suspension (commercial hair gel made of Carbopol) using a stress-controlled Paar Physica MC1+ rheometer equipped with a Couette geometry ($R_1 = 1.25$ cm and $\beta = 0.26$). In addition they carried out velocity-profile measurements in a similar geometry ($R_1 = 4$ cm and $\beta = 0.44$) using magnetic resonance imaging (MRI) techniques. Further rheometrical tests were also done with a Bohlin CVOR200 rheometer ($R_1 = 0.0125$ cm and $\beta = 0.06$). Carbopol suspensions usually exhibit a viscoplastic behavior (Roberts & Barnes, 2001). MRI techniques made it possible to obtain an accurate estimation of the flow curve and then to compare the different methods.

The data obtained by Baudez *et al.* (2004) are reported in a log-linear plot in Fig. 1.6. They were slightly noisy and a specific procedure was used to denoise and interpolate the raw data. Different nonparametric regression techniques can be used for this purpose: kernel estimator (Hart, 1999), spline smoothing (Wahba, 1990), Fourier series estimator, wavelet regression and shrinkage (Donoho & Johnstone, 1995; Kovac, 1998; Cai, 1999, 2002), Bayesian inference (Werman & Keren, 2001), etc. There is not a universal method because, depending on the noise level, the number of data, and the properties of the function to be recovered, the performance of each method in terms of denoising efficiency can vary significantly. Here, because of the small size of the data samples, the optimized Gasser-Müller kernel method (included in the Mathematica package) was used to denoise and interpolate the data [for details in the implementation, see (Hart, 1999)]. The resulting interpolating curves are plotted in Fig. 1.6.

Figure 1.7 shows the flow curves deduced by the Tikhonov regularization method (dashed line) and the wavelet-vaguelette decomposition method (solid line) for the polymeric gel. For the Tikhonov method, we used the method described in (Yeow *et al.*, 2000) with $n_k = 400$ discretization points and a smoothing parameter $\lambda = 2 \times 10^{-6}$ and 5×10^{-6}. For the WVD method, Daubechies D8 wavelet and the functional formulation were used.

For the polymeric gel, it was possible to independently obtain a reference flow curve by using the velocity profile determined by Baudez *et al.* (2004) using MRI techniques. Indeed, in a Couette geometry, the shear stress distribution across the gap is imposed: $\tau(r) = M/(2\pi r^2)$; the shear rate can be computed by differentiating the velocity profile $v(r)$: $\dot{\gamma}(r) = -r\partial(v/r)/\partial r$. Reporting a parametric plot $(\dot{\gamma}(r),\ \tau(r))$ as a function of the radial distance r makes it possible to have a clearer idea on the flow curve for the material tested. The dots in Fig. 1.7 represent the flow curve determined in this way.

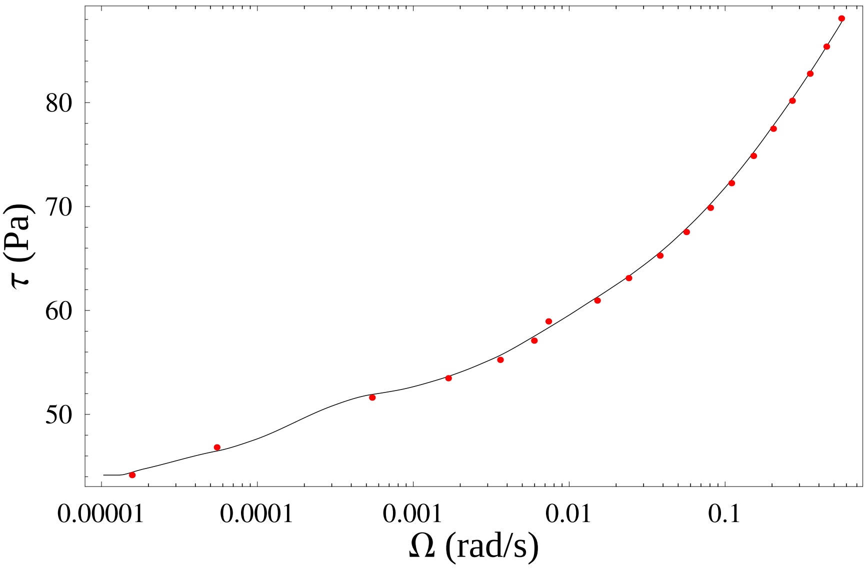

Figure 1.6 *Raw data obtained by Baudez* et al. *(2004) for a polymeric gel (Carbopol). Dots correspond to data while the solid lines represent the curve interpolating the data obtained using the Gasser-Müller kernel method (bandwidth parameter taken at 0.1).*

For the polymeric gel [see Fig. 1.7], the three methods compare well over a shear-rate range covering approximately two orders of magnitude ($5 \times 10^{-2} \leq \dot{\gamma} \leq 20$ s^{-1}), whereas differences can be observed at low and high shear rates. Because of the smoothing constraint imposed on the flow curve in the Tikhonov method, the shear stress drops quickly at low shear rates, leading to an underestimation of the yield stress (estimated at 41 Pa using independent tests). Similarly, at large shear rates, the slight convexity of the flow curve (in a log-linear representation) leads to an undue increase in the shear stress. Because of the absence of regularization constraint in the WVD method, the corresponding flow curve comes closer to the experimental flow curve inferred from MRI Measurements. We can, however, notice the bump for shear rates in the range $10^{-3} - 5 \times 10^{-2}$, which seems not natural. This is probably an artifact caused by the interpolating curve [see Fig. 1.6] since a similar bump is also observable. Additional rotational-velocity data are required to improve accuracy in the low-shear-rate limit.

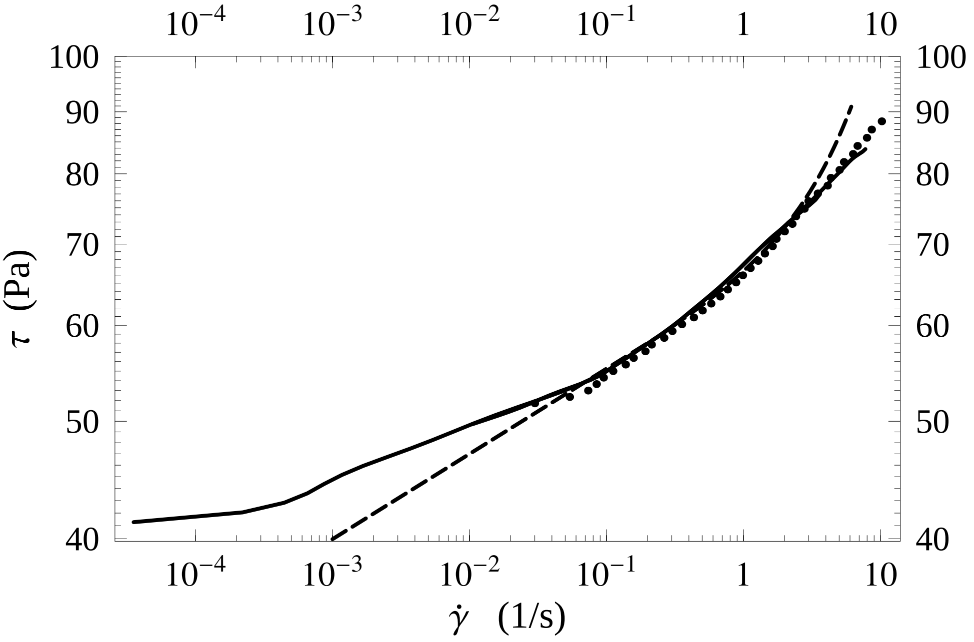

Figure 1.7 *Flow curve for the polymeric gel. The dots represent the flow curve obtained by differentiating the MRI velocity profile. The dashed lines represent the flow curves obtained using the Tikhonov method [smoothing parameter* $\lambda = 2 \times 10^{-6}$*]. The solid lines represent the flow curve determined using the WVD method.*

1.4 Rheometers and rheometrical procedures

In shear flows, the stress distribution is fully characterized when we know the shear stress $\tau = \sigma_{xy}$ and the normal stresses σ_{xx}, σ_{yy}, and σ_{zz}. A familiar and equivalent characterization is based on the use of the normal stress differences

$$N_1(\dot{\gamma}) = \sigma_{xx} - \sigma_{yy} \text{ and } N_2(\dot{\gamma}) = \sigma_{yy} - \sigma_{zz},$$

which makes it possible to get rid of the pressure term (recall that $\sigma_{xx} = -p + s_{xx}$, where s_{xx} is the extra stress).

The bulk viscosity is

$$\mu(\dot{\gamma}) = \frac{\tau}{\dot{\gamma}}.$$

Similarly, we introduce the normal-stress coefficients

$$\Psi_1 = \frac{N_1}{\dot{\gamma}^2} \text{ and } \Psi_2 = \frac{N_2}{\dot{\gamma}^2}.$$

$\rightsquigarrow$ We want to determine $\mu = f(\dot{\gamma})$ (*viscosity curve*) or equivalently $\tau = f(\dot{\gamma})$ (*flow curve*). In addition, normal stress differences may be of importance. Most often only $N_1(\dot{\gamma})$ can be measured (e;g., with a cone-plane rheometer).

1.4.1 How to determine the flow curve?

Manual or automatic procedure?

Most rheometers are now controlled by a computer, which also provides additional softwares for computing the flow curve automatically. When the experimentalist has a sufficiently good knowledge of the rheological properties of the material tested and the viscometric geometry used in the testing is standard, these softwares are very helpful.

For complex materials or for non-standard geometries, it is usually better to directly extract the measurement data (torque, rotational velocity) and use specific methods to determine the flow curves, which makes it possible:

- to use a specific experimental protocole in data acquisition or processing;
- to modify the data to take disturbing phenomena into account;
- to obtain more accurate solutions (e.g., in the inverse problem for wide-gap rheometers, by controlling the smoothness of the solution sought).

For complex fluids (the general case for natural fluids studied in geophysics and in industry), rheometry is far from being an ensemble of simple and ready-for-use techniques. On the contrary, investigating the rheological properties of a material generally requires many trials using different rheometers and procedures. In some cases, visualization techniques (such as nuclear magnetic resonance imagery, transparent interstitial fluid and tools, birefringence techniques) may be helpful to monitor microstructure changes.

How to measure the flow curve?

In most modern rheometers, the standard technique involves imposing a step-like *ramp*, i.e., a succession of stress steps (respectively, strain steps), and measuring the resulting deformation (respectively, stress). It is difficult to prescribe the duration of each step in advance because it basically depends on how quickly the material reaches its steady state.

Plotting the data

The data obtained by using a rheometer usually cover a wide range of shear rate, typically 3 or more orders of magnitude. For this reason, it is usually recommended to plot the data on a logarithmic basis. When the data are plotted, different things can be done:

- simple mathematical expressions can be fitted to the data, e.g., a power-law relation: $\tau = K\dot{\gamma}^n$;
- a yield stress can be evaluated by extrapolating the experimental curve to $\dot{\gamma} = 0$ and give an apparent intercept on the τ-axis that can be interpreted as a yield stress.

Note that the flow curve $\tau = f(\dot{\gamma})$ can be plotted as:

- shear stress as a function of shear rate
- bulk viscosity $\mu = \tau/\dot{\gamma}$ as a function of shear rate

Recall that the units used in viscometry are the following

- strain in %
- stress in Pascal [Pa] 1 Pa = kg×m^2×s^{-2}
- shear rate in 1/s (and not Hertz)
- dynamical viscosity μ in [Pa.s] 1 Pa.s = kg×m^2×s^{-1} (avoid Poise, centiPoise, etc.)
- density ϱ in [kg/m^3]
- dynamical viscosity $\nu = \mu/\varrho$ in [m^2/s] (avoid Stokes, centiStokes [cS], etc.)

1.4.2 Stress/strain step

Basic experiments and probably the simplest we can think of is (see Figure 1.8)

- to suddenly exert a stress on a material at rest over a sufficiently long time, then to measure the strain output after flow cessation: *recovery* test.

- to suddenly exert a stress on a material at rest over a sufficiently long time, then to measure the strain output after flow inception: *creep* test.
- to suddenly impose a steady shear flow, then to monitor the stress variation with time to determine how the shear stress reaches its steady value: *stress growth* test.
- to suddenly impose a steady shear flow, keep it constant over a given time interval, then cease the flow and monitor the stress variation with time after flow cessation (fluid at rest): *stress relaxation* test.
- to realize a steady shear flow over a given time interval, then remove the shear stress and monitor the strain variation with time: *constrained recoil* test. A viscoelastic material recoils because of elasticity, whereas a Newtonian fluid stops immediately.

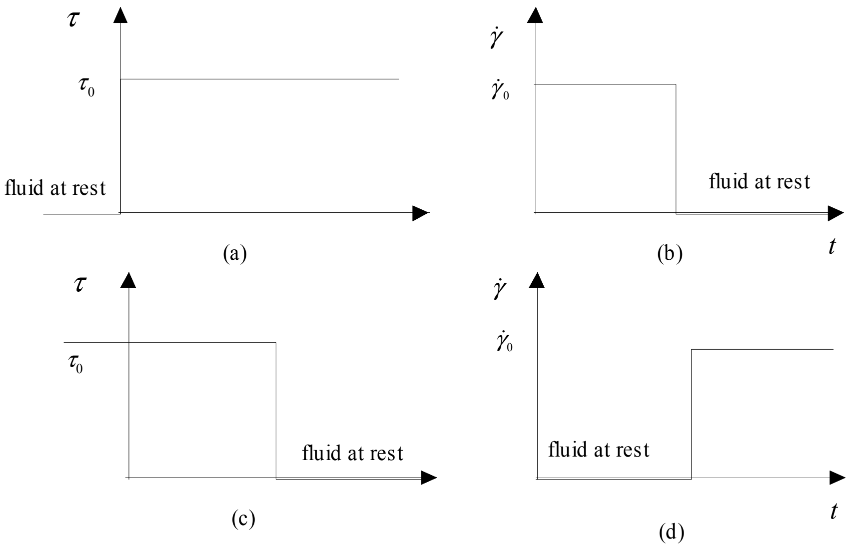

Figure 1.8 *Basic tests: (a) Creep. (b) Stress relaxation. (c) Recovery. (d) Stress growth.*

Plotting the time variation of the output signal makes it possible to exhibit some fundamental properties such as viscoelasticity or thixotropy (see below). Figure 1.9 shows the typical response for a Newtonian fluid (solid line) and a non-Newtonian fluid (dashed line). For both materials, the shear stress tends towards a limiting value, which means that the material has reached a new equilibrium (steady state). However, how the stress reaches this limiting value differs depending on the material:

- for a Newtonian fluid, the stress reaches its steady state quasi instantaneously;
- for a non-Newtonian fluids, it is common to observe an overshoot, then a decrease towards the steady value.

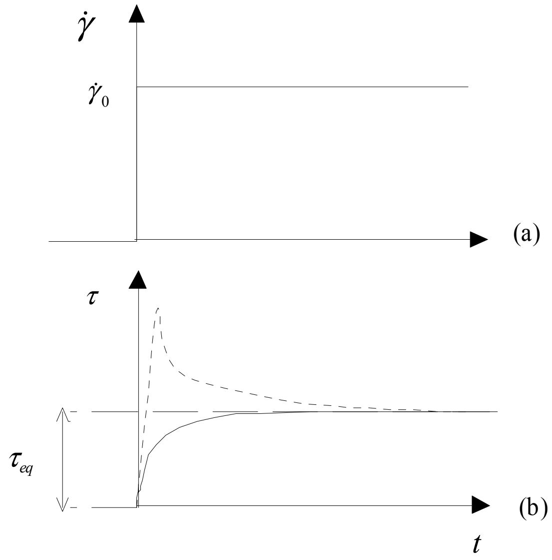

Figure 1.9 *Stress growth: shear rate imposed at* $t = 0$ *and stress response measured upon flow inception. (a) Input: constant shear rate imposed at* $t = 0$*. (b) Output: time variation of* τ *monitored upon flow inception. How the shear stress reaches the steady-state value* τ_{eq} *depends on the rheological properties: the typical response of a Newtonian fluid (solid line) and a visco-elastic material (dashed line) is depicted.*

For a non-Newtonian fluid, the *overshoot* can be understood as follows: when the material has a structure on the microscopic scale (e.g., polymers connection, particle network, etc.), deforming the material implies that the structure must be re-organized, e.g., by breaking contacts between particles in close contact for a suspension: more energy must be provided to the system for it to reach a new equilibrium. For a thixotropic material, the time needed to reach this equilibrium depends on the previous states (intensity of the shear rate, duration of the resting procedure).

1.5 Typical rheological behaviors

1.5.1 Outlining a flow curve

The *flow curve* is the relation between the shear rate $\dot{\gamma}$ and shear stress τ established from experimental measurements taken in a viscometric flow (i.e., meaning that a simple shear flow was realized by appropriate means and that we are able to derive the $\dot{\gamma} - \tau$ curve). On many occasions, the flow curve is represented in the form

$$\mu = \frac{\tau}{\dot{\gamma}} = f(\dot{\gamma}),$$

where f is a function that we want to characterize.

1.5.2 Shear-thinning/thickening

Many fluids exhibit the same kind of behaviour (see Fig. 1.10):

- at low shear rates, the viscosity is constant and we say that the viscosity lies in the Newtonian plateau;
- for increasing shear rate, the viscosity decreases (i.e., $f'(\dot{\gamma}) < 0$), the behavior is said to be *shear-thinning*. On a log-log plot, this trend is represented by a straight line when the fluid behavior can be described with a *power-law model* $f(\dot{\gamma}) = K\dot{\gamma}^n$, with $n < 1$ the *power-law index* and K the *consistency*;
- at high shear rates, the viscosity curve may start flattening out and reach another plateau.

On rare occasions, the viscosity is seen to increase with shear rates and in that case, the behavior is said to be *shear-thickening*[4].

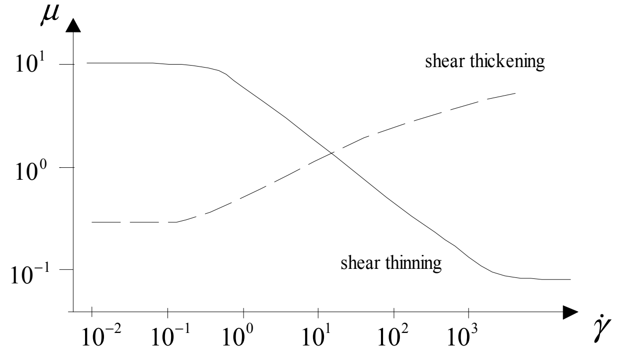

Figure 1.10 *Sketch of a shear-thinning/thikening flow.*

The Cross model is well appropriate for fitting shear-thinning fluids with two plateaux

$$\frac{\mu - \mu_\infty}{\mu_0 - \mu_\infty} = \frac{1}{1 + K\dot{\gamma}^n},$$

with μ_0 and μ_∞ the viscosities at low and high shear rates. Other similar models are the Carreau model

$$\frac{\mu - \mu_\infty}{\mu_0 - \mu_\infty} = \frac{1}{(1 + K\dot{\gamma}^2)^m},$$

and the Sisko model (a simplified version of the Cross model when $\mu_0 \gg \mu_\infty$)

$$\mu = \mu_\infty + \frac{\mu_0}{K\dot{\gamma}^n} \text{ or } \tau = \mu_\infty + \frac{\mu_0}{K}\dot{\gamma}^{1-n}.$$

---

[4] Not to confuse with dilatancy since in the past, the two expressions were used with same meaning.

1.5.3 Yield stress

Definition

For some fluids, the flow curve when plotted in the $\dot{\gamma} - \tau$ plane exhibits a *yield stress*: when the rate is decreased towards zero, the shear stress tends towards a constant value. Although extrapolating to zero is not possible when working in log-log plot, a common practice is to consider the limiting stress as a yield stress, i.e. the stress threshold below which there is no motion ($\dot{\gamma} = 0$). As shown in Fig. 1.11, the idea is to extrapolate the experimental trend towards $\dot{\gamma} = 0$. There are many problems around the interpretation of the yield stress determined in this way [e.g. see papers in the Journal of Rheology echoing the debate around the relevance of the yield stress (Harnett & Hu, 1989; Astarita, 1990; Evans, 1992; de Kee & Chan Man Fong, 1993; Spaans & Williams, 1995; Barnes, 1999)]. Care must taken in defining the yield stress as the intercept of the extrapolated flow curve with the τ-axis, especially when the experimentalist uses a rheometer with a limited range of shear rates (typically in excess of 0.1 s^{-1}). Additional tests are recommended (typically creeping test with a controlled-stress rheometer).

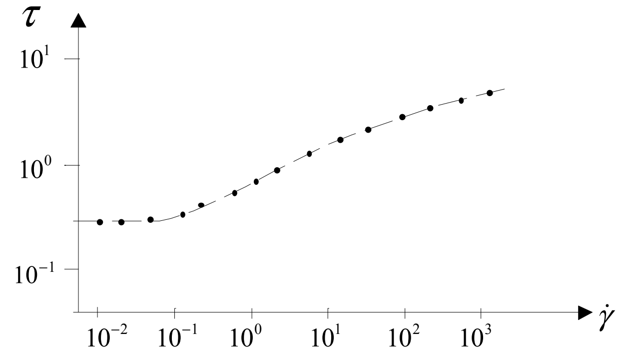

Figure 1.11 *Sketch of a flow curve representative of a yield-stress fluid. Dots represent data and the dashed line the interpolation curve extrapolated towards* $\dot{\gamma} = 0$.

Viscoplastic models

Mostly the *Bingham model* is used to interpolate the data

$$\tau = \tau_c + K\dot{\gamma},$$

with τ_c the yield stress and K a parameter called consistency. A more sophisticated model is the *Herschel-Bulkley model*, which takes nonlinear shearing effects into account

$$\tau = \tau_c + K\dot{\gamma}^n,$$

where $n < 1$ in most cases. Another candidate is the *Casson model*

$$\sqrt{\tau} = \sqrt{\tau_c} + \sqrt{K\dot{\gamma}}.$$

Accurate experimental procedure

Extrapolation of rheometrical data is not recommended to estimate the yield stress. When possible, it is better to use direct tests such as the following trial-and-error procedure:

- a low shear stress is imposed to the sample and the resulting deformation is measured. If there is no yielding, the deformation tends toward a limiting value at long times ;
- when the shear stress imposed is in excess of the yield stress, a constantly rising deformation is observed and the growth rate is the bulk viscosity

The game consists in finding the yield stress by applying successive stress levels to the sample.

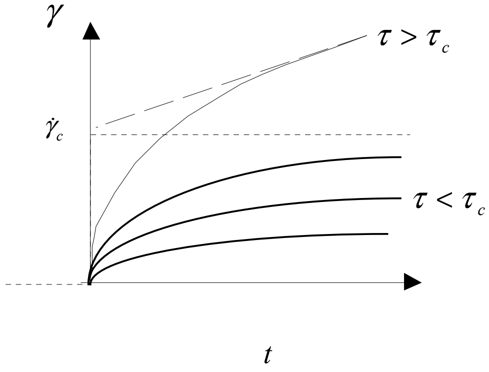

Figure 1.12 *Sketch of the strain variation with time depending on the stress level.*

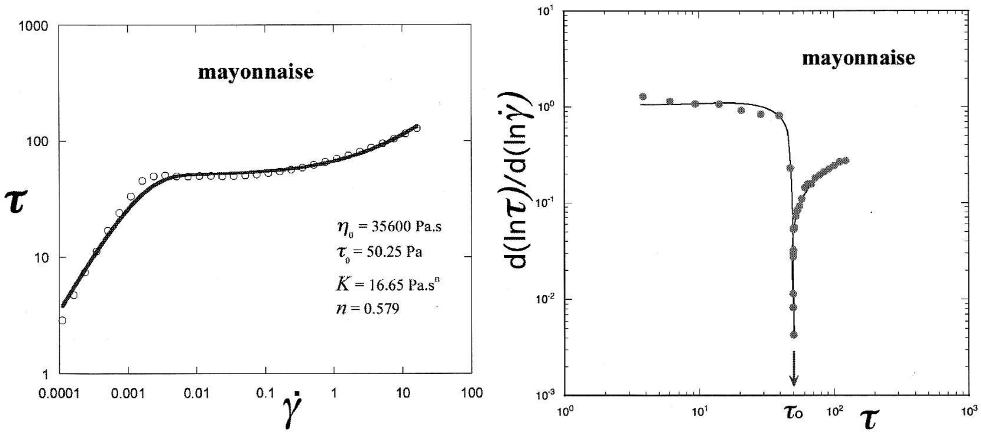

(a) (b)

Figure 1.13 *(a) Flow curve of a mayonnaise sample. (b) Estimation of the yield stress. After (Mendes & Dutra, 2004).*

Another method proposed by Mendes & Dutra (2004) involves plotting

$$\frac{\mathrm{d}\ln\tau}{\mathrm{d}\ln\dot{\gamma}} = \frac{\dot{\gamma}}{\tau}\frac{\mathrm{d}\tau}{\mathrm{d}\dot{\gamma}},$$

as a function of τ. The yield stress position is given by a sharp peak in the curve. An example is provided in Fig. 1.13.

1.5.4 Viscoelasticity

Partitioning materials into fluids and solids is an idealized view. Depending on the typical timescale, a material can be considered as a solid (e.g., exhibiting an elastic behavior) or a fluid. For instance, over 'short' timescales, a glacier is a solid, whereas at long timescales (e.g., several years), it behaves like a liquid. This constat leads many rheologists to state that everything flows, even solids flow, but very slowly. To reconcile this paradoxical absence of differences between what we usually call 'solids' and 'fluids', it is helpful to introduce the notion of relaxation time: the *relaxation time* is the characteristic time needed for a material to flow. In reference to Deborah in the Bible, rheologists also introduce the Deborah number, which is the ratio between the characteristic time/duration of an observation/experiment $t_{obs.}$ and the relaxation time t_r

$$De = \frac{t_{obs.}}{t_r}.$$

When $De \ll 1$, the observer/experimentalist has not the time to register any fluid/creep motion and the material behavior can be considered as solid. When $De \gg 1$, the material has time to relax and modify its structure as a response to the applied forces; the material behaves like a fluid.

Using this definition and using usual timescales for observation/experiments, most materials belong to either the solid or fluid classes. However, for some materials, the Deborah number is of order of unity, which means that the material can exhibit both solid and fluid properties. Viscoelasticity is a typical trait of materials exhibiting fluid/solid properties.

Linear viscoelasticity

In most textbooks and courses on rheology, the simplest way to introduce the notion of viscoelasticity is to make use of analogies with simple mechanical models consisting of springs (elastic behavior) and dashpot (viscous behavior). These analogues make it possible to have some conceptual insight into the physical behavior of complex materials by breaking down the dissipative viscous processes (time-dependent) and energy-storage processes. Two basic ingredients are used

- spring: according to Hooke's law, the strain γ is proportional to the applied stress τ, which reads

  $$\tau = G\gamma,$$

  with G the elastic modulus. Note that: (i) for a given stress, there is a limiting deformation $\gamma = G^{-1}\tau$, (ii) the behavior is independent of time. Physically, elastic elements represent the possibility of storing energy. This storage can be achieved by different processes (e.g., polymer recoil).
- dashpot: the response of the dashpot, the plunger of which is pushed at the velocity $\dot{\gamma}$ is

  $$\tau = \mu\dot{\gamma},$$

  where μ is the viscosity. Note that if we switch on a stress τ, the material response is immediate and the deformation rate is proportional to the applied rate. Physically, dashpots represent dissipative processes that occur as a result of the relative motion between molecules, particles, or polymer chains. This motion induce friction when there is contact between elements or viscous dampening if there is an interstitial fluid.

The simplest representation of a visco-elastic fluid is to combine a spring and a dashpot in series and this combination is called the *Maxwell* model. If the two elements are mounted in parallel, the combination is called a *Kelvin-Voight model* and is the simplest representation of a viscoelastic solid. There are a number of possible combinations of these two elementary models, the simplest one is the *Burgers model*, which is the association of a Maxwell and Kelvin-Voight models. These models are empirical in essence; experimentation showed that these simple models capture the basic properties of a number of viscoelastic materials, but they have their limitations.

Maxwell model. – Let us consider the response given by a Maxwell model: since the spring and the dashpot are in series, the total deformation is the sum of the elementary deformation. We deduce

$$\frac{\mathrm{d}\gamma}{\mathrm{d}t} = \frac{1}{G}\frac{\mathrm{d}\tau}{\mathrm{d}t} + \frac{\tau}{\mu},$$

whose general solution is

$$\tau(t) = Ke^{-\frac{Gt}{\mu}} + \int_{-\infty}^{t} Ge^{\frac{G(t'-t)}{\mu}}\dot{\gamma}(t')\mathrm{d}t',$$

where K is an integration constant, the lower boundary in the integral is arbitrary. If we require that the stress in the fluid is finite at $t = -\infty$, then we must set $K = 0$. Note that:

- for steady state, this equation simplifies to the Newtonian equation $\tau = \mu\dot{\gamma}$;
- for sudden changes in stress, the time derivative dominates;
- the general solution can be cast into the following form

$$\tau(t) = \int_{-\infty}^{t}\left[\frac{\mu}{t_r}e^{\frac{t'-t}{t_r}}\right]\dot{\gamma}(t')\mathrm{d}t' = \int_{-\infty}^{t}\Gamma(t-t')\dot{\gamma}(t')\mathrm{d}t,$$

where $t_r = \mu/G$ is a relaxation time. The term within the brackets is called the *relaxation modulus* and the integral takes the form of a convolution product of $\Gamma(t) = \mu e^{-t/t_r}/t_r$ and $\dot{\gamma}$. When written in this form, the Maxwell model says that the stress at the present time t depends on the strain rate at t as well as on the strain rate at all past time t' but to within a weighting factor that decays exponentially. This is the simplest representation of *fading memory.* This way of representing the stress is particularly interesting because the integrands is written as the product of two functions: the first one Γ represents the fluid properties, while the second depends on the nature of the flow (via the shear rate). All generalized viscoelastic models are specified in this form.

If we apply this model to the creep testing (see below), the deformation is described by the curve

$$\gamma = \tau\left(\frac{1}{G} + \frac{t}{\mu}\right).$$

Kelvin-Voight model. – The deformation is described by the curve

$$\gamma = \frac{\tau}{G}\left(1 - e^{-\frac{t}{t_r}}\right),$$

where $t_r = \mu/G$ is once again the relaxation time.

Burgers model. – The deformation is described by the curve

$$\gamma = \tau\left(\frac{1}{G_1} + \frac{1}{G_2}\left(1 - e^{-\frac{t}{t_r}} + \frac{t}{\mu_1}\right)\right),$$

where $t_r = \mu_2/G_2$ is the relaxation time.

Creep testing

The simplest test we can imagine is the creeping test: a constant stress is suddenly applied to the material and the strain variation with time is then monitored. The ratio

$$J(t) = \frac{\gamma(t)}{\tau},$$

is usually referred to as the *compliance.*

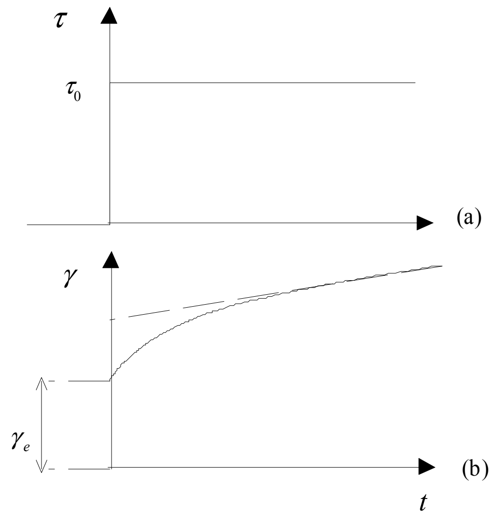

Figure 1.14 *(a) stress variation impose to the sample (b) strain measured as a response to the stress input.*

The typical response can be broken into different phases:

– immediate elastic response;
– delayed elastic response (glassy behavior), where the deformation rate becomes increasingly slow, but ends up as a slow steady-state deformation at long times;
– the steady-state viscous regime, when the material is in steady flow, with constant shear rate (the response curve is a straight line in a plot $\gamma(t)$.

The main features of this common behavior are captured by the Maxwell model (immediate elastic response + steady state behavior) or Burgers model (delayed response is also described).

Oscillatory test

Instead of conducting creeping tests over a range of time, we can run oscillatory shear experiments over a range of frequency. The basic idea is to apply a sine-wave-shaped strain (resp. stress) and measure the resulting stress (resp. strain). For instance, if we impose the deformation (here expressed in a complex form)

$$\gamma(t) = \gamma_0 \Re\left(e^{\imath\omega t}\right),$$

where γ_0 is the strain amplitude (real and positive) and ω the frequency, this means that the shear rate is also imposed

$$\dot{\gamma}(t) = \omega\gamma_0 \Re\left(e^{\imath(\omega t+\pi/2)}\right),$$

where $\dot{\gamma}_0 = \omega\gamma_0$ is the shear rate amplitude.

We measure a material response, which takes the form

$$\tau(t) = A(\omega)\gamma_0 \Re\left(e^{\imath(\omega t+\delta)}\right),$$

where δ is the phase shift, or equivalently

$$\tau(t) = B(\omega)\dot{\gamma}_0 \Re\left(e^{\imath(\omega t-\phi)}\right),$$

relative to the shear rate, with $\phi = \pi/2 - \delta$. For small deformations, the shear stress is assumed to oscillate with the same frequency, but not necessarily in phase:

$$\tau = \Re\left(\tau_0 e^{\imath\omega t}\right),$$

where it is worth noticing that the shear stress amplitude τ_0 is in general complex. It is customary to rewrite the outcome signal by breaking down the in-phase and out-of-phase contributions:

$$\tau_0 = -\imath G^* \gamma_0 \Rightarrow \tau = G'(\omega)\gamma_0 \sin \omega t + G''(\omega)\gamma_0 \cos \omega t,$$

or, in terms of shear rate,

$$\tau_0 = \eta^* \dot{\gamma}_0 \Rightarrow \tau = \eta'(\omega)\dot{\gamma}_0 \cos \omega t + \eta''(\omega)\dot{\gamma}_0 \sin \omega t,$$

with $G^* = G' + \imath G''$ the *complex modulus* and $\eta^* = \eta' - \imath\eta''$ the *complex viscosity.*

It is straightforward to deduce the following relations:

$$G^* = -\imath\omega\eta^*,$$

$$A = \sqrt{G'^2 + G''^2} \text{ and } B = \sqrt{\eta'^2 + \eta''^2},$$

$$\tan\delta = \frac{G''}{G'} \text{ and } \tan\phi = \frac{\eta''}{\eta'}.$$

There is a close correspondence between creeping and oscillatory tests:

- short times correspond to high frequency and usually an elastic response is observed
- behavior at long times is given by low frequencies and is usually of viscous type.

How to interpret the G' and G'' curves? In breaking down the output signal, we introduce functions that are directly related to

- the solid behavior, which is in phase with input signal. The function $G'(\omega) = \omega\eta''$ (in absolute value) is called the *storage modulus* since it reflects relaxation times and elastic modulus. For a perfectly elastic solid, we have $G' = G$ and $G'' = 0$;
- the liquid behavior, which is out of phase (offset of $\pi/2$) relative to the input signal. The function $G''(\omega) = \omega\eta'$ is called the *loss modulus* and characterizes the viscous behavior; it gives information about the (viscous) dissipation in the flow. For a perfectly Newtonian fluid, we have $\eta' = \mu$ and $\eta'' = 0$.

Experimentally we can plot the two curves $G'(\omega)$ and $G''(\omega)$ or equivalently $\eta'(\omega)$ and $\eta''(\omega)$. Sometimes, other quantities characterizing the rheological behavior such as $|G^*|$ or $|\mu^*|$ are also used in graphical representations.

What do we learn from oscillatory tests?

Each community in rheology has its own habits. In polymer science, using oscillatory data is quite common, whereas in the rheology of particle suspension, emphasis is usually given to creeping tests.

Figure 1.15 shows a typical example of variations of G' and G''. More information can be inferred from these curves, as shown below.

A number of interesting properties can be pinpointed by looking at G' and G'' curves:

- when $\omega \to 0$ (recall that $\omega \to 0$ corresponds to long time responses in the time domain), $G'' \approx \mu_0\omega$ since elastic effects are negligible compared to viscous effects at long times, which makes it possible to measure the viscosity at low shear rates. Note that we have always

  $$\eta'(\omega)_{\omega\to 0} = \mu(\dot{\gamma})_{\dot{\gamma}\to 0},$$

  which implies that $G'' = \eta'\omega$ tends towards 0 and is asymptotic to $\mu(\dot{\gamma})_0\omega$ (where $\mu(\dot{\gamma})_{\omega\to 0} = \mu(\dot{\gamma})_{\dot{\gamma}\to 0}$).

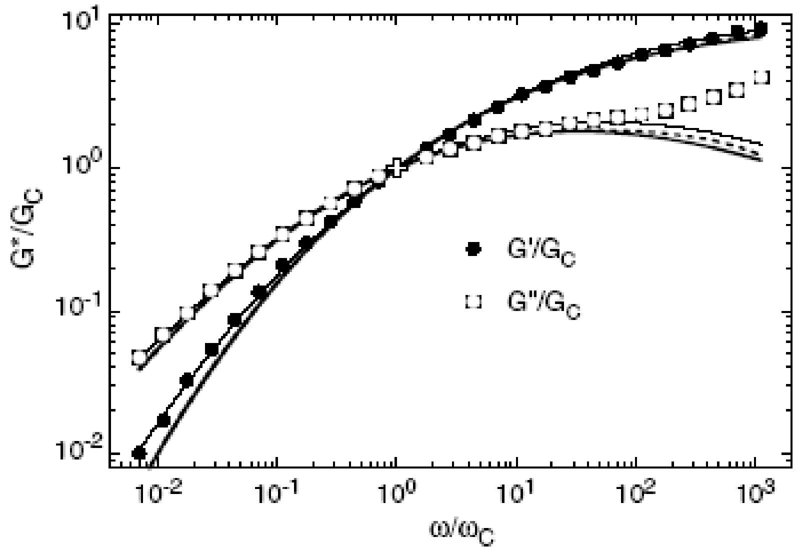

Figure 1.15 *Polysterene dynamic moduli. Points: experimental data from (Guzmán et al.,* Rheol. Acta **44** *(2005) 342 –351). Crossover ($\omega_C = 0.09$ rad/s, $G_C = 23.2$ kPa).*

- We usually observe that the ratio of the storage modulus to ω^2

$$\frac{\eta''}{\omega} = \frac{G'}{\omega^2}$$

  tends towards a finite limit when $\omega \to 0$.
- For a number of polymeric liquids (e;g., dilute polymer suspensions), it is quite customary to observe that :

$$\omega \to \infty,\ \eta' \to \eta'_\infty \text{ and } \eta'' \propto \omega^{-1}$$

  where η'_∞ is slightly larger than the solvent viscosity. This is not an absolute rule.
- the cross-over frequency at which $G' = G''$ provides an estimate of the longest relaxation time (in s/rad).
- There is an empirical relation referred to as the *Cox-Merz rule*, that relates the viscosity $\mu(\dot\gamma)$ and the magnitude of the complex viscosity $\eta^*(\omega)$. In short, this rule predicts that the magnitude $|\eta^*(\omega)|$ is equal to the viscosity at corresponding values of shear rate and frequency

$$|\eta^*(\omega)| = |\eta^*(\omega \to \dot\gamma)| = \eta'(\omega \to \dot\gamma)\sqrt{1 + \left(\frac{\eta''}{\eta'}\right)^2}$$

  This rule provides a good approximation mostly for polymers. Its use for concentrated suspensions has also been discussed (Doraiswamy *et al.*, 1991; Geissle & Hochstein, 2003).
- There is an equivalent of the Cox-Merz rule for normal stress, which is called *Laun's rule.* This rules states that the material function $\Psi_1 = N_1/\dot\gamma^2$ is well approximated by

$$\Psi_1 = \frac{N_1}{\dot\gamma^2} = \frac{2\eta''(\omega)}{\omega}\left[1 + \left(\frac{\eta''}{\eta'}\right)^2\right]^{7/10},$$

by replacing ω with $\dot\gamma$. This rule originates in the behavior of G'' when $\omega \to 0$ (see above).

Figure 1.16 *Weissenberg effect. Photo from Gareth McKinley's group at MIT.*

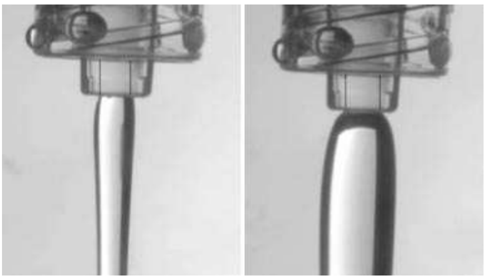

Figure 1.17 *Die swell effect. Photo from Gareth McKinley's group at MIT.*

1.5.5 Normal stress effects

Manifestation

There are many situations where normal-stress effects occur and give rise to specific phenomena. Note that these effects are typical for non-Newtonian (e.g., viscoelastic fluid) fluids. Here are some typical examples:

- Weissenberg effect or rod-climbing: when rotating in a fluid contained in a container, a cylinder disturbs the free surface shape differently depending on whether the fluid is Newtonian or not. For a Newtonian, centrifugal forces induces dipping (fluid expelled from the cylinder vicinity), whereas for elastic fluids, the fluid climbs along the cylinder (see figure 1.16).
- Die-swell effect: when an elastic fluid flows out of a tube, it swells as a result of normal stress effects, whereas for a Newtonian fluid, there is usually a contraction or the surface remains straight.

A number of odd phenomena are also observed in the development of instabilities in elastic fluids (Shaqfeh, 1996; Boger & Walters, 1993).

Origin

Normal stress effects are common with polymeric fluids and in this case, they are usually caused by the relaxation of polymer coils, which had been extended earlier. For instance, in a simple shear flow such as a flow through a die, the polymers are stretched along an elongational axis (direction of the flow), which creates additional tension in this direction due to chain elasticity. This extra tension is proportional to the elongation, which in turn is proportional to the shear rate $\dot{\gamma}$ and since the normal stress for elastic polymers is dependent on both the elongation and shear rate, we expect a quadratic dependence of the normal stress difference on the shear rate. This scaling is observed experimentally (Bird *et al.*, 1987).

Other materials such as particle suspensions may exhibit non-zero stress differences. In that case, the normal stress effect reflects a nonsymmetric stress field due to an anisotropic structure and/or complex interactions. For instance, a compacted granular medium exhibits clearly normal stress differences due to nonsymmetric force distribution within a particle network (e.g., see Fig. 3.5 in Chap. 3) (Wieghardt, 1975). Another example is provided by suspensions of non-colloidal particles, which exhibit specific particle arrangements that result in the normal stress differences (Brady & Morris, 1997; Zarraga *et al.*, 2000).

Measurement

The normal stresses or normal stress differences can be measured in a number of ways. For instance, we have seen that when a fluid flows down an inclined channel, its free surface can be slightly convex because of the normal stress difference (if the tension surface is negligible) and measuring the shape of the free surface in the cross-stream direction makes it possible to evaluate the first normal stress difference (see also pp. 102–105, Tanner, 1988). Similarly, the flow-depth profile in the rod-climbing experiment or the die swelling when extruding polymers can be used to measure normal stresses. In the latter case, Tanner (1988) shows that the ratio of the jet diameter (D_j) and the capillary diameter (D) is connected to the following stress combinations via the approximate relation

$$\frac{D_j}{D} = 0.1 + \left(1 + \frac{1}{2}\left(\frac{\sigma_{zz} - \sigma_{rr}}{2\tau}\right)^2\right),$$

for elastic polymers.

In practice, the cone-and-plate geometry is commonly used to measure the first normal stress difference. We can express the first normal coefficient as

$$\Psi_1 = \frac{2}{\pi}\frac{F}{R^2\omega^2}\varphi^2,$$

where the thrust exerted by the fluid on the cone is denoted by F, the cone angle is denoted by φ, its diameter is R, and ω is the rotational velocity of the geometry.

1.5.6 Thixotropy

Definition

Thixotropy[5] refers to the property of a material such that

- when it flows, its rheological properties vary strongly with shear rate (considerable shear thinning);
- when it is left at stand (after flow cessation), it retrieves its initial consistency (solid-like behavior) and properties.

Note that there is no strict consensus within the rheologist community concerning this definition (Barnes, 1997). For a number of people (especially in industry), thixotropy means extreme shear thinning and conferring this property to manufactured slurries such as paints is highly desirable.

Manifestation

In 1923, Schalek and Szegvari found that aqueous iron-oxide “gels have the remarkable property of becoming completely liquid through gentle shaking alone, to such an extent that the

---

[5] Coined from the Greek words $\tau\eta\iota\chi\iota\sigma$ (stirring or shaking) and $\tau\rho\epsilon\pi o$ (turning or changing).

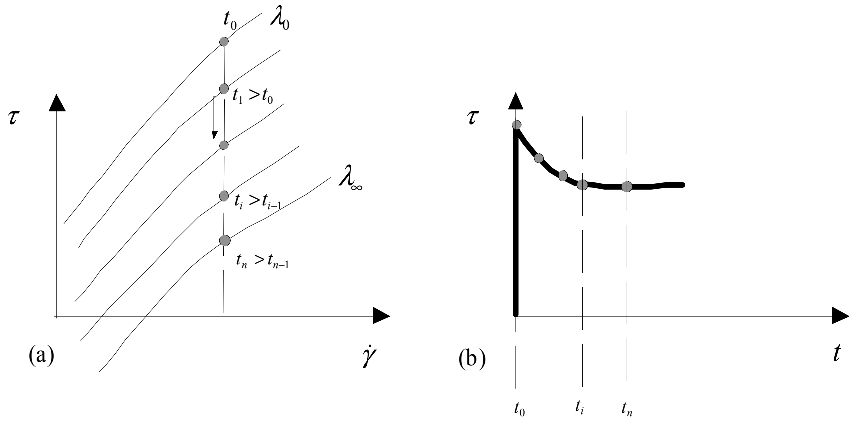

Figure 1.18 *Time decrease in shear stress: because the flow curve actually depends on the microstructure (represented here via a microstructural parameter (a), then the shear stress varies with time before eventually its steady-state value (b).*

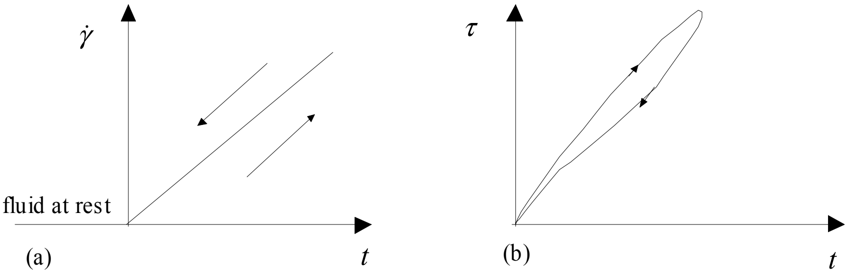

Figure 1.19 *Thixotropy loop.*

liquified gel is hardly distinguishable from the original sol. These sols were liquified by shaking, solidified again after a period of time. . . the change of state process could be repeated a number of times without any visible change in the system" (cited in Barnes, 1997). It was believed that a new kind of phase change had been found. The first manifestation of thixotropic materials is thus the fluidization of the material, a kind of yoghurt effect: when one vigorously mix a yoghurt with a spoon, the consistency alters quite abruptly.

There are several clues that can lead to thinking that a material is thixotropic:

- If we apply a constant shear rate to thixotropic material, the shear stress measured (or, equivalently, viscosity) decreases with time and it will eventually reach a limiting steady value. First this is an overshoot in the shear-stress response, then a slow decrease [see Fig. 1.18(b)]. However, the peak value depends on how carefully or vigorously the material was initially loaded into the rheometer and how long it was left to rest before shearing.
- When applying an increasing shear rate to a material, then at a given by reversing the shear rate [see Fig. 1.19(a)], one can observe a loop in the time record of stress. Some rheometers propose a special function for measuring thixotropy (by measuring the loop area), but in fact, the actual loop area depends on a number of parameters (duration of each shear-rate increment, buildup rate, etc.), which makes it difficult to propose a proper interpretation of this test.

Physical origin

Almost all materials that are shear thinning are thixotropic because it takes a finite time to bring about the rearrangements needed in the microstructural elements that result in shear thinning. Typical examples include clays and soil suspensions, creams, drilling muds, flour sus-

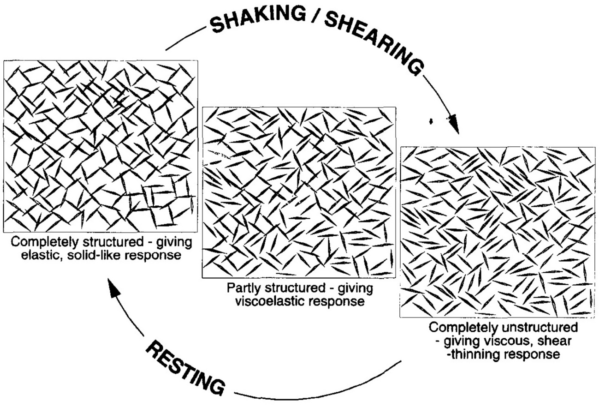

Figure 1.20 *Thixotropy as the manifestation of microstructure influence on bulk rheological behavior. After Barnes (1997).*

pensions, fibre greases, jellies, paints, etc. Three ingredients are usually required to observe a thixotropic behavior (see 1.20):

- a material made up of "structures" that progressively break down on shearing (or shaking);
- a reversible process that implies that the "structuration" of the material lost after flow inception is retrieved when the material has been left at rest for a sufficiently long time. Thus, shearing induces loss of the initial order (at rest), while resting implies rebuilding;
- the timescales characterizing each phase (structure breakdown/rebuiling) are not equal, with usually a characteristic time ranging from a few milli-seconds to a few minutes for the structure breakdown, whereas the rebuilding timescale is of order of a few hours to several days.

Indeed, when at rest, a material possesses a structure that maximalizes the shear strength (both for viscous and elastic processes): there is no order in the spatial distribution of particles and the number of contacts between particles is large. On shearing, particles start aligning, the number of contact between neighboring particles decreases, the particle spatial distribution is asymmetrical in the flow direction.

Characterization

▲ Be careful and remind that some disturbing effects (e.g., slipping) can produce effects similar to thixotropic effects.

▲ A thixotropic material is highly dependent on its past history, especially the deformation history. In theory, if we wait a sufficiently long time, a material at rest has recovered its initial state (e.g., random structure). In practice, one can define an arbitrary initial state (which does not necessarily correspond to a resting/equilibrium state) by applying high shear rates to complete break down the inner structure, then leaving the material at stand for a given time. Proceeding with the material in this way makes it possible to have the same initial state as many often as desired.

▲ When testing the rheological response of a material, it can be recommended to test it within a homogenous flow, i.e. within a flow where the shear rate is constant and uniform at any point and time. In the converse case, the state of the material being dependent on shear-rate, its local response may differ significantly depending on the position in the flow. Let us take the example of a parallel-plate rheometer, we have $\dot{\gamma} = 0$ at $r = 0$, which implies weak breakdown in the vicinity of the central axis, whereas at the periphery, the material is fully disorganized.

We suggest the following procedure:

1. Let us assume that we start from a well-specified initial state, the material being at rest. We apply a constant shear rate $\dot{\gamma}_0$ [see Fig. 1.21(a)] and measure the shear stress.
2. On applying a shear rate, the inner structure is disorganized, which requires energy. This is reflected by a shear-stress overshoot, which is followed by a slow decrease towards a limiting value corresponding to the new equilibrium induced by the new strain rate [see Fig. 1.21(b)] if we wait a sufficiently long time.
3. If we remove the shear rate, the shear stress drops to zero instantaneously (no viscoelasticity).
4. After a resting time, we apply the same rate as earlier, but since the inner structure was altered, less energy is needed to break the particle network or realign the particles, which implies that the shear-stress overshoot is less pronounced and the steady state is reached more quickly [see Fig. 1.21(b)].
5. If the overshoot is denoted by $\Delta\tau$, we can determine the function $\Delta\tau(t_{rest}$ relating the overshoot to the resting time [see Fig. 1.21(c)].

Modelling

The simplest mode we can imagine is to assume that the viscosity is dependent on a structural parameter. As a first approximation and for the sake of simplicity, we assume that (i) this parameter is scalar, (ii) it reflects the microstructure state (e.g., the floc size in a flocculated suspension, the number of contact in a colloid, available energy for a given particle configuration, etc.), (iii) it satisfies a kinetic equation in the form

$$\frac{\mathrm{d}\lambda}{\mathrm{d}t} = \frac{F(\lambda)}{t_b} - \frac{G(\lambda)}{t_e},$$

where t_b is the buildup timescale, $t_e = \dot{\gamma}^{-1}$ is a typical characteristic of the flow, F represents the increase of the scalar parameter induced by buildup, whereas G stands for the λ as a result of microstructure disorganization. These functions can de determined experimentally. Typical examples include $F = (1-\lambda)^a$ and $G = b\lambda$, with a and b two reals (see pp. 24–25, Barnes, 1997)

In short, we have $\mu = \mu(\dot{\gamma},\lambda)$, with λ variations controlled by the kinetic equation above. When solving a problem, we have to solve the momentum equations together with the kinetic equation.

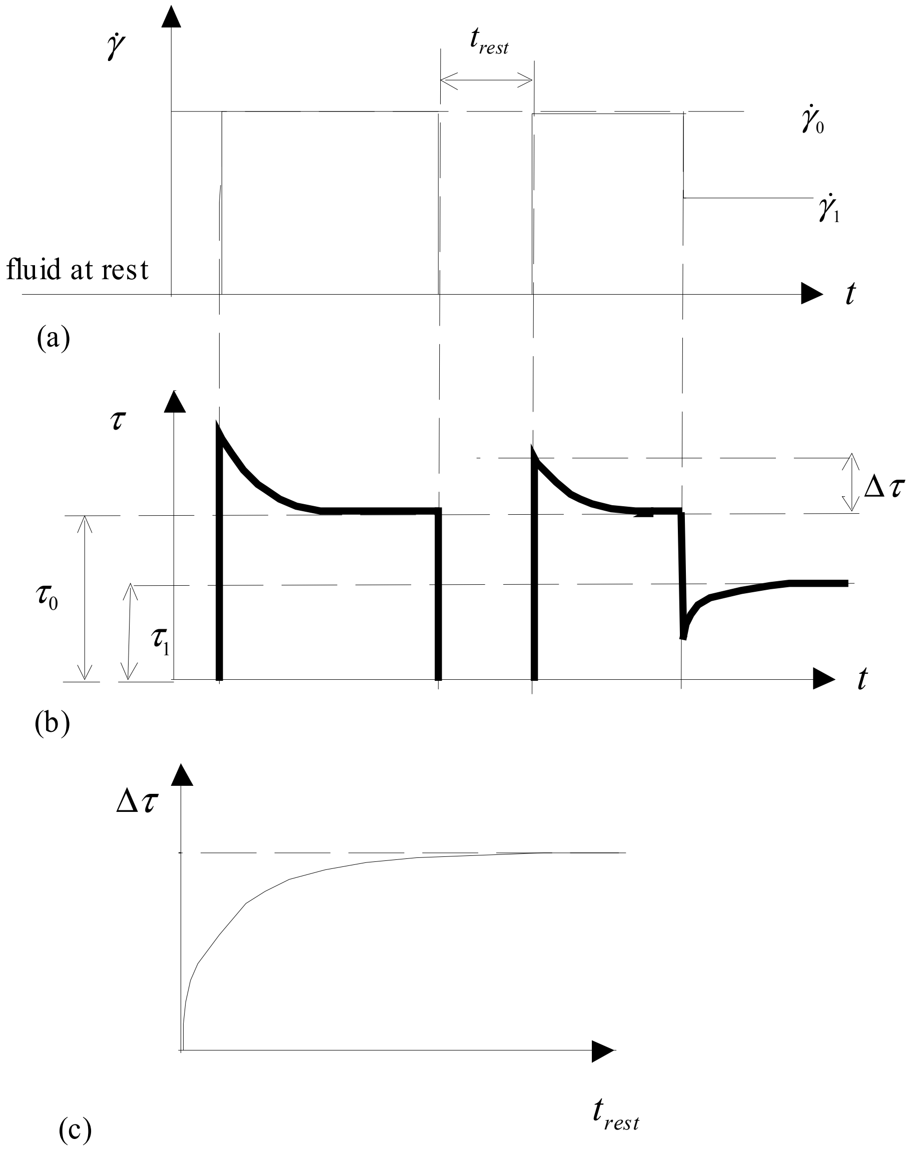

Figure 1.21 *Typical evolution of shear stress (b) in response to a shear-rate history (a). Iterating the procedure with different values of shear-rate levels leads to determining the stress jump* $\Delta\tau$ *as a function of the resting time* t_{rest}.

1.6 Problems encountered in rheometry

1.6.1 Problems with rheometers

In rheometry, many disturbing effects may arise. They often reflect the influence of the microstructure. For instance, for a particle suspension, especially made up of nonbuoyant particles, sedimentation and migration of particles can significantly alter the stress distribution and thus the measured torque. Likewise, for concentrated pastes, a fracture inside the sheared sample may sometimes be observed, usually resulting from a *localization of shear* within a thin layer. Other disturbing effects are experimental problems pertaining to the rheometer type. For instance, when using a rotational viscometer with a smooth metallic shearing surface, wall slip can occur. Apart from effects resulting from microstructural changes, which are a part of the problem to study, it is sometimes possible to reduce disturbing effects or to account for them in the flow-curve computation.

Problems coming from electronic defects

As for any electronic apparatus, a rheometer may encounter problems that cause trouble when taking measurement. The typical sources of error include

- calibration defect: test the response of the rheometer by using a previously calibrated fluid, usually stable oil (e.g., silicone). These may be purchased from chemical product suppliers, who propose ISO-9002 registered and NIST-traceable fluids.
- zero drift: test the rheometer with a Newtonian fluid.

End effects

More important are probably the problems related to wall and end effects. Any rheometer is subjected to end effects, which have to be corrected or taken into account in the computation of the flow curve. Typical examples are the following

- end effects in a channel are due to the finite length of the channel as well as the sidewalls, both producing potentially significant variations in the flow depth;
- in a Couette rheometer, the measured torque includes a contribution due to the shearing over the bottom surface of the bob. Such a contribution is substantially reduced using a bob with a hole hollowed on the bottom surface so that air is trapped when the bob is immersed in the fluid. But this can be inefficient for particle suspensions, such as granular materials, and in this case, the bottom contribution to the resulting torque must be directly assessed using the method proposed by Barnes & Carnali (1990);
- for a parallel-plate rheometer, the fluid surface at the peripheral free surface may bulge out or creep, inducing a significant variation in the measured torque, possibly varying with time.

Wall effects: slipping and adherence

A substantial source of problems arises with particle suspensions due to the presence of a wall (Barnes, 1995):

- a wall modifies the particle arrangement: this phenomenon called *particle depletion* involves a decrease in particle concentration close to the wall, which leads to the development of a lubricated fluid layer close to the solid boundary and to the slipping of the bulk.
- depending on the fluid properties, there may be interactions between the metallic surface and the constituents of the liquid. For specific materials like flocculated suspensions (floc

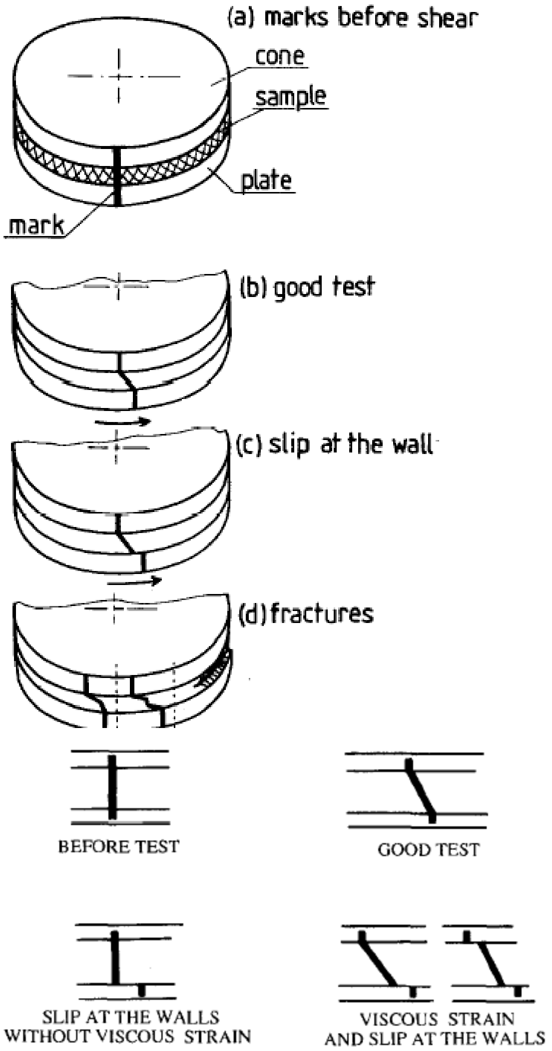

Figure 1.22 *Detection of slipping and shear localization for shear tests. After (Magnin & Piau, 1987, 1990).*

size is shear-rate dependent) or for fibrous materials, the presence of a solid boundary may alter the local structure within the liquid, thus local viscosity.

Slipping problems can be pinpointed experimentally by marking the sample with very fine non-active powder at the free surface and on the edges of the cone and plate, as shown in figure 1.22(a). Slipping and sample rupture is detected by observing how lines deform during the test. When the deformation is homogeneous, as expected or desired, the marked lines are straight, as shown in 1.22(b). Slipping is made visible through discontinuities of the marks.

Slipping may significantly disturb measurements :

- under-evaluation of bulk viscosity
- improper evaluation of the yield stress for a viscoplastic material

Some solutions are:

- A strategy involves measuring the slipping velocity directly and then computing an effective shear rate.
- Still another possibility requires using the same rheometer with different sizes, as first proposed by Mooney for the capillary rheometer.
- Rheometer suppliers provide specific grooved or corrugated geometries. Sandblasting with a coarse grit or gluing a sand paper can also be used to roughen a metallic surface.

- A growing number of applications are based on vane shear cell Barnes & Nguyen (2001).
- When there are chemical interactions (chemical attack with ion production) or physical interactions (van der Waals force) between the fluid constituents and the walls, specific surface treatment must be used.

Be careful: some techniques such as using rough surfaces do not remove the slipping problem, but only shift it: instead of slipping, the material undergoes shear localization within the sample.

Rupture within the sample

With rupture, we mean:

- shear localization: shear is concentrated within a narrow strip inside the sample, which implies a jump in shear rate on the bulk scale
- slipping between two layers of material.

Deformation of the free surface

In most viscometric flows, there is a free surface. This surface may deform as a result of different processes:

- normal stress effect: rod-climbing effect or bulging of the free surface for flows down inclines
- inertial effect: for the coaxial cylinder rheometer at high velocities, there is a gradient in the flow depth to balance the inertial centrifuge forces. For the parallel-plate rheometer, fluid may be expelled because of radial acceleration
- evaporation, particle migration etc. at the periphery of the sample for parallel-plate rheometer.

Finite-size effects

Furthermore, many natural fluids encountered in geophysics are suspensions with a large size distribution. The size of the rheometer should be determined such that its typical size (e.g., the gap in a rotational viscometer) is much larger than the largest particle size.

The solution involves using large-sized rheometers, e.g., wide gap Couette cells.

1.6.2 Limitations of the viscometric treatment

The ‘simple-fluid’ assumption

The viscometric treatment relies on the crucial assumption that the extra-stress tensor is a one-to-one function of the strain-rate tensor only (class of simple fluids). Many classes of material studied in geophysics are not in fact incompressible, homogeneous, isotropic, or merely expressible in the form $\boldsymbol{\sigma} = -p\mathbf{1} + \mathbf{s}(\mathbf{d})$.

For instance, for materials with time-dependent properties (thixotropic materials, viscoelastic materials), the constitutive equation can be expressed in the form $\boldsymbol{\sigma} = -p\mathbf{1} + \mathbf{s}(\mathbf{d})$ only for a steady state. Another example is provided by granular flows. In this case, when applied to experimental data obtained by studying dry granular flows down an inclined channel (Ancey *et al.*, 1996), the viscometric treatment leads to the conclusion that the flow curve should be a decreasing function of the shear rate in violation of a stability criterion imposing that the flow curve be an increasing function. Although such a decrease in the flow curve cannot be directly interpreted in terms of a constitutive equation, it provides interesting rheological information that can be explained on the basis of microstructural theories (Ancey & Evesque, 2000).

Development of instabilities

At high speed, a number of instabilities occur:

- development of secondary flow and recirculation cell, e.g., Saffman-Taylor instability in Couette cells
- turbulence development
- particle migration, particle jamming or settling

The possible solution is to

- visualize the internal flow structure to detect secondary flow;
- place tracers in the fluid to determine their trajectory, then the streamlines;
- check the consistency of the data. For instance for a parallel-plate rheometer, the viscometric treatment is valid provided centrifugal forces are negligible compared to the second normal stress difference: $\varrho R^2 w^2 \ll N_2$, where w is the orthoradial component of the velocity. Such an effect can be detected experimentally either by observing secondary flows or by noticing that doubling both the gap and the rotational velocity (thus keeping the shear rate constant) produces a significant variation in the measured torque.

1.6.3 Technical issues related to the derivation of the flow curve

Recall that:

- The softwares provided by rheometer manufacturers for computing the flow curve or other rheological properties makes use of standard methods. For instance, for the Couette cell (coaxial cylinder rheometer), the narrow-gap approximation is used, which implies that the user should develop his own software to deal with wide-gap rheometer.
- For most viscometers, computing the shear rate from experimental data can raise serious problems. A major source of uncertainty is that in most viscometric procedures the shear rate is expressed as a derivative – for instance $\partial q/\partial h$ in (1.11) – which must be estimated from experimental data. To do so, different procedures are available but they do not always provide the same results, especially when data are noisy (Borgia & Spera, 1990).

A typical example of these problems is given by the concentric-cylinder rheometer (or Couette rheometer). The shear rate is inferred from the rotational velocity Ω and the torque (per unit depth) C using the following relationship:

$$\Omega = -\frac{1}{2}\int_{C/(2\pi R_1^2)}^{C/(2\pi R_2^2)} \dot\gamma(\tau)\mathrm{d}\ln\tau. \tag{1.18}$$

When the gap between the two cylinders is narrow, it is possible to approximate the shear rate as: $\dot\gamma = R_1\Omega/(R_2 - R_1) + o(1 - R_2/R_1)$.

However, such a geometry is not very suitable to studying particle suspensions (slipping, size effects, etc.) and usually a wide gap is preferred. For methods of this kind, computing the shear rate requires:

- specifying the type of constitutive equation in advance, integrating it to obtain the relation between the torque and the rotational velocity, and fitting the relation to experimental data.
- using a more effective and practical method of solving the inverse problem such as
  - the Tikhonov regularization method proposed by Yeow *et al.* (2000): this procedure does not require the algebraic form of the $\tau - \dot\gamma$ curve to be specified and has the advantage of filtering out noise.

- the wavelet-vaguelette decomposition method proposed by Ancey (2005) which is not based on a regularization step and thus is more appropriate for complex fluids.

The only viscometer which poses no problem in converting experimental data into a $\tau - \dot{\gamma}$ curve is the parallel-plate rheometer. In this case, the shear rate distribution is imposed by the experimentalist: $\dot{\gamma} = \Omega R/h$. But such a relationship holds provided centrifugal forces are negligible compared to the second normal stress difference: $\varrho R^2 w^2 \ll N_2$, where w is the orthoradial component of the velocity. Such an effect can be detected experimentally either by observing secondary flows or by noticing that doubling both the gap and the rotational velocity (thus keeping the shear rate constant) produces a significant variation in the measured torque.

1.6.4 Problems related to sample preparation

A sample that will be tested in a rheometer must be representative of large batches of material from which it is extracted. Specific care should be taken in obtaining and preparing particle suspensions when the sample has been collected in the field (e.g., a sample of debris flow) or in industrial facilities due to segregation effects.

1.7 Non-standard techniques: what can be done without a rheometer?

1.7.1 Viscosity: free fall of a bead

Consider an isolated spherical particule of radius a falling under the action of gravity in a fluid that is assumed to be Newtonian with viscosity μ and unbounded (no wall close to the particle). If the sphere moves very slowly, its Reynolds number

$$\mathrm{Re} = \frac{\varrho_p a u}{\mu},$$

with ϱ_p the particle density and u the particle velocity relative to the fluid. When $\mathrm{Re} \ll 1$, then the force exerted by the fluid on the particle is given by Stokes' law

$$F = 6\pi\mu a u.$$

If we can measure the velocity u when the particle reaches a steady regime, we can determine the fluid viscosity from the force balance $0 = -\varrho_p g + \varrho_f g + F$, where fluid density has been denoted by ϱ_f

$$\mu = \frac{2}{9}(\varrho_p - \varrho_f)\frac{ga^2}{u}.$$

A practical version of this measurement technique is the rolling-ball viscometer (Bird *et al.*, 1987).

1.7.2 Yield stress: Slump test

In the laboratory, it is frequently impossible to investigate the rheological properties of a particle suspension using a rheometer. For instance, with snow or magma, such tests are almost always impractical. For debris suspensions, it is usually impossible to carry out measurements with the complete range of particle size. This has motivated researchers to developed approximate rheometric procedures and to investigate the relations between field observations and rheological properties. For instance, given the sole objective of determining the yield stress, the semi-empirical method referred to as a slump test can provide an estimate of the yield stress for a viscoplastic material. This method involves filling a cylinder with the material to be tested, lifting the cylinder off and allowing the material to flow under its own weight. The profile of the final mound of material as well as the difference (δ) between the initial and final heights is linked to the yield stress. Pashias & Boger (1996) have found:

$$\frac{\delta}{h} = 1 - 2\frac{\tau_c}{\varrho g h}\left(1 - \ln\left(2\frac{\tau_c}{\varrho g h}\right)\right), \tag{1.19}$$

where h is the cylinder height, ϱ the material density (see also Schowalter & Christensen, 1999). Close examination of experimental data published by Pashias and Boger shows a deviation from the theoretical curve for yield stress values in excess of approximately $0.15\varrho g h$. For yield stress values lower than $0.15\varrho g h$ (or for $\delta/h > 0.4$), uncertainty was less than 10% for their tests. The explanation of the deviation for higher yield stress values lies perhaps in the weakness of the assumption on the elastoplastic behavior for very cohesive materials. Coussot *et al.* (1996) developed an alternative approach based on an interpretation of the deposit shape. They showed that the free surface profile (the relationship between the material height y and the distance from the edge x) depends on the yield stress only. On a flat horizontal surface, the free surface profile has the following expression

$$\frac{\varrho g y}{\tau_c} = \sqrt{2\frac{\varrho g x}{\tau_c}}. \tag{1.20}$$

Comparisons between rheological data deduced from a parallel-plate rheometer and free surface profile measurements showed an acceptable agreement for fine mud suspensions and debris flow materials. Uncertainty was less than 20%, within the boundaries of acceptable uncertainty for rheometrical measurement. The major restriction in the use of equation (1.20) stems from the long-wave approximation, which implies that the mound height must far outweigh the extension of the deposit: $h - \delta \gg \tau_c/(\varrho g)$. The method proposed by Coussot *et al.* (1996) can be extended to different rheologies and boundary conditions. In the field, such a method applied to levee profiles of debris flow can provide estimates of the bulk yield stress provided that the assumption of viscoplastic behavior holds.

A number of other tests have been developed in civil engineering tests (e.g., Abram's test for evaluating concrete workability) and in the industry (e.g., Bostwick's test in food engineering), which usually provide information on how easily a material flows. More recently, some theoretical analyses have tried to elaborate on the interpretations that can be done with these empirical (McKarthy & Seymour, 1994; Piau & Debiane, 2005).

Chapter 2

Rheology and Continuum Mechanics

Prerequisites

- fluid mechanics: mass, momentum, energy balance equations
- mathematics: differential analysis, tensorial analysis, algebra tools

Objectives

- to provide the mathematical ground supporting continuum mechanics
- to review the fundamental principles used in formulating a constitutive equations
- to provide physical insight into the mathematical operators used in mechanics

Content

Within the framework of continuum mechanics, the details of the material microstructure are forgotten and we only examine the bulk behavior, e.g. how does a material deform when it experiences a given state of stress? Mathematically, we introduce the *constitutive equation*, which relates deformations and/or rates of deformation to stresses. Essentially continuum mechanics provides tools and rules that make it possible to:

- express constitutive equations in a proper form, i.e., in a tensorial form that satisfies the rules of physics;
- obtain equations that govern the bulk motion.

Most phenomenological laws we can infer from experiments are in a scalar form. For instance, in rheometry, the only information we obtain in most cases is the flow curve, i.e., the relation $\tau = f(\dot{\gamma})$, whereas we need more information to model the three-dimensional behavior of fluids. The question is how to express a 3D constitutive equations. We shall see that the reply is not as easy as it can be thought at first glance. We start with the Newtonian case, the simplest case that we can imagine. We then continue by reviewing the basic equations used in continuum mechanics (conservation of mass, momentum, and energy). Emphasis is then given to providing a few examples of application.

2.1 Why is continuum mechanics useful? An historical perspective

Newton's and Trouton's experiments were run on very viscous materials, but their interpretation, if cursorily made, leads to different values of viscosity.

2.1.1 Paradoxical experimental results?

In 1687, Isaac Newton proposed that "the resistance which arises from the lack of slipperiness of the parts of the liquid, other things being equal, is proportional to the velocity with which the parts of the liquid are separated from one another". This forms the basic statement behind the theory of Newtonian fluid mechanics. Translated into modern scientific terms, this sentence means that the resistance to flow (per unit area) τ is proportional to the velocity gradient U/h:

$$\tau = \mu \frac{U}{h}, \tag{2.1}$$

where U is the relative velocity with which the upper plate moves and h is the thickness of fluid separating the two plates (see Fig. 2.1). μ is a coefficient intrinsic to the material, which is termed *dynamic viscosity*. This relationship is of great practical importance for many reasons:

- it is the simplest way of expressing the constitutive equation for a fluid (linear behavior);
- it provides a convenient experimental method for measuring the constitutive parameter μ by measuring the shear stress exerted by the fluid on the upper plate moving with a velocity U (or conversely by measuring the velocity when a given tangential force is applied to the upper plate).

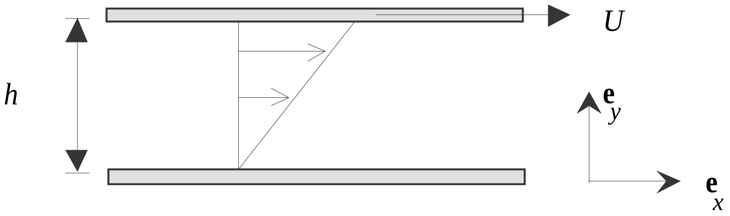

Figure 2.1 *Illustration of a fluid sheared by a moving upper plate*

In 1904, Trouton did experiments on mineral pitch involving stretching the fluid with a given velocity. Figure 2.2 depicts the principle of this experiment. The fluid undergoes a uniaxial elongation achieved with a constant elongation rate $\dot{\alpha}$, defined as the relative deformation rate: $\dot{\alpha} = \dot{l}/l$, where l is the fluid sample length. For his experiments, Trouton found a linear relationship between the applied force per unit area σ and the elongation rate:

$$\sigma = \mu_e \alpha = \mu_e \frac{1}{l}\frac{dl}{dt}. \tag{2.2}$$

This relationship was structurally very similar to the one proposed by Newton but it introduced a new material parameter, which is now called *Trouton viscosity*. This constitutive parameter was found to be three times greater than the Newtonian viscosity inferred from steady simple-shear experiments: $\mu_e = 3\mu$. At first glance, this result is both comforting since behavior is still linear (the resulting stress varies linearly with the applied strain rate) and disturbing since the value of the linearity coefficient depends on the type of experiment.

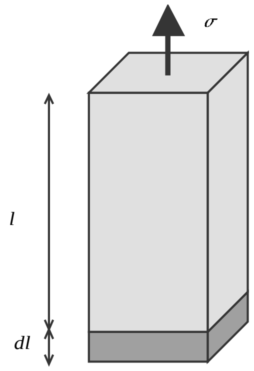

Figure 2.2 *Typical deformation of a material experiencing a normal stress* σ

2.1.2 How to remove the paradox?

In fact, Trouton's result does not lead to a paradox if we are careful to express the constitutive parameter in a tensorial form rather than a purely scalar form. This was achieved by Navier and Stokes, who independently developed a consistent three-dimensional theory for Newtonian viscous fluids. For a simple fluid, the stress tensor σ can be cast in the following form:

$$\sigma = -p\mathbf{1} + \mathbf{s}, \tag{2.3}$$

where p is called the fluid pressure and $\mathbf{s}$ is the extra-stress tensor representing the stresses resulting from a relative motion within the fluid. It is also called the *deviatoric stress tensor* since it represents the departure from equilibrium. The pressure term used in Eq. (2.3) is defined as (minus) the average of the three normal stresses $p = -\mathrm{tr}\,\boldsymbol{\sigma}/3$. This also implies that ($\mathrm{tr}\,\mathbf{s} = 0$). The pressure used in Eq. (2.3) is analogous to the hydrostatic fluid pressure in the sense that it is a measure of the local intensity of the squeezing of the fluid. The connection between this purely mechanical definition and the term pressure used in thermodynamics is not simple. For a Newtonian viscous fluid, the Navier-Stokes equation postulates that the extra-stress tensor is linearly linked to the strain-rate tensor $\mathbf{d} = (\nabla\mathbf{u} + {}^t\nabla\mathbf{u})/2$:

$$\mathbf{s} = 2\eta\mathbf{d}, \tag{2.4}$$

where $\mathbf{u}$ is the local fluid velocity and η is called the *Newtonian viscosity.* It is worth noticing that the constitutive equation is expressed as a relationship between the extra-stress tensor and the local properties of the fluid, which are assumed to depend only on the instantaneous distribution of velocity (more precisely, on the departure from uniformity of that distribution). There are many arguments from continuum mechanics and analysis of molecular transport of momentum in fluids, which show that the local velocity gradient $\nabla\mathbf{u}$ is the parameter of the flow field with most relevance to the deviatoric stress. On the contrary, the pressure is not a constitutive parameter of the moving fluid. When the fluid is compressible, the pressure p can be inferred from the free energy, but it is indeterminate for incompressible Newtonian fluids. If we return to the previous experiments, we infer from the momentum equation that the velocity field is linear: $\mathbf{u} = U\mathbf{e}_x y/h$. We easily infer that the shear rate is: $\dot\gamma = \partial u/\partial y = U/h$ and then comparing (2.4) to (2.1) leads to: $\eta = \mu$.

Thus, the Newtonian viscosity corresponds to the *dynamic viscosity*, measured in a simple-shear flow. In the case of a uniaxial elongation, the components of the strain-rate tensor are when inertia can be neglected:

$$\mathbf{d} = \begin{bmatrix} \dot\alpha & 0 & 0 \\ 0 & -\dot\alpha/2 & 0 \\ 0 & 0 & -\dot\alpha/2 \end{bmatrix}. \tag{2.5}$$

At the same time, the stress tensor can be written as:

$$\boldsymbol{\sigma} = \begin{bmatrix} \sigma & 0 & 0 \\ 0 & 0 & 0 \\ 0 & 0 & 0 \end{bmatrix}. \tag{2.6}$$

Comparing (2.3), (2.5), and (2.6) leads to: $p = -\eta\dot{\alpha}$ and $\sigma = 3\eta\dot{\alpha}$, that is: $\mu_e = 3\eta$, confirming that the Trouton elongational viscosity is three times greater than the Newtonian viscosity. It turns out that Trouton's and Newton's experiments reflect the same constitutive behavior. This example shows the importance of an appropriate tensorial form for expressing the stress tensor. In the present case, the tensorial form (2.4) may be seen as a simple generalization of the simple shear expression (2.1).

2.2 Fundamentals of Continuum Mechanics

2.2.1 Kinematics

It is customary to start a continuum mechanics course with the notion of Lagrangian and Eulerian descriptions:

- in an Eulerian description of the matter, attention is focused on what happens in a given volume control regardless of the history of particles contained in this volume;
- in a Lagrangian description, we follow up the motion of each particle that was at a given position at $t = 0$.

This duality in the matter description disappears very quickly from students' memory. Fluid mechanicians make use of Eulerian tools almost exclusively since for Newtonian fluids, the physics is governed by the past history, whereas solid mechanicians give preference to the Lagrangian description because for small deformations, there is not much differences between the descriptions.

However, in an advanced course on rheology and continuum mechanics, emphasis is given to the dual nature of materials which can exhibit both solid-like and fluid-like properties. Much attention has been paid to providing a unified vision of continuum mechanics that is sufficiently general to be applied to a wide range of rheological behaviors. This unified view extends the classic mechanics in several ways:

- large deformations to cope with viscoplasticity and viscoelasticity;
- thermodynamics to take irreversible processes into account.

Here we will focus our attention to a classic description of material deformation and the reader is referred to specialized books that expound more sophisticated theories of deformation (Bird *et al.*, 1987; Tanner, 1988; Morrison, 2001).

In the following, we shall following focus on Eulerian form of the equations of motion, but keep in mind that, especially in advanced fluid mechanics, Lagrangian representations of the equations are very useful (e.g., see Pope, 2000; Minier & Peirano, 2001; Zdunkowski & Bott, 2003, in the field of turbulence or atmospheric flows).

The gradient tensor

In order to characterize the deformation of a body, it is usually helpful to determine how neighboring points behave, i.e. how the increment $\mathrm{d}\mathbf{X}$ in an initial frame is transformed (see Fig. 2.3), including:

- stretching/contraction of length,
- rotation of elements due to solid rotation and shearing.

We take three neighboring points in the initial frame of reference $\mathcal{C}_0$, called A, B, and C, forming a right angle (see Fig. 2.3). Because of deformation, there may be

- stretching in a direction $\mathbf{e}_1$ or $\mathbf{e}_2$,
- solid rotation around a given axis with an angle α,
- pure shear, i.e. the angle $\theta_0 = \pi/2$ between $\mathbf{X}_1 = \mathbf{AB}$ and $\mathbf{X}_2 = \mathbf{BC}$ has been altered.

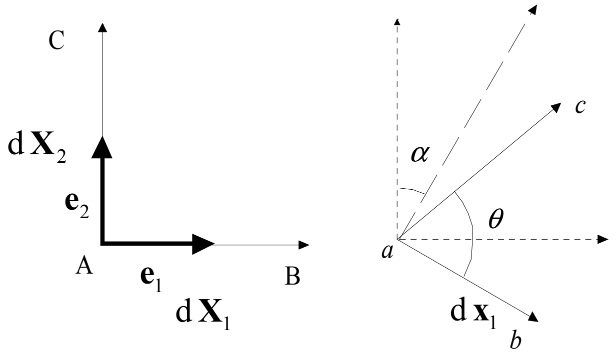

Figure 2.3 *Deformation of a right angle.*

For this purpose, we introduce the transformation

$$\mathrm{d}\mathbf{X} \rightarrow \mathrm{d}\mathbf{x},$$

where $\mathbf{x}(\mathbf{X},\, t)$ is the position occupied at time t by a particle that was earlier at $t = 0$ at the position $\mathbf{X}$ in the initial frame of reference $\mathcal{C}_0$. Positioning $\mathbf{x}$ can be made in the same frame of reference $\mathcal{C}_0$ or in another frame $\mathcal{C}(t)$. Differentiating the relation $\mathbf{x} = \mathbf{x}(\mathbf{X},\, t)$ leads to

$$\mathrm{d}\mathbf{x} = \mathbf{F} \cdot \mathrm{d}\mathbf{X},$$

where $\mathbf{F}$ is called the *gradient tensor*. When we use the same frame to refer to the current and initial configurations, we can introduce the displacement vector $\mathbf{u}$ such that

$$\mathbf{x} = \mathbf{u} + \mathbf{X},$$

from which we infer

$$F_{ij} = \delta_{ij} + \frac{\partial u_i}{\partial X_j}.$$

The deformation of the angle (AB, AC) can be determined by using the scalar product

$$\mathrm{d}\mathbf{x}_1 \cdot \mathrm{d}\mathbf{x}_2 = (\mathbf{F} \cdot \mathrm{d}\mathbf{X}_1) \cdot (\mathbf{F} \cdot \mathrm{d}\mathbf{X}_2),$$

which can be transformed into

$$\mathrm{d}\mathbf{x}_1 \cdot \mathrm{d}\mathbf{x}_2 = \mathrm{d}\mathbf{X}_1 \cdot (\mathbf{C} \cdot \mathrm{d}\mathbf{X}_2),$$

where $\mathbf{C} = \mathbf{F}^T \cdot \mathbf{F}$ is a symmetric tensor called the *stretch tensor* or *Cauchy-Green tensor.* The relative variation of the scalar product is then

$$\mathrm{d}\mathbf{x}_1 \cdot \mathrm{d}\mathbf{x}_2 - \mathrm{d}\mathbf{X}_1 \cdot \mathrm{d}\mathbf{X}_2 = 2\mathrm{d}\mathbf{X}_1 \cdot (\mathbf{E} \cdot \mathrm{d}\mathbf{X}_2),$$

where

$$\mathbf{E} = \frac{1}{2}(\mathbf{C} - \mathbf{1}) = \frac{1}{2}(\mathbf{F}^T \cdot \mathbf{F} - \mathbf{1}),$$

is the *strain tensor of Green-Lagrange.*

Let us now express the stretching of a length increment $\mathrm{d}s = \sqrt{\mathrm{d}\mathbf{x}_1 \cdot \mathrm{d}\mathbf{x}_1}$

$$\mathrm{d}s_1 = (\mathbf{e}_1 \cdot \mathbf{C} \cdot \mathbf{e}_1)^{1/2} \mathrm{d}S,$$

where $\mathrm{d}S_1 = \sqrt{\mathrm{d}\mathbf{X}_1 \cdot \mathrm{d}\mathbf{X}_1}$. We deduce the relative stretching, i.e. the strain in direction $\mathbf{e}_1$

$$\epsilon_1 = \frac{\mathrm{d}s_1 - \mathrm{d}S_1}{\mathrm{d}S_1} = (\mathbf{e}_1 \mathbf{C} \mathbf{e}_1)^{1/2} - 1 = \sqrt{1 + 2E_{11}} - 1.$$

We can also characterize the angle θ

$$\cos\theta = \frac{\mathrm{d}\mathbf{x}_1 \cdot \mathrm{d}\mathbf{x}_2}{\mathrm{d}s_1 \mathrm{d}s_2} = \frac{2E_{12}}{\sqrt{1+2E_{11}}\sqrt{1+2E_{22}}},$$

which shows that

- the diagonal components give information on strains in the axis directions;
- the off-diagonal terms specify how a angle of an initially right wedge is deformed.

In order to get rid of the solid rotation that is not related to deformation, we make use of a theorem, called the *polar decomposition* theorem, that says that any tensor can be broken down in a unique way into an orthogonal[1] tensor $\mathbf{R}$ (representing block rotation) and symmetric (pure deformation) tensor [length-increment variation + angle variation]. Applied to the gradient tensor, this theorem allows us to write:

$$\mathbf{F} = \mathbf{R} \cdot \mathbf{U} = \mathbf{V} \cdot \mathbf{R},$$

where $\mathbf{U}$ (resp. $\mathbf{V}$) is the right (resp. left) pure strain tensor.

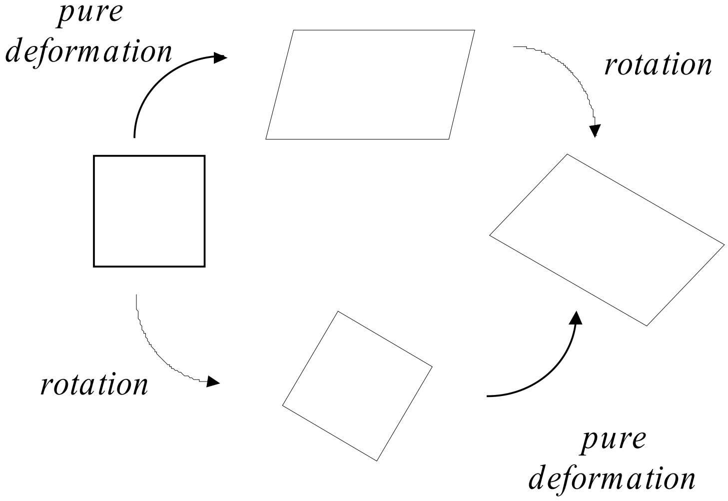

Figure 2.4 *Polar decomposition of the gradient tensor.*

This theorem can also be applied to other tensors such as $\mathbf{C}$ and $\mathbf{E}$, but in that case we can take benefit from the symmetry[2] of these tensors together with the symmetry in $\mathbf{U}$ (or $\mathbf{V}$). In their eigenvector bases, deformation corresponds to length variations with no angle variation.

In addition to the length, we can also characterize the deformation of surfaces and volumes. The transformation of an infinitesimal volume $\mathrm{d}V$ in the initial frame is given by the Jacobian J of the transformation $\mathrm{d}\mathbf{X} \to \mathrm{d}\mathbf{x}$

$$\mathrm{d}v = J\mathrm{d}V \text{ with } J = |\det \mathbf{F}|.$$

Similarly, an oriented infinitesimal element of surface $\mathrm{d}\mathbf{A}$ can be expressed as $\mathrm{d}\mathbf{A} = \mathrm{d}\mathbf{X}_1 \times \mathrm{d}\mathbf{X}_2$, which is transformed into

$$\mathrm{d}\mathbf{a} = \mathrm{d}\mathbf{x}_1 \times \mathrm{d}\mathbf{x}_2 = J(\mathbf{F}^{-1})^T \cdot \mathrm{d}\mathbf{A}.$$

For instance, let us consider a shear strain in the form

$$x_1 = X_1 + \gamma(t)X_2,\ x_2 = X_2, \text{ and } x_3 = X_3,$$

---

[1] Recall that if a tensor is orthogonal, then $\mathbf{R}^T \cdot \mathbf{R} = \mathbf{R} \cdot \mathbf{R}^T = \mathbf{1}$ and $\det \mathbf{R} = 1$.

[2] Recall that a real-valued symmetric tensor can be diagonalized and its eigenvector basis is orthogonal.

where $\gamma(t)$ is called the shear amplitude and (x_1, x_2, x_3) is the coordinates in a Cartesian frame. We find that this transformation keeps the volumes constant ($J = 1$) and

$$\mathbf{F} = \begin{bmatrix} 1 & \gamma & 0 \\ 0 & 1 & 0 \\ 0 & 0 & 1 \end{bmatrix},\ \mathbf{C} = \begin{bmatrix} 1 & \gamma & 0 \\ \gamma & 1+\gamma^2 & 0 \\ 0 & 0 & 1 \end{bmatrix},\ \text{and } \mathbf{E} = \begin{bmatrix} 0 & \gamma/2 & 0 \\ \gamma/2 & \gamma^2/2 & 0 \\ 0 & 0 & 1 \end{bmatrix}.$$

Small deformations

When deformations are small, we can linearize the tensors to get rid of nonlinear terms. Essentially this means that the displacement $\mathbf{u} = \mathbf{x} - \mathbf{X}$ between the current and initial positions is very small. We can deduce that

- there is not much differences between the frame $\mathcal{C}_0$ and $\mathcal{C}(t)$, which can then be assumed to be the same;
- we can write $\mathbf{F} = \mathbf{1} + \mathbf{H}$ with $\mathbf{H} = \nabla_X \mathbf{x}$ with “small” entries.

We deduce that the Cauchy-Green tensor can be linearized in the following way

$$\mathbf{C} = \mathbf{F}^T \cdot \mathbf{F} = \mathbf{1} + \mathbf{H} + \mathbf{H}^T = 1 + 2\boldsymbol{\epsilon},$$

where $\boldsymbol{\epsilon}$ is called the (linearized) strain tensor and is defined as the symmetric part of $\mathbf{H}$

$$\boldsymbol{\epsilon} = \frac{1}{2}(\mathbf{H} + \mathbf{H}^T) = \frac{1}{2}\left(\nabla_X \mathbf{x} + \nabla_X \mathbf{x}^T\right) = \mathbf{E}.$$

Rate of strain

In order to characterize the velocity, we introduce the time derivative of $\mathbf{x}(\mathbf{X}, t)$. In a Lagrangian system, $\mathbf{X}$ corresponds to the initial condition at $t = 0$, whereas in an Eulerian system, $\mathbf{X}$ is the position previously occupied by a particle and is a function of time.

The time derivative of an infinitesimal length increment is

$$\frac{\mathrm{d}}{\mathrm{d}t}\mathrm{d}\mathbf{x} = \dot{\mathbf{F}} \cdot \mathrm{d}\mathbf{X} = \dot{\mathbf{F}} \cdot \mathbf{F}^{-1} \cdot \mathrm{d}\mathbf{x} = \mathbf{L} \cdot \mathrm{d}\mathbf{x},$$

where $\mathbf{L} = \dot{\mathbf{F}} \cdot \mathbf{F}^{-1} = \nabla_x \mathbf{v}$ is called the *velocity gradient tensor*. It is customary to break down into a symmetric and antisymmetric contribution

$$\mathbf{d} = \frac{1}{2}(\mathbf{L} + \mathbf{L}^T) \text{ and } \mathbf{w} = \frac{1}{2}(\mathbf{L} - \mathbf{L}^T).$$

The symmetric part $\mathbf{d}$ describes the strain rate and hence is called the *strain-rate tensor* (sometimes the stretching tensor), whereas the antisymmetric part $\mathbf{w}$ called the *vorticity tensor* (sometimes the spin tensor) corresponds to the rotational of the velocity field.

Recall that when a tensor $\mathbf{w}$ is antisymmetric, this implies the existence of a vector $\boldsymbol{\omega}$ such that for any vector $\mathbf{n}$, we have $\mathbf{w} \cdot \mathbf{n} = \boldsymbol{\omega} \times \mathbf{n}$. Let us expand the velocity $\mathbf{v}(\mathbf{x} + \mathrm{d}\mathbf{x})$

$$\mathbf{v}(\mathbf{x} + \mathrm{d}\mathbf{x}) = \mathbf{v}(\mathbf{x}) + \nabla_x \mathbf{v} \cdot \mathrm{d}\mathbf{x} + \cdots = \mathbf{v}(\mathbf{x}) + \mathbf{d}(\mathbf{x}) \cdot \mathrm{d}\mathbf{x} + \boldsymbol{w}(\mathbf{x}) \cdot \mathrm{d}\mathbf{x} + \cdots,$$

which means that to first order, we have

$$\mathbf{v}(\mathbf{x} + \mathrm{d}\mathbf{x}) = \mathbf{v}(\mathbf{x}) + \mathbf{d} \cdot \mathrm{d}\mathbf{x} + \boldsymbol{\omega} \times \mathrm{d}\mathbf{x}.$$

This means that the local variation in the velocity field can be broken down into a strain-rate contribution and another contribution corresponding to solid rotation

Refined kinematical description

Here we have deliberately ignored the issues related to the frames in which the tensor components are written. We have just introduced the configurations $\mathcal{C}_0$ and $\mathcal{C}(t)$ and any quantity can be defined in either configuration. Another approach is to introduce curvilinear coordinate system that is linked to the material deformations: when the body deforms, the initial axes of $\mathcal{C}_0$ deform in the same way and define a system of material coordinates that is embedded in the material and deform with it, as shown in Figure 2.5.

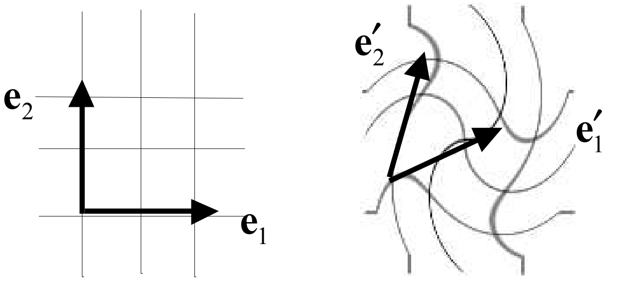

Figure 2.5 *Polar decomposition of the gradient tensor.*

The idea of a convected coordinate system embedded in a flowing film and deforming with it was developed by Oldroyd (1950) in the 1950s. This idea was motivated by the desire to formulate constitutive equations that are (i) independent of any frame of reference, (ii) independent of the position, and translational and rotational motion, of the element as a whole in space, and (iii) independent of the states of neighboring material elements.

2.2.2 Stress tensor

Definition of the stress tensor

We are going to introduce a new tensor called the *stress tensor*, which is used to compute the stresses exerted on an infinitesimal surface δS oriented by the outward unit vector $\mathbf{n}$. The stress $\boldsymbol{\tau}$ exerted on δS is defined as the ratio of the forces $\mathbf{f}$ per unit surface when δS becomes smaller and smaller:

$$\boldsymbol{\tau} = \lim_{\delta S \to 0} \frac{\mathbf{f}}{\delta S}.$$

Using Cauchy's lemma (force balance on a tetrahedron), it can be shown the existence of a tensor $\boldsymbol{\sigma}$, the *stress tensor*, such that

$$\boldsymbol{\tau} = \boldsymbol{\sigma} \cdot \mathbf{n}, \tag{2.7}$$

which means that the stress linearly varies with the normal $\mathbf{n}$. In a Cartesian frame, this tensor is represented by a symmetric matrix.

It is worth reminding that this construction is based on a postulate, which implies that other constructions are possible (e.g., micropolar or Cosserat medium) (Germain, 1973a,b). More generally, it is possible to use the virtual power principle to derive all the fundamental equations used in continuum mechanics and in that case, the stress tensor can formally be derived from the inner energy dissipation rate Φ

$$\sigma_{ij} = \frac{\partial \Phi}{\partial d_{ij}}. \tag{2.8}$$

This approach to continuum mechanics turns out to be fruitful for a number of problems in elasticity (membrum and shell theory) and in fluid mechanics. Indeed, on some occasions, it is easier to compute the energy dissipated in a system and, in that case, to compute the stress tensor using (2.8); for instance, a number of approximate computations of the bulk viscosity of a dilute particle suspension were done in this way (Einstein, 1911; Frankel & Acrivos, 1967).

Pressure and extra-stress

For a simple fluid at rest, the stress tensor reduces to

$$\boldsymbol{\tau} = -p\mathbf{1},$$

where p is called the *pressure.* From the thermodynamic viewpoint, the pressure is a function of the density ρ and temperature T: $p = p(\rho,\, T)$. Making use of the (Helmholtz) free energy $F = E - TS$, with S entropy, E internal energy, then we can show

$$p = \rho^2 \frac{\partial F}{\partial \rho}.$$

When the density is constant (incompressible material) or the flow is isochoric, the thermodynamic definition of pressures is no longer valid and the *thermodynamic pressure* must be replaced by the *hydrodynamic pressure.* The latter is an undetermined function that can be specified on solving the governing equations with specific boundary conditions.

When an incompressible simple fluid at rest is slightly disturbed, we can imagine that the stress can be expressed as

$$\boldsymbol{\sigma} = -p\mathbf{1} + \mathbf{s},$$

where $\mathbf{s}$ is called the extra-stress tensor and represents the departure from the static equilibrium. We shall see that for a wide class of fluids, this extra-stress is a function of the strain-rate tensor alone $\mathbf{d}$, which leads to posing: $\boldsymbol{\tau} = -p\mathbf{1} + \mathbf{s}(\mathbf{d})$. The simplest dependence of $\mathbf{s}$ on $\mathbf{d}$ that we can imagine is the linear relation: $\mathbf{s} = 2\mu\mathbf{d}$, i.e., the Newtonian constitutive equation. There is another motivation for writing the stress tensor as the sum of a pressure term and an additional contribution $\mathbf{s}$. Indeed, for an incompressible fluid, the mass balance imposes some constraints on the motion; there are internal stresses $\boldsymbol{\sigma'}$ that make the fluid incompressible. If these stresses are assumed to induce no energy dissipation, then for any deformation, we must have $\Phi = \mathrm{tr}\,(\boldsymbol{\sigma}\mathbf{d}) = 0$ or, in other words, $\boldsymbol{\sigma'} = -p\mathbf{1}$ since $\mathrm{tr}\,\mathbf{d} = 0$ (incompressible fluid). In the sequel, we shall see that there are some rules that must be satisfied in specifying a particular form of constitutive equation.

This way of expressing the stress tensor can be generalized to any type of material. It is customary in rheology to break down the stress tensor into two parts:

$$\boldsymbol{\sigma} = -p\mathbf{1} + \mathbf{s},$$

where p is now called the *mean pressure*

$$p = -\frac{1}{3}\mathrm{tr}\,\boldsymbol{\sigma},$$

and $\mathbf{s}$ is called the *deviatoric stress tensor* since it represents the departure from an equivalent equilibrium state.

Describing the rheological behavior of a material involves determining the relation between the stress tensor $\boldsymbol{\sigma}$ and the gradient tensor $\mathbf{F}$. The relation $\boldsymbol{\sigma} = \mathcal{F}(\mathbf{F})$, where $\mathcal{F}$ is a functional is called the *constitutive equation.* When the material is incompressible, the constitutive equation is usually defined with the extra-stress tensor since the stress tensor is defined to within an arbitrary function (pressure): $\mathbf{s} = \mathcal{F}(\mathbf{F})$.

▲ Keep in mind that pressure may have a meaning that differs depending on the context: thermodynamic pressure, hydrodynamic pressure, mean pressure.

2.2.3 Admissibility of a constitutive equations

There are a number of rules that must be used to produce constitutive equations that are admissible from the rational and physical standpoints. The establishment of these rules have been the subject of long debates and has been approached in a number of ways, the interrelation of which are by no means easy to understand (Oldroyd, 1950; Truesdell, 1966, 1974). Here we will deal with general principles without expounding all the details.

Objectivity or material indifference

A constant behavior in physics is to express laws that do not depend on a particular system of reference. Let us try now to apply this fundamental principle to the formulation of constitutive equation. We assume that a constitutive equation is a mathematical relation between the stress and the deformation, using a short-hand notation, we express

$$\boldsymbol{\sigma} = \mathcal{F}(\mathbf{F})$$

where $\mathcal{F}$ is a functional depending on the gradient tensor $\mathbf{F}$. We have seen earlier that $\mathbf{F}$ can include solid rotation. Solid rotation as wells as translation of a reference or a change of clock frame must not modify the physics, which implies that we must get rid of solid rotation and translation when expressing a constitutive equation.

Principle 1: *A constitutive equations is invariant under any change of reference frame.*

In practice this means that we make a change of variable

$$\mathbf{x}' = \mathbf{R}\cdot\mathbf{x} + \mathbf{b} \text{ and } t' = t + a,$$

which means that the image $\mathbf{x}'$ experiences a rotation (the tensor $\mathbf{R}$ can be time-dependent) and a translation ($\mathbf{b}$ is a constant vector) with respect to the original point $\mathbf{x}$; in addition there is change in the time reference (a being a constant), which merely shows that time can appears explicitly as variable in an objective tensor. Then, for a quantity to be objective we must check that:

- a scalar remains the same: $s' = s$,
- a vector must satisfy $\mathbf{x} = \mathbf{R}\cdot\mathbf{x}$
- a tensor $\mathbf{T}$ is objective if it transforms objective vectors into objective vectors, i.e., $\mathbf{T}'\cdot\mathbf{x}' = \mathbf{R}\cdot\mathbf{T}\cdot\mathbf{x}$ or equivalently
$$\mathbf{T}' = \mathbf{R}\cdot\mathbf{T}\cdot\mathbf{R}^T.$$

The issue lies in the dependence of $\mathbf{F}$ on a particular frame. For instance, we introduce a rotation of the reference frame, the gradient tensor is the new frame is

$$F'_{ij} = \frac{\partial x'_i}{\partial X_j} = \frac{\partial x'_i}{\partial x_k}\frac{\partial x_k}{\partial X_j},$$

with $R_{ik} = \partial x'_i/\partial x_k$ an orthogonal tensor that corresponds to a frame rotation: $\mathbf{x}' = \mathbf{R}\cdot\mathbf{x}$ (see Figure 2.6). We deduce that $\mathbf{F}' = \mathbf{R}\cdot\mathbf{F}$, which is not admissible.

Now, if we make use of the Cauchy tensor

$$\mathbf{C}' = \mathbf{F}'^T\cdot\mathbf{F}' = \mathbf{F}^T\cdot\mathbf{R}^T\cdot\mathbf{R}\cdot\mathbf{F} = \mathbf{F}^T\cdot\mathbf{F} = \mathbf{C},$$

which shows that $\mathbf{C}$ is not an objective tensor since it does depend on the frame. Similarly, it can be shown that the strain tensor $\mathbf{E}$ and the strain-rate tensor $\mathbf{d}$ are objective.

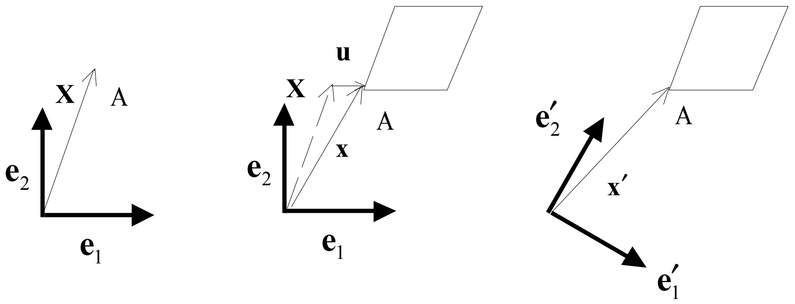

Figure 2.6 *Change of reference.*

Determinism

Principle 2: *The history of the thermo-kinetic process experienced by the material fully determines the current rheological and thermodynamic state of the material.* This principle must be relaxed slightly when the material is incompressible because the stress state is determined to within the hydrostatic pressure (which depends on the boundary conditions and the problem geometry).

Local action

Principle 3: *The thermodynamic process of a material at a given point is completely determined by the history of the thermo-kinetic process to which the neighborhood of the point was submitted.* In other words, the stress tensor at a given point does not depend on movements occurring at finite distance from this point.

2.2.4 Specific properties of material

A material is said to be

- *homogeneous* when the constitutive equation does not depend on the point considered;
- *isotropic* when the material response is invariant under rotation, i.e., when we consider a direction or another, we measure the same response.
- characterized by a *fading memory* when the material response depends on the very recent history.

The reader can refer to the book by Hutter & Jöhnk (2004) for further developments on *symmetry* in materials and their consequences in the constitutive equations.

2.2.5 Representation theorems

Cayley-Hamilton theorem

In algebra, the *Cayley-Hamilton theorem* says that from a second order tensor $\mathbf{M}$, we can build a third-order polynomial

$$P_M(\lambda) = \det(\mathbf{M} - \lambda\mathbf{1}) = -\lambda^3 + M_I\lambda^2 - M_{II}\lambda + M_{III},$$

where M_I, M_{II}, and M_{III} are called the fundamental invariants of $\mathbf{M}$, with

$$M_I = \operatorname{tr}\mathbf{M},\ M_{II} = \frac{1}{2}\left((\operatorname{tr}\mathbf{M})^2 - \operatorname{tr}\mathbf{M}^2\right),\ \text{and } M_{III} = \det\mathbf{M}.$$

The zeros of this polynomial are the eigenvalues of $\mathbf{M}$ and, moreover, we have the relation

$$P_M(\mathbf{M}) = 0.$$

The remarkable result is that it is possible to define three independent scalar quantities that are objective, i.e., they do not depend on the frame in which we can express $\mathbf{M}$ since they are scalar. From this viewpoint, it is equivalent to write $f = f(\mathbf{M})$ or $f = f(M_I,M_{II},M_{III})$. The benefit is twofold

- it is mostly easier to handle scalar quantities than tensors;
- we can reduce the number of variables needed for describing the behavior. For instance, instead of a second-order symmetric tensor (with 6 independent variables), we can use the three invariants without loss of information.

We will now show that it is possible to interpret the invariants physically.

Physical interpretation

Any combination of invariants is invariant. Using this principle, we can build invariants that are physically meaningful. For the stress tensor $\boldsymbol{\sigma}$ and the strain tensor $\boldsymbol{\epsilon}$, we introduce

- the first invariants of the stress tensor and the strain tensor are defined as

$$I_{1,\sigma} = \text{tr}\ \boldsymbol{\sigma} = 3\sigma_m \text{ and } I_{1,\epsilon} = \text{tr}\ \boldsymbol{\epsilon} = \frac{\Delta V}{V},$$

  showing that the first invariant of the stress tensor gives an idea of the mean pressure at a given point, while the first invariant of the strain tensor specifies the relative volume variation.
- the second invariant is usually defined as

$$I_{2,\sigma} = \text{tr}\ \mathbf{s}^2 \text{ and } I_{2,\epsilon} = \text{tr}\ \mathbf{e}^2,$$

  where $\mathbf{s} = \boldsymbol{\sigma} - \sigma_m \mathbf{1}$ is the deviatoric stress tensor and $\mathbf{e} = \boldsymbol{\epsilon} - I_{1,\epsilon}\mathbf{1}/3$ is the deviatoric strain tensor. The second invariant indicated how large the departure from the mean state is.
- the third invariant is mostly defined as

$$I_{3,\sigma} = \text{tr}\ \mathbf{s}^3 \text{ and } I_{3,\epsilon} = \text{tr}\ \mathbf{e}^3.$$

  We can show that the third invariant makes it possible to define a phase angle in the deviatoric plane[3].

$$\cos\phi = -\frac{\sqrt{6}I_3}{I_2^{3/2}}.$$

To illustrate these notions, let us assume that we know the stress tensor at a given point M. The stress tensor being symmetric, we know that there there is an orthogonal basis made up of the eigenvectors of $\boldsymbol{\sigma}$. In the stress space, where the coordinates are given by the eigenvalues of $\boldsymbol{\sigma}$ (hereafter referred to as σ_i with $1 \le i \le 3$), the stress state at M is represented by a point.

---

[3] plane passing through H and the normal of which is the first trissectrice

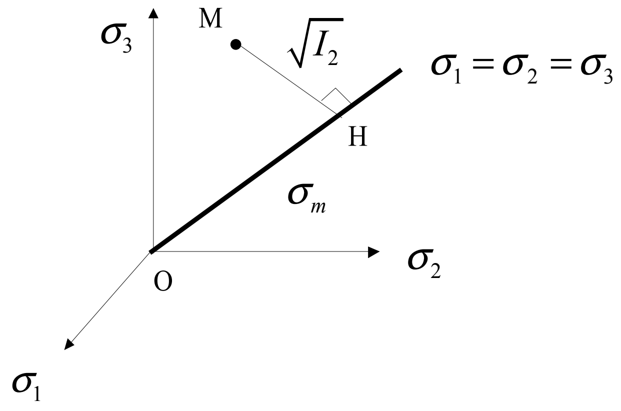

Figure 2.7 *Stress space.*

The position of this stress point can be given in terms of the Cartesian coordinates or in terms of invariants. Indeed, let us call H the projection of M onto the first trissectrice (straight line $\sigma_1 = \sigma_2 = \sigma_3$). To position M, we need the distances OH and HM together with an angle ϕ with respect to an arbitrary direction in the deviatoric plane. It is straightforward to show that

- OH represents the mean stress at M;
- HM represents the departure from an isotropic state and $|HM|^2 = I_{2,\sigma} = s_1^2 + s_2^2 + s_3^2$ where s_i are the eigenvalues of the deviatoric stress tensor.

Representation theorems

Representation theorems are an ensemble of rules that specify how to transform a tensor-valued expression into an expression involving invariants (Boehler, 1987; Zheng, 1994).

For instance, let us assume that we have to compute the strain energy function W of an elastic body. We can write that $W = W(\mathbf{E})$, where $\mathbf{E}$ is the strain tensor, or we can write $W = W(E_i)$ with E_i with $1 \leq i \leq 6$ the six independent components of $\mathbf{E}$. Using invariants, we can also write

$$W = W(I_{1,\epsilon},\, I_{2,\epsilon},\, I_{3,\epsilon}).$$

In doing so, we reduce the number of variables from 6 to 3. If we assume that there is a preferred direction of deformation $\mathbf{n}$, then we can write $W = W(\mathbf{E},\, \mathbf{n})$ (i.e., 9 variables) or

$$W = W(I_{1,\epsilon},\, I_{2,\epsilon},\, I_{3,\epsilon},\, \mathbf{n}\cdot\mathbf{E}\cdot\mathbf{n},\, \mathbf{n}\cdot\mathbf{E}^2\cdot\mathbf{n}),$$

reducing the number of variables from 9 to 5.

Representation of tensor-valued functions in complete irreducible forms has been proved to be very helpful in formulating nonlinear constitutive equations for isotropic or anisotropic materials.

2.2.6 Balance equations

Transport theorem

In any course on functional analysis, one can find the Leibnitz formula that shows how to derive an integral real-valued function, the boundaries of which may vary

$$\frac{\mathrm{d}}{\mathrm{d}x}\int_{a(x)}^{b(x)} f(x,\, t)\mathrm{d}t = \int_{a(x)}^{b(x)} \frac{\partial f(x,\, t)}{\partial x}\mathrm{d}t + f(b(x))\frac{\mathrm{d}b}{\mathrm{d}x} - f(a(x))\frac{\mathrm{d}a}{\mathrm{d}x}.$$

Leibnitz relation can be generalized to multiple integrals, i.e. integration is made on volumes instead of intervals. One obtains the following relation called *transport theorem*

$$\boxed{\frac{\mathrm{d}}{\mathrm{d}t}\int_V f\mathrm{d}V = \int_V \frac{\partial f}{\partial t}\mathrm{d}V + \int_S f\mathbf{u}\cdot\mathbf{n}\mathrm{d}S,} \tag{2.9}$$

where V is the control volume containing a given mass of fluid, S is the surface bounding this volume, and $\mathbf{n}$ is the vector normal to the surface S ; $\mathbf{n}$ is unitary ($|\mathbf{n}| = 1$) and outwardly oriented. This relation written here for a scalar function f holds for any vectorial function $\mathbf{f}$.

Equation (2.9) is fondamental since it makes it possible to derive all the equations needed in continuum mechanics. It can be interpreted as follows Any variation in f with time within the control volume V results from

- local change in f with time;
- flux of f through S (flux = inflow – outflow through V).

An helpful variant of the transport theorem is obtained by using the Green-Ostrogradski theorem :

$$\boxed{\frac{\mathrm{d}}{\mathrm{d}t}\int_V f\mathrm{d}V = \int_V \left(\frac{\partial f}{\partial t} + \nabla\cdot(f\mathbf{u})\right)\mathrm{d}V}.$$

This expression shall be used to derive local equations in the following.

▲ **Be careful**: a control volume is most often a material volume, i.e., it is made up of a collection of particles that are followed up in their motion; its borders are fluid and move with the fluid, which means that the boundary velocity corresponds to the local velocity at the boundary. On some occasions, we can also define an arbitrary control volume, the velocity of which $\mathbf{u}$ at the border surface S does not correspond to that of the fluid.

Another important variant of the transport theorem is the *Reynolds theorem* that applies to integrands that take the form ρf, with ρ the fluid density.

$$\boxed{\frac{\mathrm{d}}{\mathrm{d}t}\int_V \rho f\mathrm{d}V = \int_V \rho\frac{\mathrm{d}}{\mathrm{d}t}f\mathrm{d}V.} \tag{2.10}$$

Conservation of mass

Let us apply the transport theorem (2.9) to $f = \rho$:

$$\frac{\mathrm{d}}{\mathrm{d}t}\int_V \rho\mathrm{d}V = \int_V \frac{\partial\rho(\mathbf{x},t)}{\partial t}\mathrm{d}V + \int_S \rho\mathbf{u}\cdot\mathbf{n}\mathrm{d}S.$$

Making use of the divergence theorem (Green-Ostrogradski), we find

$$\frac{\mathrm{d}}{\mathrm{d}t}\int_V \rho\mathrm{d}V = \int_V \left(\frac{\partial\rho(\mathbf{x},t)}{\partial t} + \nabla\cdot(\rho\mathbf{u})\right)\mathrm{d}V = 0.$$

Note that the total mass is constant because we follow up a finite number of particles and there is no production or loss of particles.

When ρ is continuous, then we can pass from a control-volume formulation to a local equation

$$\boxed{\frac{\partial\rho(\mathbf{x},t)}{\partial t} + \nabla\cdot\rho\mathbf{u} = 0.} \tag{2.11}$$

This equation is often called *continuity equation*. It can also be cast in the following form:

$$\frac{1}{\rho}\frac{\mathrm{d}\rho}{\mathrm{d}t} = -\rho\nabla\cdot\mathbf{u}.$$

▲ Recall that passing from global to local equations is permitted only if the field is continuous. This is not always the case, e.g. when there is a *shock* inside the control volume. Specific equation must be used (see below).

Here are other helpful definitions

- a flow is said *isochoric* when $\frac{1}{\rho}\frac{\mathrm{d}\rho}{\mathrm{d}t} = 0$ (e.g., when the Mach number is less than unity, air flow is isochoric);
- a material is said *incompressible* when ρ is constant at any point and any time (water can be considered as incompressible under normal flow conditions).

Conservation of momentum

One applies the transport theorem (2.9) tho the momentum $f = \rho\mathbf{u}$:

$$\frac{\mathrm{d}}{\mathrm{d}t}\int_V \rho\mathbf{u}\mathrm{d}V = \int_V \frac{\partial \rho\mathbf{u}}{\partial t}\mathrm{d}V + \int_S \rho\mathbf{u}(\mathbf{u}\cdot\mathbf{n})\mathrm{d}S.$$

There are many variants of this equation, based either on different ways of expressing the material derivative of $\rho\mathbf{u}$ or on different ways of expressing the velocity (e.g., streamline function, vorticity). On applying the divergence theorem, one gets:

$$\frac{\mathrm{d}}{\mathrm{d}t}\int_V \rho\mathbf{u}\mathrm{d}V = \int_V \left(\frac{\partial \rho\mathbf{u}}{\partial t} + \nabla\cdot\rho\mathbf{u}\mathbf{u}\right)\mathrm{d}V,$$

or equivalently

$$\frac{\mathrm{d}}{\mathrm{d}t}\int_V \rho\mathbf{u}\mathrm{d}V = \int_V \rho\left(\frac{\partial \mathbf{u}}{\partial t} + \nabla\cdot\mathbf{u}\mathbf{u}\right)\mathrm{d}V.$$

The fundamental principle of Mechanics is that any time variation in momentum results from applying body or surface force(s) on the control volume

$$\frac{\mathrm{d}}{\mathrm{d}t}\int_V \rho\mathbf{u}\mathrm{d}V = \text{forces applied on } V.$$

Once again, we can obtain a local expression of the momentum balance equation if the fields are continuous:

$$\frac{\partial \rho\mathbf{u}}{\partial t} + \nabla\cdot\rho\mathbf{u}\mathbf{u} = \rho\mathbf{g} + \nabla\cdot\boldsymbol{\sigma},$$

or

$$\boxed{\rho\frac{\partial \mathbf{u}}{\partial t} + \rho\mathbf{u}\cdot\nabla\mathbf{u} = \rho\mathbf{g} + \nabla\cdot\boldsymbol{\sigma} = \rho\mathbf{g} - \nabla p + \nabla\cdot\mathbf{s}} \tag{2.12}$$

▲ **Be aware** that $\mathbf{u}\cdot\nabla\mathbf{u}$ does not mean the product between $\mathbf{u}$ and the tensor $\nabla\mathbf{u}$. Rigorously speaking, it would be better to write $(\mathbf{u}\cdot\nabla)\mathbf{u}$, the parentheses are used to say that $\mathbf{u}\cdot\nabla$ is a differential operator applied to $\mathbf{u}$.

2.2.7 Conservation of energy

Kinetic energy

The transport theorem (2.9) is now applied to the kinetic energy $f = E_c = \frac{1}{2}\rho|\mathbf{u}|^2$:

$$\frac{\mathrm{d}}{\mathrm{d}t}\int_V \frac{1}{2}\rho|\mathbf{u}|^2\mathrm{d}V = \int_V \frac{\partial E_c}{\partial t}\mathrm{d}V + \int_S \frac{1}{2}\rho|\mathbf{u}|^2(\mathbf{u}\cdot\mathbf{n})\mathrm{d}S.$$

As earlier for the momentum equation, there are variants of this equation depending on how the material derivative of E_c is expressed. Making use of the divergence theorem leads to

$$\frac{\mathrm{d}}{\mathrm{d}t}\int_V E_c \mathrm{d}V = \int_V \left(\frac{\partial E_c}{\partial t} + \nabla \cdot \left(\frac{1}{2}\rho|\mathbf{u}|^2\mathbf{u}\right)\right)\mathrm{d}V,$$

Note that the equation can be inferred from (2.12) by multiplying it by $\mathbf{u}$, then replacing terms such as $\mathbf{u}\partial\mathbf{u}$ with $\partial|\mathbf{u}|^2/2$, and then integrating over the control volume V. We then deduce the bulk expression of the *kinetic energy theorem*

$$\frac{\mathrm{d}}{\mathrm{d}t}\int_V E_c \mathrm{d}V = \text{power supplied to the volume } V - \text{power dissipated in } V,$$

$$\frac{\mathrm{d}}{\mathrm{d}t}\int_V E_c \mathrm{d}V = \int_V \rho\mathbf{u}\cdot\mathbf{g}\mathrm{d}V + \int_V \mathbf{u}\cdot(\nabla\cdot\boldsymbol{\sigma})\mathrm{d}V.$$

When the fields are continuous and making use of

$$\mathbf{u}\cdot(\nabla\cdot\boldsymbol{\sigma}) = \nabla\cdot(\mathbf{u}\cdot\boldsymbol{\sigma}) - \boldsymbol{\sigma}:\nabla\mathbf{u},$$

we can derive the local equation

$$\boxed{\frac{\partial E_c}{\partial t} + \nabla\cdot(E_c\mathbf{u}) = \rho\mathbf{u}\cdot\mathbf{g} + \nabla\cdot(\mathbf{u}\cdot\boldsymbol{\sigma}) - \boldsymbol{\sigma}:\nabla\mathbf{u}.} \tag{2.13}$$

We refer to $\Phi = \boldsymbol{\sigma} : \nabla\mathbf{u}$ as the *energy dissipation rate.* Using the decomposition of the strain rate tensor into its symmetric and antisymmetric parts, we also obtain

$$\Phi = \boldsymbol{\sigma} : \mathbf{d} = \mathrm{tr}\ (\boldsymbol{\sigma} : \cdot).$$

⇛ Recall that the energy balance theorem contains nothing more that the momentum balance equation does. For a regular problem, we can select either theorem; the choice is a matter of personal convenience or strategy (for alleviating computation). On some occasions, only one of these equations can be used in practice. For instance, when studying shock formation, it is usually better to use momentum balance equations because shocks induce energy dissipation that is not easy to compute.

⇛ In many practical applications (incompressible fluid in a steady regime), the energy balance equation can be transformed into the Bernoulli equation

$$\boxed{\frac{\partial E_c}{\partial t} + \nabla\cdot\left(\mathbf{u}\frac{\rho|\mathbf{u}|^2 + 2p_*}{2}\right) = \nabla\cdot(\mathbf{u}\cdot\mathbf{s}) - \mathbf{s}:\mathbf{d},}$$

where $p_* = p + \psi$ is the *generalized pressure*, with $\psi = \rho g z$ the gravity potential ($\rho\mathbf{g} = -\nabla\psi$). The *Bernoulli theorem* is obtained by assuming that

- the flow is steady, i.e. $\partial E_c/\partial t = 0$;
- the Reynolds number is high (the fluid is inviscid).

We then obtain

$$\nabla\cdot\left(\mathbf{u}\frac{\rho|\mathbf{u}|^2 + 2p_*}{2}\right) = \mathbf{u}\cdot\nabla\left(\frac{\rho|\mathbf{u}|^2}{2} + p_*\right) = 0,$$

which means that

$$\boxed{\Psi = \frac{1}{2}\rho|\mathbf{u}|^2 + p_* = \frac{1}{2}\rho|\mathbf{u}|^2 + p + \rho g z} \tag{2.14}$$

is constant along a streamline.

First axiom of thermodynamics

The first law of thermodynamics applied to a control volume V is the following statement

$$\begin{aligned}\text{rate of change of total energy} = \ & \text{rate of change of work of the forces applied to } V \\ & + \text{rate of heat addition.}\end{aligned} \quad (2.15)$$

We define the following quantities

- The *total energy* is the sum of the internal energy $E = \rho e$ (e internal energy per unit mass) and the kinetic energy $\rho u^2/2$.
- The rate of work is the power of the forces applied to the boundary and the body forces (e.g., gravity).
- The heat supplied to the control volume results from heat generated at points within V and from heat transmitted through the boundaries. The heat supply density is denoted by r and the heat flux is written $q = \mathbf{q}\cdot\mathbf{n}$, with $\mathbf{q}$ the heat flux vector (Stokes relation). When the Fourier law holds, the heat flux vector is related to the gradient temperature $\mathbf{q} = -\kappa\nabla T$, where κ is the *heat conductivity.*

Translated into mathematical terms, this statement becomes

$$\boxed{\frac{\mathrm{d}}{\mathrm{d}t}\int_V \rho\left(e+\frac{1}{2}u^2\right)\mathrm{d}V = \int_V \rho\mathbf{u}\cdot\mathbf{g}\mathrm{d}V + \int_A \mathbf{u}\cdot(\boldsymbol{\sigma}\cdot\mathbf{n})\mathrm{d}A + \int_V \rho r\mathrm{d}V - \int_A \mathbf{q}\cdot\mathbf{n}\mathrm{d}A,}$$

where A is the surface bounding V. The local form is

$$\rho\frac{\mathrm{d}}{\mathrm{d}t}\left(e+\frac{1}{2}u^2\right) = \rho\mathbf{u}\cdot\mathbf{g} + \nabla\cdot(\boldsymbol{\sigma}\mathbf{u}) - \nabla\mathbf{q} + \rho r.$$

Making use of the kinetic energy theorem leads to the following relation

$$\boxed{\rho\frac{\mathrm{d}e}{\mathrm{d}t} = \Phi - \nabla\mathbf{q} + \rho r,}$$

where $\Phi = \boldsymbol{\sigma} : \mathbf{d}$ is the dissipation rate (also called stress power). Variations in the internal energy are caused by (viscous) dissipation, the flux of heat, and/or a source/sink of heat.

Second axiom of thermodynamics

We end our discussion on energy conservation by recalling the second principle used in thermodynamics, which reflects the irreversibility of time processes associated with energy dissipation. The second law states that

$$\rho\dot{f} - \Phi + \rho\dot{T}s + \frac{1}{T}\mathbf{q}\cdot\nabla T \le 0$$

with $f = e - Ts$ the free energy per unit mass, s the entropy per unit mass, Φ the energy dissipation rate, $\mathbf{q}$ the heat flux vector, and T the temperature.

2.2.8 Jump conditions

In practice, there a number of situations where there are rapid changes in the flow features over relatively short distances. For instance, a high-speed airplane or spatial capsule creates a shock wave as it breaks the sound barrier., as shown in Figures 2.8 and 2.9

Figure 2.8 *A U.S. Navy airplane creates a shock wave as it breaks the sound barrier. The shock wave is visible as a large cloud of condensation formed by the cooling of the air. A smaller shock wave can be seen forming on top of the canopy.(U.S. Navy photo by John Gay).*

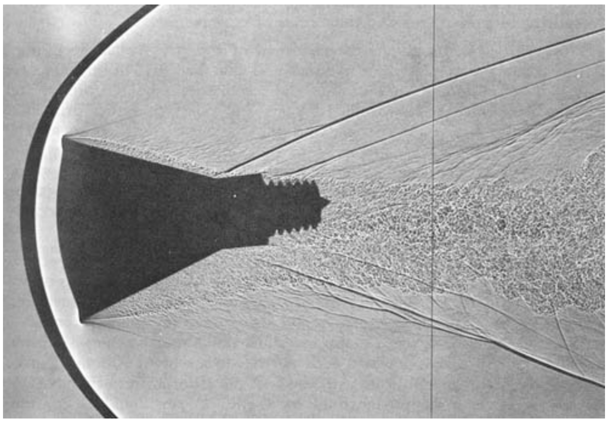

Figure 2.9 *A shadowgraph of the Project Mercury reentry capsule, showing the bow-shock wave in front of it and the flow fields behind the capsule. Photograph from NASA).*

In theory, it is usually appropriate to consider the shock as a discontinuity surface, i.e. a surface through the flow variables (density, velocity, etc.) may be become discontinuous. The local balance equations are valid on either side of the jump, but not at the shock surface. This implies that we have to specify the jump conditions on the flow variables induced by a shock. Note that a discontinuity surface may be an existing boundary (e.g. a free surface) or it may be created under some flow conditions. Spontaneous creation or disappearance of a shock surface is typical for hyperbolic partial differential equations (Courant & Friedrich, 1948). We will focus here on the latter case.

Let us first consider the scalar case. We have to solve a hyperbolic problem in the form:

$$\frac{\partial f(x,\,t)}{\partial t} + \frac{\partial G[f(x,\,t)]}{\partial x} = a(x,\,t),$$

where G is a function and a another function called the source term. Note that the equations looks like the balance equations we have seen earlier. Usually such an equation originates from the conservation of a quantity in a given control volume, i.e. an equation in the following integral form

$$\frac{\mathrm{d}}{\mathrm{d}t}\int_V f(x,\,t)\mathrm{d}x = G[f(x_2,\,t)] - G[f(x_1,\,t)] + \int_V a(x,\,t)\mathrm{d}x,$$

where the control volume corresponds to the range $[x_1, x_2]$ in the scalar case. When f is continuous over V, the two equations are equivalent. Let us assume that there is a moving point $x = s(t)$ within $[x_1, x_2]$ at which f admits a discontinuity. Making use of the Leibnitz rule, we have

$$\frac{\mathrm{d}}{\mathrm{d}t}\int_{x_1}^{x_2} f(x,\,t)\mathrm{d}x = \int_{x_1}^{s(t)} \frac{\partial f(x,\,t)}{\partial t}\mathrm{d}x + \int_{s(t)}^{x_2} \frac{\partial f(x,\,t)}{\partial t}\mathrm{d}x - \dot{s}[\![f]\!],$$

where have broken down $[x_1, x_2] = [x_1, s(t)] + [s, x_2(t)]$ and where $[\![f]\!]$ is the jump experienced by f:

$$[\![f]\!] = \lim_{x->s,\ x>0} f(x) - \lim_{x->s,\ x<0} f(x).$$

Then taking the limits $x_1 \to s$ and $x_2 \to s$, leads to

$$[\![G[f(x,\,t)] - \dot{s}f(x,\,t)]\!] = 0,$$

where $A = \int a(x,\,t)\mathrm{d}x$. The quantity is $G[f] - f\dot{s}$ is conserved through the shock. We can also deduce the shock velocity

$$\dot{s} = \frac{[\![G[f(x,\,t)]]\!]}{[\![f(x,\,t)]\!]}.$$

For instance, we can retrieve the *Rankine-Hugoniot shock conditions* used in gas dynamics if we take

- $f = \rho u$ (u being a velocity and ρ a density), $G[f] = \frac{1}{2}\rho u^2 + p$, and $a = 0$ (with p the pressure), we have the (scalar) momentum equation along an axis. The shock condition is then $[\![p + \frac{1}{2}\rho u^2]\!] = \dot{s}[\![\rho u]\!]$ at $x = s(t)$.
- $f = \rho$, $G[f] = \rho u$, and $a = 0$, we have the (scalar) mass equation along an axis. The shock condition is then $[\![\rho u]\!] = \dot{s}[\![\rho]\!]$ at $x = s(t)$. If we introduce the relative velocity $u' = u - \dot{s}$, we have also $[\![\rho u']\!] = 0$, which means that in the frame relative to the shock, the mass flux is conserved.

This equation can be generalized to higher dimensions without any problem.

▲ When dealing with shocks, it is very important to use the original conservation equations (in an integral form) from which the local equation has been derived. Typically, when the field are continuous, the equations

$$\frac{\partial \rho u}{\partial t} + u\frac{\partial \rho u}{\partial x} = 0,$$

and

$$\frac{\partial u}{\partial t} + u\frac{\partial u}{\partial x} = 0,$$

are equivalent because of the continuity equation. However, the former equation comes directly from the conservation of momentum (hence it is called the *conservative* form and ρu a conservative variable), whereas the latter is a simplification (called *non-conservative* form). It we reintegrate these equations to obtain the shock conditions, we will not find the same shock velocity. For this reason, care must be taken in computing shock conditions related to a hyperbolic partial differential equation.

2.3 Phenomenological constitutive equations

In many cases, most of the available information on the rheological behavior of a material is inferred from simple shear experiments. But, contrary to the Newtonian (linear) case, the tensorial form cannot be merely and easily generalized from the scalar expression fitted to experimental data. In this chapter, we have seen that:

- First, building a three-dimensional expression of the stress tensor involves respecting a certain number of formulation principles. These principles simply express the idea that the material properties of a fluid should be independent of the observer or frame of reference (principle of material objectivity) and the behavior of a material element depends only on the previous history of that element and not on the state of neighboring elements (Bird *et al.*, 1987).
- Then it is often necessary to provide extra information or rules to build a convenient expression for the constitutive equation.

We shall illustrate this with several examples.

2.3.1 Newtonian behavior

We start with an application of the representation theorem and the virtual power principle. We have an isotropic, incompressible, homogenous material assumed to be viscous. When it deforms, the energy dissipation rate Φ is fonction of the state of deformation, or more specifically of the strain rate $\mathbf{d}$, hence we write

$$\Phi = \Phi(\mathbf{d}),$$

but, making use of the representation, we can directly deduce the equivalent but more reduced form

$$\Phi = \Phi(d_I,\, d_{II},\, d_{III}),$$

where d_i represents the ith invariant of the strain-rate tensor. Since the material is isotropic, Φ does not depend on d_{III}; since it is incompressible, we have $d_I = 0$. Now we assume that we have a linear behavior, i.e., the energy rate dissipation must be a quadratic function of the invariants since dissipation = stress × strain rate $\propto$ strain rate^2. So we get

$$\Phi = \Phi(d_I,\, d_{II},\, d_{III}) = -\alpha d_{II},$$

with $\alpha > 0$ a constant and $d_{II} = -\frac{1}{2}\mathrm{tr}\,\mathbf{d}^2 = -\frac{1}{2}d_{kl}d_{kl}$ (Einstein's convention used). The extra-stress tensor is defined as

$$s_{ij} = \frac{\partial \Phi}{\partial d_{ij}} = \alpha \frac{1}{2}\frac{\partial d_{kl}d_{kl}}{\partial d_{ij}} = \alpha d_{kl}\delta_{ik}\delta jl = \alpha d_{ij},$$

from which we retrieve the Newtonian constitutive equation by posing $\alpha = 2\mu$.

2.3.2 Viscoplastic behavior

When a fluid exhibits viscoplastic properties, we usually fit experimental data with a Bingham equation as a first approximation (Bird *et al.*, 1983):

$$\dot\gamma > 0 \Rightarrow \tau = \tau_c + K\dot\gamma \tag{2.16}$$

Equation (2.16) means that

- for shear stresses in excess of a critical value, called the yield stress, the shear stress is a linear function of the shear rate;

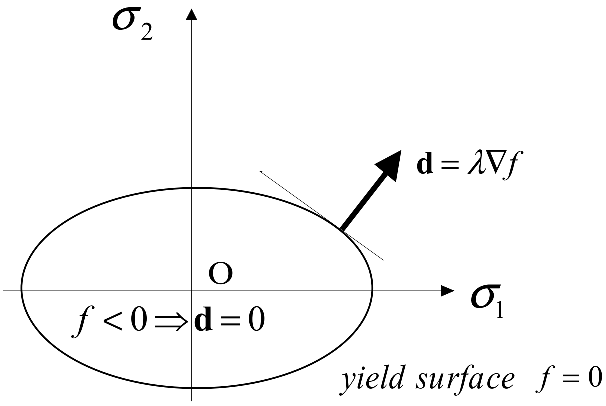

Figure 2.10 *Yield surface delimiting two domains*

- conversely when $\tau \leq \tau_c$ there is no shear within the fluid ($\dot\gamma = 0$).

The question arises as to how the scalar expression can be transformed into a tensorial form. The usual but not the only way is to consider a process, called *plastic rule*, as the key process of yielding.

A plastic rule includes two ingredients.

- First, it postulates the existence of a surface in the stress space (σ_1,σ_2,σ_3) delimiting two possible mechanical states of a material element (σ_i denotes a principal stress, that is an eigenvalue of the stress tensor), as depicted in Fig. 2.10. The surface is referred to as the *yield surface* and is usually represented by an equation in the form $f(\sigma_1,\sigma_2,\sigma_3) = 0$. When $f < 0$, behavior is generally assumed to be elastic or rigid. When $f = 0$, the material yields.
- Second it is assumed that, after yielding, the strain-rate is directly proportional to the surplus of stress, that is, the distance between the point the representing the stress state and the yield surface. Translated into mathematical terms, this leads to write: $\dot\gamma = \lambda\nabla f$ with λ a proportionality coefficient (Lagrangian multiplier).

How must the yield function f be built to satisfy the principle of material objectivity? For f to be independent of the frame, it must be expressed not as a function of the components of the stress, but as a function of its invariants:

- The first invariant $I_1 = \mathrm{tr}\,\boldsymbol{\sigma} = \sigma_1 + \sigma_2 + \sigma_3$ represents the *mean stress* multiplied by 3 ($|\mathbf{OP}| = I_1/3$ in Fig. 2.11),
- the second invariant $I_2 = (\mathrm{tr}^2\boldsymbol{\sigma} - \mathrm{tr}\boldsymbol{\sigma}^2)/2 = -\mathrm{tr}(\mathbf{s}^2)/2$ can be interpreted as the deviation of a stress state from the mean stress state ($|\mathbf{PM}|^2 = -2I_2$ in Fig. 2.11) and is accordingly called the *stress deviator.*
- The third invariant $I_3 = -\mathrm{tr}\,\mathbf{s}^3/6$ reflects the angle in the deviatoric plane made by the direction **PM** with respect to the projection of -axis and is sometimes called the *phase* ($\cos^2 3\varphi = I_3^2/I_2^3$ in Fig. 2.11).

If the material is isotropic and homogenous, the yield function f is expected to be independent of the mean pressure and the third invariant. Thus we have $f(\sigma_1,\sigma_2,\sigma_3) = f(I_2)$. In plasticity, the simplest yield criterion is the *von Mises criterion*, asserting that yield occurs whenever the deviator exceeds a critical value (whose root gives the yield stress): $f(I_2) = \sqrt{-I_2} - \tau_c$. As depicted in Fig. 2.11, the yield surface is a cylinder of radius τ_c centered around an axis $\sigma_1 = \sigma_2 = \sigma_3$. If we draw the yield surface in the extra-stress space, we obtain a sphere of radius $\sqrt{2}\tau_c$.

Once the stress state is outside the cylinder defined by the yield surface, a flow occurs within the material. In a linear theory it is further assumed that the strain rate is proportional to the

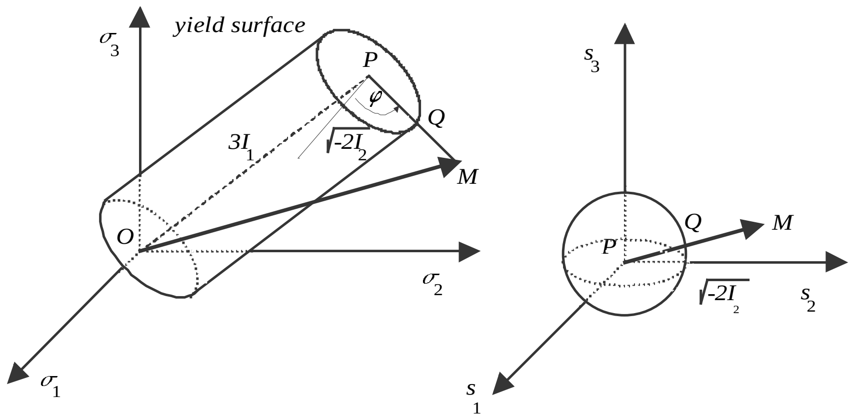

Figure 2.11 *On the left, the yield surface in the stress space when the von Mises criterion is selected as yield function. A stress state is characterized by its three principal stresses and thus can be reported in the stress space. The three invariants of the stress tensor can be interpreted in terms of co-ordinates*

increment in stress (distance from the point representing the stress state M to the yield surface) and collinear to the normal $\partial f/\partial \mathbf{s}$. This leads to the expression:

$$\mathbf{d} = \lambda\left(\sqrt{I_2} - \tau_c\right)\frac{\mathbf{s}}{\sqrt{I_2}} \tag{2.17}$$

For convenience, we define the proportionality coefficient as: $\lambda^{-1} = 2\eta$. It is generally more usual to express the constitutive equation in the converse form. First, the second invariant of the strain rate tensor J_2 can be expressed as $J_2 = -\mathrm{tr}(\mathbf{d}^2)/2 = \left(\lambda\left(\sqrt{-I_2} - \tau_c\right)\right)^2$. Then we deduce the usual form of the Bingham constitutive equation:

$$\mathbf{d} = 0 \Leftrightarrow \sqrt{-I_2} \leq \tau_c \tag{2.18}$$

$$\mathbf{d} \neq 0 \Leftrightarrow \boldsymbol{\sigma} = -p\mathbf{1} + \left(2\eta + \frac{\tau_c}{\sqrt{-J_2}}\right)\mathbf{d} \tag{2.19}$$

It is worth noting that contrary to the Newtonian case, the general tensorial expression (2.18) cannot not easily be extrapolated from the steady simple-shear equation (2.16).

2.3.3 Viscoelasticity

When studying the linear 1D Maxwell model in § 1.5.4, we obtained an equation in the form

$$\frac{\mathrm{d}\gamma}{\mathrm{d}t} = \frac{1}{G}\frac{\mathrm{d}\tau}{\mathrm{d}t} + \frac{\tau}{\mu},$$

where G is the elastic modulus and μ denotes viscosity. We would like to transform this empirical equation into a 3D tensorial expression and naively we write

$$2\mu\mathbf{d} = \frac{\mu}{G}\frac{\mathrm{d}\boldsymbol{\sigma}}{\mathrm{d}t} + \boldsymbol{\sigma},$$

but it is not difficult to see that this expression does not satisfy the objectivity principle. According to this principle, the stress tensor does not depend on the frame in which we use it (or its components) or, in other words, it must be invariant under any rotation. Let us consider the stress tensor when the frame of reference is rotated. We have

$$\boldsymbol{\sigma}' = \mathbf{R}\cdot\boldsymbol{\sigma}\cdot\mathbf{R}^T$$

the image of $\boldsymbol{\sigma}$, where $\mathbf{R}$ is an orthogonal tensor. Taking the time derivative leads to

$$\frac{\mathrm{d}}{\mathrm{d}t}\boldsymbol{\sigma}' = \frac{\mathrm{d}\mathbf{R}}{\mathrm{d}t}\cdot\boldsymbol{\sigma}\cdot\mathbf{R}^T + \mathbf{R}\cdot\frac{\mathrm{d}\boldsymbol{\sigma}}{\mathrm{d}t}\cdot\mathbf{R}^T + \mathbf{R}\cdot\boldsymbol{\sigma}\cdot\frac{\mathrm{d}\mathbf{R}^T}{\mathrm{d}t} \neq \mathbf{R}\cdot\frac{\mathrm{d}\boldsymbol{\sigma}}{\mathrm{d}t}\cdot\mathbf{R}^T,$$

which shows that $\dot{\boldsymbol{\sigma}}$ is not objective. To overcome this issue, we have to define a kind of time derivative that satisfies the objectivity principle. For this purpose, note that if we replace $\boldsymbol{\sigma}$ with $\mathbf{R}^T\cdot\boldsymbol{\sigma}'\cdot\mathbf{R}$ and introduce $\boldsymbol{\Omega} = \dot{\mathbf{R}}\cdot\mathbf{R}^T$, we have $\dot{\boldsymbol{\sigma}}' = \mathbf{R}\cdot\boldsymbol{\sigma}\cdot\mathbf{R} + \boldsymbol{\Omega}\cdot\boldsymbol{\sigma}' + \boldsymbol{\sigma}'\cdot\boldsymbol{\Omega}^T$, which can be transformed by making use of the antisymmetry of $\boldsymbol{\Omega}$: $\dot{\boldsymbol{\sigma}}' = \mathbf{R}\cdot\dot{\boldsymbol{\sigma}}\cdot\mathbf{R}^T + \boldsymbol{\Omega}\cdot\boldsymbol{\sigma}' - \boldsymbol{\sigma}'\cdot\boldsymbol{\Omega}$. If we want to transform this derivative into an objective derivative, we have to get rid of the last two contributing terms. There are different possibilities. Oldroyd introduced the Oldroyd (or convective contravariant) derivative as follows:

$$\overset{\triangle}{\boldsymbol{\sigma}} = \dot{\boldsymbol{\sigma}} - \mathbf{L}\cdot\boldsymbol{\sigma} - \boldsymbol{\sigma}\cdot\mathbf{L}^T,$$

where $\mathbf{L}$ is the velocity gradient tensor. In this way, it is possible to

- provide a proper tensorial formulation of the constitutive equation;
- make an empirical law (primarily valid for small deformations) consistent with large deformations.

The stress tensor is then solution to

$$2\mu\mathbf{d} = \frac{\mu}{G}\overset{\triangle}{\mathbf{s}} + \mathbf{s}.$$

Note that in this particular case, we do not have necessarily tr $\mathbf{s}$, which is a typical example of a fluid for which the extra-stress tensor differs from the deviatoric the stress tensor.

Chapter 3

Rheophysics

Prerequisites

- fluid mechanics: conservation law
- mathematics: differential analysis, probability, algebra tools

Objectives

- to provide the mathematical basis underpinning kinetic theory
- to review a few averaging techniques
- to deal with approximate methods for finding tractable analytical expressions
- to introduce the readers with the modelling of particle suspension

Content

My presentation focuses on dynamic properties of particle suspensions. Because the behavior is complex, study of idealized situations makes it easier to understand the physics behind. We start the chapter by outlining the relationship existing between a single particle and a fluid phase. Dimensionless numbers such as the Reynolds and the Stokes numbers are very helpful in characterizing the strength of the phase coupling. On extreme cases, when the particle is the slave or completely independent of the fluid phase, fully analytical derivations of the bulk constitutive equation are possible. We show that using appropriate averaging procedures make it possible to construct the bulk stress tensor from the governing equations describing the motion on the bulk scale. At the end of this chapter, we give some clues to understand the physics of concentrated suspensions that offer a substantial and challenging field of investigations.

3.1 Fundamentals of rheophysics

3.1.1 Movement of a single sphere and consequences on the flow regime

An overview

In the rheology of particle suspensions, the starting point in any rheophysical approach is to examine the behavior of individual components on a particle scale, then to infer the bulk rheological behavior by using an appropriate average process. In order to avoid overly general explanations, we assume that

(i) the interstitial fluid is Newtonian, with viscosity μ and density ρ_f;
(ii) the particles are rigid, spherical, and of equal size (radius a, density ρ_p).

Fluid motion is described by the Navier-Stokes equations:

$$\frac{\partial \mathbf{u}_f}{\partial t} + \mathbf{u}_f \cdot \nabla \mathbf{u}_f = -\frac{1}{\rho_f}\nabla p + \frac{1}{\rho_f}\nabla \cdot \boldsymbol{\sigma}_f, \tag{3.1}$$

$$\nabla \cdot \mathbf{u}_f = 0, \tag{3.2}$$

where $\mathbf{u}_f$ is the fluid velocity, p is the generalized pressure (including the fluid pressure and gravity potential), and $\boldsymbol{\sigma}_f$ is the stress tensor (here $\boldsymbol{\sigma}_f = 2\mu\mathbf{d}$ where $\mathbf{d}$ denotes the strain-rate tensor). The equation of motion for the particle can be written in the following Lagrangian form:

$$\frac{d\mathbf{u}_p}{dt} = \mathbf{g} + \frac{1}{m_p}\mathbf{F}(\mathbf{u}_p,\mathbf{u}_f), \tag{3.3}$$

where $\mathbf{F}(\mathbf{u}_p,\mathbf{u}_f)$ is the force field resulting from the interaction between the fluid and the particle, m_p is the particle mass, and $\mathbf{u}_p$ the velocity of the mass center. The boundary conditions at the solid/fluid interface reflect non-penetration and fluid adherence: $\mathbf{u}_f \cdot \mathbf{k} = 0$, where $\mathbf{k}$ denotes the outwardly-oriented unit normal.

Note that

- the force field $\mathbf{F}(\mathbf{u}_p,\mathbf{u}_f)$ is not yet defined;
- when expressing the dependence of $\mathbf{F}$ on the flow variables, we assume that it depends on the instantaneous particle velocity and the (Eulerian) velocity field (given by the Navier-Stokes equations).

The interplay between the two sets of equations is obvious since to solve the Navier-Stokes equations, we need to know the boundary conditions, hence the particle position, and in the meantime, to know this particle position, we have to determine the fluid velocity field.

To obtain a more physical picture of the fluid/particle interplay, we introduce dimensionless numbers and transform the equations above into dimensionless expressions. Let us introduce a velocity scale U for the fluid. The timescale for the fluid motion near the particle is then: $t_f = a/U$. The characteristic time for the particle is defined as a relaxation time, that is, the time needed for its velocity to vary substantially as a result of the fluid action. If F is the order of magnitude of the fluid-particle interaction, examining Eq. (3.3) leads to selecting: $t_p = m_pU/F$. The equations of motion can now be written in dimensionless form as follows (dimensionless variables have a tilde):

$$\mathrm{Re}_p\left(\frac{\partial \tilde{\mathbf{u}}_f}{\partial \tilde{t}} + \tilde{\mathbf{u}}_f \cdot \nabla \tilde{\mathbf{u}}_f\right) = -\frac{P\rho_f a}{\mu U}\nabla \tilde{p} + \Delta \tilde{\mathbf{u}}_f \tag{3.4}$$

where P is the pressure scale [here $P = \mu U/(\rho_f a)$] and

$$\mathrm{Re}_p = \rho_f U a/\mu,$$

is the *particle Reynolds number*. For the particle, one obtains:

$$\mathrm{St}\frac{d\tilde{\mathbf{u}}_p}{d\tilde{t}} = \frac{m_p}{F}\mathbf{g} + \tilde{\mathbf{F}}(\tilde{\mathbf{u}}_p,\tilde{\mathbf{u}}_f), \tag{3.5}$$

where

$$\mathrm{St} = \frac{t_p}{t_f} = \frac{m_p U^2}{Fa},$$

is called the *Stokes number*[1]. Two asymptotic regimes can be achieved depending on the value of the Stokes number:

- St ≫ 1. The fluid has no time to adjust its velocity to the variations in the particle velocity and, conversely, the particle is not affected by the rapid variations in the fluid velocity (but naturally it continues to be affected by the slow variations). In practice, this means that the fluid and the particle evolve in a quasi-autonomous way and, therefore, their motion can be considered separately. On a macroscopic scale, such suspensions retain a genuinely two-phase character and the equations of motion take the form of two interrelated equations (one for each phase).
- St → 0. The particle has time to adjust its velocity to any change in the fluid velocity field. As an illustration, one says that the particle is the slave of the fluid phase. On a macroscopic scale, this means that the suspension behaves as a one-phase medium.

From this discussion, one must keep in mind that, if in essence any particle suspension is a two-phase material on a particle scale, the suspension can behave as a one-phase fluid on a macroscopic scale. In addition the only asymptotic regimes for which it is possible to deduce the fluid-particle interaction in a completely theoretical way are the regimes $\mathrm{St} \to 0$ and $\mathrm{Re}_p \to 0$ and $\mathrm{St} \to \infty$ and $\mathrm{Re}_p \to \infty$.

Potential flow past a sphere

When Re_p is large, we can neglect the viscous forces. If the fluid flow is irrotational and steady with a uniform velocity $\mathbf{U}$, then introducing the streamline function ψ and the velocity potential ϕ ($\mathbf{u} = \nabla\phi$), we can transform the governing equations into the Laplace equation

$$\nabla^2\phi = 0.$$

There is a well-known solution to this equation when the fluid is unbounded and comprises a particle alone (see § 2.9, § 6.8, Batchelor, 1967)

$$\phi(\mathbf{r}) = \mathbf{U}\cdot\mathbf{r}\left(1 + \frac{a^3}{2|\mathbf{r}|^3}\right),$$

from which we deduce the velocity components

$$u_r = U\cos\theta\left(1 - \frac{a^3}{r^3}\right) \text{ and } u_\theta = U\cos\theta\left(1 + \frac{a^3}{2r^3}\right),$$

in spherical coordinates ($\mathbf{r}$ is measured relative to the sphere center). The streamlines are given by

$$\psi = \frac{1}{2}Ur^2\sin^2\theta\left(1 - \frac{a^3}{r^3}\right),$$

from which we can deduce the path lines (trajectories) of fluid particles (see Fig. 3.1).

---

[1] When $\mathrm{Re}_p \to 0$, then the viscous force underwent by the particle is $F = 6\pi\mu a U$ (demonstration given below), which leads to the classic expression given in several books for the Stokes number: $\mathrm{St} = \frac{2}{9}\frac{a^2 U}{\nu}$.

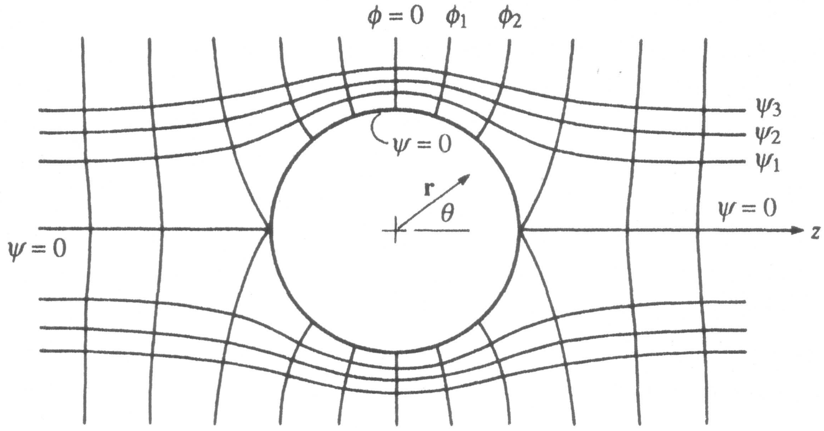

Figure 3.1 *Streamlines and isopotential lines for an inviscid flow (at high Reynolds number) past a stationary sphere.*

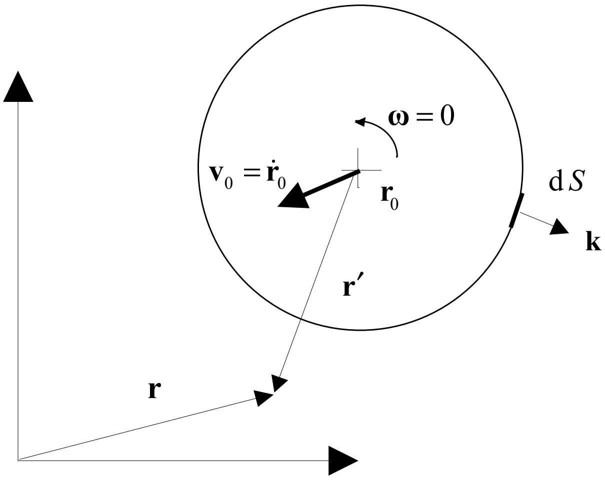

Figure 3.2 *Notation used in the computation.*

The problem of more complicated velocity fields has been long investigated (Lhuillier, 1982*b*; Auton *et al.*, 1988; Howe *et al.*, 2001). Here we proposed some results by following the derivation proposed by Lhuillier (1982*b*,*a*) (see also Drew & Passman, 1999, pp. 162–163), who assumed that the velocity field in the absence of particles is in the form

$$\mathbf{u}(\mathbf{r},\, t) = \mathbf{u}_\infty(t) + \mathbf{G}(t) \cdot \mathbf{r} + \frac{1}{2}\mathbf{r}\mathbf{r} : \mathbf{H}(t),$$

where $\mathbf{u}_\infty(t)$ stands for a time-dependent uniform motion, the second term on the right-hand side $\mathbf{G}(t) \cdot \mathbf{r}$ represents a deformation gradient, while the last term is a high-order (quadratic) term representing a gradient of strain rate (note that this equation is a kind of Taylor expansion, thus is a quite general representation of velocity fields).

Now we add a single particle of radius a and we refer to its position (position of the center of mass) as $\mathbf{r}_0$. The boundary conditions at the surface of this particle ($|\mathbf{r} - \mathbf{r}_0| = a$) are

$$\mathbf{v}_p \cdot \mathbf{k} = \mathbf{u} \cdot \mathbf{k} = \nabla\phi \cdot \mathbf{k},$$

with $\mathbf{u}$ the fluid velocity, $\mathbf{v}_p$ the velocity of the particle at the solid interface, and $\mathbf{k}$ the outward normal to the surface. Far from the sphere, we assume that the velocity match the velocity in the absence of the particle. The potential function related to the disturbed velocity field and consistent with the boundary conditions at the free surface of a particle is found to be

$$\phi(\mathbf{r},\, t|\mathbf{r}_0) = \mathbf{u}_\infty(t)\cdot\mathbf{r} + \frac{1}{2}\mathbf{G}(t) : \mathbf{r}\mathbf{r} + \frac{a^3}{2r'^3}\left(\mathbf{u}_0 - \frac{\mathrm{d}\mathbf{r}_0}{\mathrm{d}t}\right)\cdot\mathbf{r}' + \frac{a^5}{3r'^5}\mathbf{G} : \mathbf{r}'\mathbf{r}',$$

where for simplicity, we omit the **H**-dependent terms and where $r' = |\mathbf{r} - \mathbf{r}_0|$, $\mathbf{u}_0 = \mathbf{u}(\mathbf{r}_0)$, $\mathbf{r}_0$ is the position of the center of mass of the particle, i.e, the fluid velocity at the position actually occupied by the center of mass (see Fig. 3.2). The first two terms on the right-hand side represent the potential in the absence of the particle (i.e., the velocity field very far from the particle), whereas the two other contributions represent how the particle disturbs the fluid velocity field. Taking the gradient of the potential function provided the velocity field disturbed by a particle located at $\mathbf{r}_0$ and moving at velocity $\dot{\mathbf{r}}_0$

$$\mathbf{u}(\mathbf{r},\, t|\mathbf{r}_0) = \mathbf{u}(\mathbf{r},\, t) + \frac{1}{2}\left(\frac{a}{r'}\right)^3(\mathbf{u}_0 - \dot{\mathbf{r}}_0)\cdot\left(\mathbf{1} - 3\frac{\mathbf{r}'\mathbf{r}'}{r'^2}\right) + \frac{2}{3}\left(\frac{a}{r'}\right)^5\mathbf{r}'\cdot\mathbf{G}\cdot\left(\mathbf{1} - \frac{5}{2}\frac{\mathbf{r}'\mathbf{r}'}{r'^2}\right).$$

We can compute the force exerted by the fluid on the particle, which arises from the pressure at the body surface

$$\mathbf{F} = \int_A (-p)\mathbf{k}\mathrm{d}A.$$

Using the Bernoulli equation for unsteady irrotational flows, we infer that the pressure is

$$\frac{\partial\phi}{\partial t} + \frac{1}{2}|\mathbf{u}|^2 + \frac{p}{\rho_f} - \mathbf{g}\cdot\mathbf{r} = constant,$$

where we note that the potential functions cannot be steady because of the motion of the sphere and the constant can be embedded in ϕ. We then deduce

$$\mathbf{F} = \rho_f\int_A \frac{\partial\phi}{\partial t}\mathbf{k}\mathrm{d}A + \frac{1}{2}\rho_f\int_A \mathbf{u}\cdot\mathbf{u}\mathbf{k}\mathrm{d}A - \rho_f\int_A \mathbf{g}\cdot\mathbf{r}\mathbf{k}\mathrm{d}A.$$

We finally obtain

$$\boxed{\frac{\mathbf{F}}{\frac{4\pi}{3}a^3\rho_f} = -\mathbf{g} + \frac{\mathrm{d}\mathbf{u}}{\mathrm{d}t} + \frac{1}{2}\left(\frac{\mathrm{d}\mathbf{u}}{\mathrm{d}t} - \dot{\mathbf{r}}_0\right),}$$

where $\mathrm{d}\mathbf{u}/\mathrm{d}t$ represents the acceleration of the undisturbed flow at the center of mass of the sphere. The last term on the right-hand side is called the *added-mass effect*. Note that in the absence of fluid acceleration, the net force (i.e., ignoring the gravity force) is zero. This result is well-known in fluid mechanics and is often referred to as the d'Alembert paradox.

Stokes flow past a sphere

Conversely, when the Reynolds number comes close to zero $\mathrm{Re}_p \to 0$, a good approximation to the equations of motion is provided by the Stokes equation

$$\nabla\cdot\mathbf{u} = 0, \tag{3.6}$$

$$\nabla p = \mu\nabla^2\mathbf{u}. \tag{3.7}$$

These equations exhibit two specific properties that deserve a few comments:

- since the time derivative has been removed, the equations provide a pseudo-static description of the motion;
- the equations are linear, hence we can use the *superposition principle* to find solutions to complicated boundary-value problems. This is the key point in most analytical and numerical treatment used for solving the Stokes equations.

By taking the divergence of the momentum equation, it can be shown that the pressure is a harmonic function while the velocity field is biharmonic:

$$\nabla^2 p = 0 \text{ and } \nabla^4 \mathbf{u} = 0,$$

which may simplify the problem, especially when there is a free surface (e.g., see Garabedian, 1966; Pozrikidis, 1992).

We are trying to determine the viscous force exerted on a particle by the surrounding fluid as a function of the particle velocity. There are two sub-problems encompassed in the original formulation:

- *mobility* problem: we assume that we know the viscous force and torque experienced by the particle and we seek its velocity;
- *resistance* problem: we seek the force and torque experienced by the particle when its velocity is prescribed.

The former solutions to the Stokes equations were constructed by using the method called 'the separation of variables' (Lamb, 1932). Nowadays, it is more usual to use the *singular solution* method (Green's function) extensively used in elasticity and electrostatics. The original momentum equations is replaced by

$$\nabla p = \mu \nabla^2 \mathbf{u} + \delta(\mathbf{x} - \mathbf{x}_0)\mathbf{f}(\mathbf{x}), \tag{3.8}$$

where $\mathbf{f}$ is a singular point force and δ is the Dirac function. Physically this equation means that when a force $\mathbf{F}$ is exerted on a sphere immersed in a unbounded Newtonian fluid, one expects that sufficiently far from the sphere, the velocity and pressure fields are the same as those caused by a force of the same magnitude concentrated at point $\mathbf{x}_0$, i.e., the details of the flow in close vicinity around the sphere are lost. The first building block for constructing the solution is to seek a 'far-field' approximation. Using the Fourier transform of the modified momentum equation (3.8) or using the vorticity formulation of this momentum equation (Landau & Lifschitz, 1987), we can show that the fluid velocity field is

$$\mathbf{u}(\mathbf{x}) = \frac{1}{8\pi\mu}\left(\frac{\mathbf{1}}{x} + \frac{\mathbf{x}\mathbf{x}}{x^3}\right)\cdot\mathbf{f},$$

while the pressure field takes the form

$$p(\mathbf{x}) = \frac{1}{4\pi x^3}\mathbf{x}\cdot\mathbf{f},$$

where for the sake of simplicity, we have posed $\mathbf{x}_0 = 0$ (see pp. 32–33, Russel *et al.*, 1995), (see pp. 36–39, Kohr & Pop, 2004). In the velocity field expression, the multiplier of $\mathbf{f}$ is called the *Oseen tensor* (or Oseen-Burgers tensor) or the *free-space Green function*[2]

$$\mathbf{u}(\mathbf{x}) = \mathbf{I}\cdot\mathbf{f}, \text{ with } \mathbf{I} = \frac{1}{8\pi\mu}\left(\frac{\mathbf{1}}{x} + \frac{\mathbf{x}\mathbf{x}}{x^3}\right).$$

The linearity of the solution appears clearly in this expression. This singular solution to the modified Stokes equations is usually called the *Stokeslet*. In the literature, Stokeslet refers to both the force density $\mathbf{f}$ and the velocity field induced by this force. Sometimes, $\mathbf{f}$ is introduced as $\mathbf{f} = 8\pi\mu\boldsymbol{\alpha}$, with $\boldsymbol{\alpha}$ the strength (Kim & Karrila, 1991).

---

[2] There is a classification of Green functions depending on the topology of the domain of flow (bounded, unbounded, semi-bounded). The free-space Green function corresponds to an infinite fluid domain.

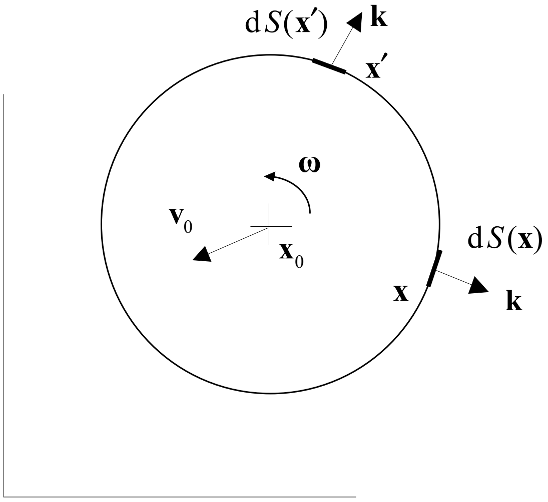

Figure 3.3 *Integration on the sphere surface.*

Let us now compute the force exerted by the fluid on a particle by following the approach developed by Batchelor (1972). We assume that there is a spherical rigid particle of radius a at $\mathbf{x} = \mathbf{x}_0$. The velocity field before the introduction is $\mathbf{u}_\infty(\mathbf{x})$ and is assumed to be known (note that at infinity, this field is still correct to order $O(1/x)$, but is not valid close to the particle). A surface distribution of force of density $\mathbf{f} = \boldsymbol{\sigma}_f \cdot \mathbf{k}$ is now applied to the particle surface S. Using the superposition principle[3], we deduce that the additional velocity at point $\mathbf{x}$ due to this force distribution is

$$\mathbf{u}' = -\int_S \mathbf{I}(\mathbf{x}-\mathbf{x}')\cdot \mathbf{f}\mathrm{d}S(\mathbf{x}'),$$

The total velocity $\mathbf{u}(\mathbf{x}) = \mathbf{u}' + \mathbf{u}_\infty$ must match the particle velocity distribution

$$\mathbf{v}(\mathbf{x}) = \mathbf{v}_0 + \boldsymbol{\omega}\times(\mathbf{x}-\mathbf{x}_0),$$

with $\boldsymbol{\omega}$ the rotational velocity of the particle and $\mathbf{v}_0$ the mean particle velocity (taken at the center of mass). Hence we have

$$\int_S \mathbf{I}(\mathbf{x}-\mathbf{x}')\cdot \mathbf{f}\mathrm{d}S(\mathbf{x}') = \mathbf{v}_0 - \mathbf{u}_\infty + \boldsymbol{\omega}\times(\mathbf{x}-\mathbf{x}_0). \tag{3.9}$$

Multiplying by $\mathrm{d}S(\mathbf{x})$ and integrating on S yields

$$\frac{2}{3}\frac{a}{\mu}\int_S \mathbf{f}\mathrm{d}S(\mathbf{x}') = \int_S (\mathbf{v}_0 - \mathbf{u}_\infty)\mathrm{d}S(\mathbf{x}),$$

where we make use of[4]

$$\int_S \mathbf{k}\mathbf{k}\mathrm{d}S = \frac{4\pi}{3}a^2\mathbf{1},\ \int_S \mathbf{1}\mathrm{d}S = 4\pi a^2\mathbf{1},\ \text{hence}\ \int_S \mathbf{I}(\mathbf{x}-\mathbf{x}')\mathrm{d}S(\mathbf{x}) = \frac{2}{3}\frac{a}{\mu}\mathbf{1}.$$

Identifying the left-hand side of (3.9) with the viscous force to within a multiplier, we deduce that

$$\mathbf{F} = \int_S \mathbf{f}\mathrm{d}S(\mathbf{x}') = \frac{3}{2}\frac{\mu}{a}\int_S (\mathbf{v}_0 - \mathbf{u}_\infty)\mathrm{d}S(\mathbf{x}) = 6\pi\mu a\mathbf{v}_0 - \frac{3}{2}\frac{\mu}{a}\int_S \mathbf{u}_\infty(\mathbf{x})\mathrm{d}S(\mathbf{x}).$$

---

[3] In fact we use the single-layer method that makes it possible to derive the velocity when a distribution of stress is prescribed on a boundary of the flow domain (Pozrikidis, 1992)

[4] The integration is straightforward if we make a change of variable, i.e., replacing $\mathbf{x} - \mathbf{x}'$ with $\mathbf{r}$ centered at $\mathbf{x}_0$; see Fig. 3.3.

By using a Taylor series of the velocity field $\mathbf{u}_\infty$ at $\mathbf{x} = \mathbf{x}_0$, we get

$$\mathbf{u}_\infty(\mathbf{x}) = \mathbf{u}_\infty(\mathbf{x}_0) + ((\mathbf{x}-\mathbf{x}_0)\cdot\nabla)\,\mathbf{u}_\infty(\mathbf{x}_0) + \frac{1}{2}\left((\mathbf{x}-\mathbf{x}_0)\cdot\nabla\right)^2\mathbf{u}_\infty(\mathbf{x}_0) + \cdots,$$

where we can transform the second-order operator $((\mathbf{x}-\mathbf{x}_0)\cdot\nabla)^2$ on the right-hand side into $((\mathbf{x}-\mathbf{x}_0)(\mathbf{x}-\mathbf{x}_0)\nabla\nabla :)$ (do not forget the double dot for the inner product). Integrating on S, we get

$$\boxed{\mathbf{F} = 6\pi\mu a\left(\mathbf{u}_\infty(\mathbf{x}_0) + \frac{1}{6}((a^2\nabla^2)\mathbf{u}_\infty)|_{\mathbf{x}_0} - \mathbf{v}_0\right).}$$

This equation is known as the *Faxén equation*, which is a second-order correction to the Stokes force: identifying $\mathbf{v}_g = \mathbf{u}_\infty(\mathbf{x}_0) - \mathbf{v}_0$ as the particle velocity relative to the fluid, we can interpret this equation as:

- a zero-order term $\mathbf{F} = 6\pi\mu a\mathbf{v}_g + O(a^2)$ which is referred to as the Stokes force;
- a second-order contribution taking into account the perturbation of the fluid velocity field as a result of shearing.

The key points to keep in mind are

- When the velocity $\mathbf{u}$ is known, we can derive the force $\mathbf{F}$, which is linearly linked to $\mathbf{u}$ and *vice versa*. In the latter case, the mobility tensor of the sphere is $\mathbf{M} = (6\pi\mu a)^{-1}\mathbf{1}$ and we can express $\mathbf{v}_g = \mathbf{M}\cdot\mathbf{F}$. This is the key ingredient used in *Stokesian-dynamics* numerical models (Brady & Bossis, 1988).
- The method based on the singular solutions to the Stokes equation, which was used to obtain the results above, are likely to be the simplest one we can imagine. For comparison see the more complete, but more complicated *boundary integral* methods (Pozrikidis, 1992) or the proofs provided in fluid-mechanics textbooks (Lamb, 1932; Happel & Brenner, 1965; Batchelor, 1967; Bird *et al.*, 1987).

General solution to the Stokes problem for unsteady flow conditions[5] have also been found (Mazur & Bedeaux, 1974; Coimbra & Rangel, 1998). The resulting equation is often called the *Basset-Boussinesq-Oseen equation.*

3.1.2 From a single sphere to a bulk: averaging

There are several fundamental properties that an averaging operator should satisfy to be helpful in deriving averaged equations. Let us represent the operator by a angular brackets: $\langle f\rangle$ reads the averaged value of f. Here are these fundamental properties:

- *First Reynolds rule*: let c_1 and c_2 two constants and f_1 and f_2 two fields. Linearity of the averaging procedure implies that

  $$\langle c_1 f_1 + c_2 f_2\rangle = c_1\langle f_1\rangle + c_2\langle f_2\rangle.$$

- *Second Reynolds rule*:

  $$\langle g\langle f\rangle\rangle = \langle g\rangle\langle f\rangle,$$

  which also implies that averaging twice does not alter the outcome since taking $g = 1$, we get $\langle\langle f\rangle\rangle = \langle f\rangle$.
- *Leibnitz rule*: we can interchange time derivative and operating operator

  $$\left\langle\frac{\partial f}{\partial t}\right\rangle = \frac{\partial\langle f\rangle}{\partial t},$$

---

[5] i.e., by assuming that the convective acceleration term in the Navier-Stokes momentum equation (2.3) alone vanishes

but be aware that f may be admit jump within the material volume, which implies that averaging such a function requires a bit more attention (see §9, Drew & Passman, 1999).

- *Gauss rule*: we can interchange space derivative and operating operator

$$\left\langle \frac{\partial f}{\partial x} \right\rangle = \frac{\partial \langle f \rangle}{\partial x}.$$

There are several ways of averaging a heterogenous medium. A great deal of literature has been devoted to averaging procedures (e.g., see Jongschaap & Doeksen, 1983; Murdoch & Bedeaux, 1994; Drew & Passman, 1999). Data acquisition based on time averaging is probably a pervasive way of measuring averaged quantities since it is the easiest method in practice, but for theoretical purposes, volume or ensemble averaging is more appropriate. We will outline the definition and fundamental properties of these two operators in the following.

Volume averaging

Averaging any quantity f consists in

$$\bar{f}(\mathbf{x},t) = \frac{1}{\mathcal{V}} \int_{\mathcal{V}} f(\mathbf{x},t) d\mathcal{V}. \tag{3.10}$$

This operator is advantageous in that it can be permuted with time or space derivation, with the subtlety that the integration volume includes both fluid and solid phases (see below).

Ensemble averaging

One of the most robust and efficient procedures is to consider (fictitiously) that we are able to carry out as many runs as desired (we will refer to them as *realizations*) with the same conditions at the macroscopic scale (same boundary conditions, same number of particles, etc.):

$$\langle f \rangle (\mathbf{x},t) = \int_{\mathcal{P}} f(\mathbf{x},t|\mathcal{R}) \mathrm{d}P(\mathcal{R}), \tag{3.11}$$

where $\mathcal{R}$ denotes a particular configuration/state of the system and $P(\mathcal{R})$ the probability of observing the system in this configuration/state. $f(\mathbf{x},t|\mathcal{R})$ is the value taken by f when the system is in a given state $\mathcal{R}$. Statistical mechanics provides a good examples of ensemble averaging; in this case, a system is characterized by its energy E and the probability is of an exponential form $\mathrm{d}P = e^{-cE}\mathrm{d}E$, with c a constant.

For suspensions in a Stokes regime, the configuration of the system can be related to the position of the N particles within the suspension. Indeed, the system is entirely determined when the particle positions and velocities are known since the fluid velocity can be deduced directly from this information. The ensemble average is then the average over all the possible realizations; the ensemble $\mathcal{C}_N$ of all possible realizations constitute the *space of states* of the system at hand, i.e. $\mathcal{C}_N$ is the set of parameters required to describe the setting. The dimension of $\mathcal{C}_N$ is the degree of freedom of the system studied. We introduce the probability P of observing N particles in a given configuration $\mathcal{C}_N$. The ensemble average of any quantity f is then:

$$\langle f \rangle (\mathbf{x},t) = \int_{\mathcal{C}_N} d\mathcal{C}_N P(\mathcal{C}_N) f(\mathbf{x},t|\mathcal{C}_N), \tag{3.12}$$

where $\mathcal{C}_N = (\mathbf{x}_1, \dot{\mathbf{x}}_1, \cdots, \mathbf{x}_N, \dot{\mathbf{x}}_N)$.

For a granular material, for which interstitial fluid effects can be ignored (or decoupled), it is also possible to use ensemble averages by utilizing the notion of configuration. However, in that case, more information is needed since particles are in close contact and can transmit forces over long distances. The space of states must accordingly of higher dimension: $\mathcal{C}_N = (\mathbf{x}_1,\, \dot{\mathbf{x}}_1,\, \ddot{\mathbf{x}}_1 \cdots,\, \mathbf{x}_N,\, \dot{\mathbf{x}}_N,\, \ddot{\mathbf{x}}_N)$, where we can replace replace the acceleration $\ddot{\mathbf{x}}$ with forces $\mathbf{F}$ exerted on particles. If in the model we have to use the rotational velocity, we must once again increase the dimension of the space of states by including the particle spin as a state variable: $\mathcal{C}_N = (\mathbf{x}_i,\, \dot{\mathbf{x}}_i,\, \mathbf{F}_i, \boldsymbol{\omega}_i)_{1\leq i\leq N}$, and so forth.

Compared to volume averaging, ensemble averaging does not require the notion of volume of control that can be cumbersome when dealing with finite-size samples (see below for an example related to concentrated suspensions). An inconvenient is that it involves assigning probabilities to configurations of the systems, which may require a very large quantity of information to deal with continuous phases. Another potential drawback is that ensemble averaging can only be used for finite systems, i.e., it is not possible to consider an unbounded volume.

3.1.3 Averaged balance equations

We consider equal-size spherical rigid particles (of radius a) within a Newtonian fluid. The suspension is assumed to be statistically homogeneous. The number of particles per unit volume (density number) is n and is related to the solid concentration ϕ (ϕ = volume occupied by particles to total volume) since we have $n = \phi/(4\pi a^3/3)$.

The approach first involves averaging the local equations of motion (volume averaging), then using an ensemble average, when required, to go farther in the interpretation of individual contributions. The operator “volume average” is constructed by taking a control volume $\mathcal{V}$ assumed to sufficiently wide to contain a large number of articles, but in the meantime sufficiently small with the respect to a typical lengthscale of the bulk for it to be considered as a continuum.

Bulk mass balance equation

For solid and fluid phases, the local mass balance equation is in the form

$$\frac{\partial \rho_i}{\partial t} + \nabla\cdot(\rho_i \mathbf{u}) = 0,$$

with $i = p$ (particle) or $i = f$ (fluid). We define the *bulk (volume-averaged) density* as $\bar{\rho} = \phi\rho_p + (1-\phi)\rho_f$ with ϕ the solid concentration. We also define a *characteristic function* (Lundgren, 1972):

- $H(\mathbf{x}) = 1$ if $\mathbf{x}$ is inside a particle;
- $H(\mathbf{x}) = 0$ if $\mathbf{x}$ lies within the fluid.

We call $\mathcal{V}_p$ the sub-volume of $\mathcal{V}$ containing the particles and $\mathcal{A}_p$ the surface bounding $\mathcal{V}_p$.

Multiplying the mass equation for solid particles by the characteristic function H and the mass equation for the continuous phase by $1-H$ and integrating over the control volume $\mathcal{V}$, we obtain

$$\int_{\mathcal{V}} \left(H\frac{\partial \rho_p}{\partial t} + (1-H)\frac{\partial \rho_f}{\partial t} + H\nabla\cdot(\rho_p\mathbf{u}) + (1-H)\nabla\cdot(\rho_f\mathbf{u}) \right) \mathrm{d}\mathcal{V} = 0,$$

that can be transformed into

$$\int_{\mathcal{V}} \left(\frac{\partial \bar{\rho}}{\partial t} + \nabla\cdot(\bar{\rho}\mathbf{u}) - \rho_p\frac{\partial H}{\partial t} - \rho_f\frac{\partial (1-H)}{\partial t} - \rho_p\nabla\cdot(H\mathbf{u}) - \rho_f\nabla\cdot((1-H)\mathbf{u}) \right) \mathrm{d}\mathcal{V} = 0,$$

where we need to characterize how the characteristic function H varies with time and space.

For this purpose, it is worth noting that particle suspensions are characterized by the presence of solid/fluid interfaces, which implies discontinuities in the material property (e.g., the local density may vary between a solid particle and the bounding fluid). Usually the fields studied here are smooth and can undergo jumps at material interfaces, which means that their time and/or space derivative may be meaningless. This issue is overcome by using generalized functions (i.e., distributions). It is customary to introduce *test functions*, which have a finite support, are continuous, and admit derivative at all orders. For instance, if ψ denotes a test function with a support $\mathcal{D}$ included in a larger domain $\mathcal{B}$ (i.e., $\psi(\mathbf{x},\, t) = 0$ for $\mathbf{x} \in \mathcal{B}$, but $\mathbf{x} \notin \mathcal{D}$), we have

$$\int \psi(\mathbf{x},\, t) f(\mathbf{x},\, t)\mathrm{d}\mathbf{x} = 0 = \int \frac{\partial \psi(\mathbf{x},\, t)}{\partial t} f(\mathbf{x},\, t)\mathrm{d}\mathbf{x}\mathrm{d}t + \int \frac{\partial f(\mathbf{x},\, t)}{\partial t} \psi(\mathbf{x},\, t)\mathrm{d}\mathbf{x},$$

which leads to the formula

$$\int \frac{\partial f(\mathbf{x},\, t)}{\partial t} \psi(\mathbf{x},\, t)\mathrm{d}\mathbf{x} = -\int \frac{\partial \psi(\mathbf{x},\, t)}{\partial t} f(\mathbf{x},\, t)\mathrm{d}\mathbf{x},$$

which is very helpful in getting rid of discontinuous derivatives. This equation remains nearly the same when we replace the time derivative with a space derivative. Here, applying this procedure to the characteristic functions leads to

$$\frac{\partial H_i}{\partial t} + \mathbf{u} \cdot \nabla(H_i) = 0,$$

with $i = f$ or p and where the following short-hand notations $H_p = H$ and $H_f = 1 - H$ have been used. This equation is sometimes referred to as the *topological equation* (Drew & Passman, 1999). Then, applying the Gauss and Leibnitz rules to interchange the time/space derivatives with the volume averaging operator, we deduce the bulk mass equation

$$\boxed{\frac{\partial \bar{\rho}}{\partial t} + \nabla \cdot (\bar{\rho}\mathbf{u}) = 0.}$$

Bulk momentum balance equation

Multiplying Equation (3.1) with $1 - H$, then integrating over the control volume $\mathcal{V}$, making use of the mass conservation ($\partial H/\partial t + \mathbf{u} \cdot \nabla H = 0$), the relation $\nabla H = \mathbf{k}$ over $\mathcal{A}_p$ with $\mathbf{k}$ the unit outward normal to $\mathcal{A}_p$ (and $\nabla H = 0$ otherwise), and the Reynolds decomposition $\mathbf{u}_f = \bar{\mathbf{u}}_f + \mathbf{u}'_f$, we eventually obtain

$$\rho_f \left(\frac{\partial \bar{\mathbf{u}}_f}{\partial t} + \nabla \cdot \bar{\mathbf{u}}_f \bar{\mathbf{u}}_f \right) = -\nabla \bar{p} + \frac{1}{\mathcal{V}} \int\limits_{\mathcal{A}_p} (\boldsymbol{\sigma}_f - p\mathbf{1}) \cdot \mathbf{k} d\mathcal{A} + \nabla \cdot \frac{1}{\mathcal{V}} \int\limits_{\mathcal{V}_f} (\boldsymbol{\sigma}_f - \rho_f \mathbf{u}'{}_f \mathbf{u}'{}_f) d\mathcal{V}. \tag{3.13}$$

In this equation, the mean fluid velocity is

$$\bar{\mathbf{u}}_f(\mathbf{x},t) = \frac{1}{\mathcal{V}} \int\limits_{\mathcal{V}} (1 - H(\mathbf{x},t))\, \mathbf{u}_f(\mathbf{x},t) d\mathcal{V} = \frac{1-\phi}{\mathcal{V}_f} \int\limits_{\mathcal{V}_f} \mathbf{u}_f(\mathbf{x},t) d\mathcal{V},$$

where we used $\int\limits_{\mathcal{V}} (1 - H) d\mathcal{V} = 1 - \phi$. Here, the mean fluid velocity is $1 - \phi$ the mean bulk velocity.

For the solid phase, we have to transform the Lagrangian equation of motion into an Eulerian equivalent. The rigid-sphere assumption implies that the solid kinematic field is: $\mathbf{u}_p(\mathbf{x},t) = \mathbf{u}_p(\mathbf{y},t) + \boldsymbol{\omega}_p \times (\mathbf{x} - \mathbf{y})$, with $\mathbf{y}$ the position of the center of mass and $\boldsymbol{\omega}_p$ the rotation velocity. Since the gradient of a rotational field is zero, the local equation is for a solid particle: $\rho_p \partial \mathbf{u}_p / \partial t = \rho_p \mathbf{g} + \nabla \cdot \boldsymbol{\sigma}_p$, with the following difficulty: the particle being rigid, the stress field is undetermined. This is in fact a minor issue since we will integrate the stress field over the particle volume, the Green-Ostrogradski allows us to connect this field to the forces acting on the particle surface. Proceeding as earlier by multiplying the equation above by H, then integrating it on $\mathcal{V}$, we find

$$\rho_p\left(\frac{\partial\bar{\mathbf{u}}_p}{\partial t}+\nabla\cdot\bar{\mathbf{u}}_p\bar{\mathbf{u}}_p\right)=\phi\rho_p\mathbf{g}+\nabla\cdot(\bar{\boldsymbol{\sigma}}_p-\rho_p\overline{\mathbf{u}'_p\mathbf{u}'_p})-\nabla\cdot\frac{1}{\mathcal{V}}\int\limits_{\mathcal{A}_p}\boldsymbol{\sigma}_p\cdot\mathbf{k}d\mathcal{A}. \tag{3.14}$$

Since at the particle surface we have $\boldsymbol{\sigma}_p\cdot\mathbf{k}=(\boldsymbol{\sigma}_f-p\mathbf{1})\cdot\mathbf{k}$, the last term on the right-hand side, representing the stresses exerted on the particle surface, is equivalent to the term in (**??**). These terms reflect momentum transfer between phases through their interface.

The local bulk velocity is defined as follows: $\mathbf{u}(\mathbf{x},t)=H\mathbf{u}_p(\mathbf{x},t)+(1-H)\mathbf{u}_f(\mathbf{x},t)$. The *bulk volume-averaged velocity* is then: $\bar{\mathbf{u}}(\mathbf{x},t)=\bar{\mathbf{u}}_p(\mathbf{x},t)+\bar{\mathbf{u}}_f(\mathbf{x},t)$. We can also define a bulk velocity based on mass averaging (rather than volume): $\bar{\rho}\bar{\mathbf{u}}_m=\rho_p\bar{\mathbf{u}}_p+\rho_f\bar{\mathbf{u}}_f$, with $\bar{\rho}=\phi\rho_p+(1-\phi)\rho_f$. The two velocities coincide when the solid and fluid densities are equal. A helpful approximation can be used when one of the densities is very low compared to the other and the velocities of each phase are of same magnitude. Using the same dimensional argument as earlier, we can show that we meet such a case for a suspension of particles within a gas with St $\gg 1$ and $\rho_p\gg\rho_f$; the same situation is met with emulsions ($\rho_p\ll\rho_f$ and St $\gg 1$ or St $\to 0$). Note that the mass conservation is satisfied $\nabla\cdot\bar{\mathbf{u}}=\nabla\cdot\bar{\mathbf{u}}_m=0$ (ϕ is assumed to be constant).

Summing (**??**) et (**??**) leads to the bulk momentum equation:

$$\bar{\rho}\left(\frac{\partial\bar{\mathbf{u}}_m}{\partial t}+\nabla\cdot\bar{\mathbf{u}}_m\bar{\mathbf{u}}\right)=-\nabla\bar{p}^\star+\nabla\cdot\frac{1}{\mathcal{V}}\int\limits_{\mathcal{V}}(\boldsymbol{\sigma}-\rho\mathbf{u}'\mathbf{u}')d\mathcal{V}, \tag{3.15}$$

with $\bar{p}^\star=\bar{\Phi}+\bar{p}_f$ (where $\nabla\bar{\Phi}=-\bar{\rho}\mathbf{g}$). This equation is not very helpful as long as we are not able to give it the classic form of momentum balance equation for a continuum; here this means that we must have $\bar{\mathbf{u}}_m\approx\bar{\mathbf{u}}$ so that the terms on the left-hand side can be identified as a material derivative. If this condition is satisfied, then we can identify the term on the right-hand side under the divergence operator as a stress tensor. We refer to it as the *bulk extra-stress tensor*:

$$\boxed{\bar{\boldsymbol{\sigma}}=\frac{1}{\mathcal{V}}\int\limits_{\mathcal{V}}(\boldsymbol{\sigma}-\rho\mathbf{u}'\mathbf{u}')d\mathcal{V},} \tag{3.16}$$

which is the definition used by Batchelor (1970) for the bulk stress tensor. Further computation reveals that this stress tensor can be divided into a fluid contribution (Batchelor, 1970; Ancey *et al.*, 1999):

$$\boxed{\bar{\boldsymbol{\sigma}}^{(f)}=2\mu\bar{\mathbf{d}}-\frac{1}{\mathcal{V}}\int\limits_{\mathcal{V}_f}\rho_f\mathbf{u}'\mathbf{u}'d\mathcal{V},} \tag{3.17}$$

and a solid contribution (Ancey *et al.*, 1999):

$$\boxed{\bar{\boldsymbol{\sigma}}^{(p)}=\frac{1}{\mathcal{V}}\int\limits_{\mathcal{A}_p}\boldsymbol{\sigma}\cdot\mathbf{x}\mathbf{k}d\mathcal{A}-\frac{1}{\mathcal{V}}\int\limits_{\mathcal{V}_p}\rho_p\mathbf{u}'\mathbf{u}'d\mathcal{V}+\mathbf{G}(\omega_p),} \tag{3.18}$$

where $\mathbf{G}(\omega_p)$ represents an antisymmetric function ω_p, which is not detailed here because in most cases of practical interest, $\mathbf{G}$ vanishes (Ancey *et al.*, 1999; Batchelor, 1970; Prosperetti, 2004).

Energy balance equation

Let us focus our attention on particle suspensions that behave as one-phase material at the bulk scale. Similarly to the momentum balance, we can derive the energy balance equation. Here

$\varepsilon = e + u^2/2$ denotes the total energy per unit volume, where e is the internal energy and $u^2/2$ is the kinetic energy per unit volume. It can be shown that (Ancey *et al.*, 1999):

$$\frac{d\rho\bar{e}}{dt} + \frac{1}{2}\frac{d}{dt}\overline{\rho\mathbf{u}'^2} = \bar{\boldsymbol{\sigma}} : \bar{\mathbf{d}} + \nabla\cdot\mathbf{q} + \int_{\mathcal{A}_p} \mathbf{k}\cdot[\![\boldsymbol{\sigma}\cdot\mathbf{u}]\!]d\mathcal{A}. \tag{3.19}$$

The first term on the left-hand side represents the variation in internal energy, while the second one is related to the fluctuating kinetic energy (where appears a "granular temperature" $T = \overline{\mathbf{u}'\cdot\mathbf{u}'}/3$ representing particle agitation). On the right-hand side member, the first term represents the work supplied during the simple shear motion (for the simple shear motion, we have $\bar{\boldsymbol{\sigma}}\cdot\bar{\mathbf{d}} = \tau\dot{\gamma}$ with τ the shear stress and $\dot{\gamma}$ the shear rate), the second term $\mathbf{q} = -\overline{\boldsymbol{\sigma}\cdot\mathbf{u}'}$ is a flux of energy related to velocity fluctuations, whereas the third one reflects energy dissipation induced by contact between particles (this term originates from the sliding between particles in contact).

Another interpretation is drawn from (3.19) on a control volume de $\mathcal{V}$ bounded by $\mathcal{A}$. Rearranging the terms, we deduce (Ancey & Evesque, 2000) :

$$\int_{\mathcal{V}} \bar{\boldsymbol{\sigma}} : \bar{\mathbf{d}}d\mathcal{V} = \int_{\mathcal{A}} \left(\frac{1}{2}\rho T\mathbf{u}\cdot\mathbf{k} + \mathbf{q}\cdot\mathbf{k}\right)d\mathcal{A} + \int_{\mathcal{V}} (\dot{\bar{\varepsilon}} - \langle\mathbf{k}\cdot[\![\boldsymbol{\sigma}\cdot\mathbf{u}]\!]\rangle)d\mathcal{V}. \tag{3.20}$$

The first term represents energy production resulting from shear. There are two ways of dissipating energy

- energy diffusion, which acts as a redistribution of energy (no real creation). Here this diffusion operates through the advection of fluctuating kinetic energy (budget[6] between the fluctuating kinetic energy supplied to or provided by the control volume) and, on the other hand, the fluctuating kinetic energy dissipate energy at the boundaries[7].
- The second mode of dissipation is related to processes of internal dissipation through an increase:
  - in internal energy (heat production resulting from viscous dissipation or inelastic deformations inside particles, hence increase in thermodynamic temperature),
  - dissipation resulting from slipping contacts between particles.

For dilute suspensions, there is no energy dissipation induced by solid particles, which implies that the primary mode of energy dissipation is related to internal energy. For concentrated suspensions, there are

- energy dissipation at the solid boundaries when particle agitation is sufficiently high;
- energy dissipation induced by slipping contacts between particles

Concerning energy dissipation, concentrated and dilute suspensions behave differently. A striking property results from this difference: for Newtonian fluids, there is equivalence between energy and momentum balance equations; notably we can derive the stress in this way: $\sigma_{ij} = \partial\bar{\Phi}/\partial\bar{d}_{ij}$. For concentrated suspensions, such a procedure requires that we specify the energy dissipated by particle contact, which is not easy to determine.

3.1.4 Passing from volume averages to ensemble averages

While volume averaging is likely to be the more appropriate method for averaging equations of motion, ensemble averaging turns out to be more efficient when pushing the computation of individual contributions farther.

---

[6] Note that this budget is zero for a uniform steady flow, as shown in la figure 3.5, because either the velocity vanishes on the volume boundary or there is a balance between inward flux and outward flux of energy.

[7] This is the case when the boundaries contain a solid wall.

Conditional averaging

We start with the simplest description of the configuration of a system made up of particles, i.e., we want to describe the position of N particles. Earlier, we have introduced the characteristic function $H(\mathbf{x})$, which takes the value 1 when $\mathbf{x}$ lies inside a particle and 0 otherwise. If we consider that all particles have the same radius a and the position of their center of mass is given by $\mathbf{y}_i$, then we can write

$$H(\mathbf{x},\,t)=\sum_{i=1}^{N}\mathcal{H}(a-|\mathbf{x}-\mathbf{y}_i|),$$

where $\mathcal{H}$ is the Heaviside function. The number density carries the same information by providing the position of the centers of mass

$$n(\mathbf{x},\,t)=\sum_{i=1}^{N}\delta(\mathbf{x}-\mathbf{y}_i),$$

where δ is the Dirac function. What we want know is to reduce the amount of information required to describe the system. For this purpose, we introduce the distribution function P_N, which is the probability of observing N particles occupying the position $\mathbf{y}_i$.

$P_N(t,\mathbf{y}_1,\mathbf{y}_2,\cdots,\mathbf{y}_N)=$ probability that at position $\mathbf{y}_i$, there is the center of mass of one particle.

The information contained in P is still very large and we can define reduced distribution functions, which are the marginal probability distribution of finding a finite number of particles at given place. For instance, $P_1(t,\,\mathbf{y}_1)$ gives the probability that the center of mass of one particles is placed at $\mathbf{y}_1$

$$P_1(t,\,\mathbf{y}_1)=\int_{\mathcal{D}^{N-1}}P_N(t,\,\mathbf{y}_1,\,\mathbf{y}_2,\cdots,\mathbf{y}_N)\mathrm{d}\mathbf{y}_2\mathrm{d}\mathbf{y}_3\cdots\mathrm{d}\mathbf{y}_N,$$

where $\mathcal{D}$ is the domain of integration. We can also define the conditional probability, which the probability of observing $N-1$ particles when the position of one particle is known to be at $\mathbf{y}_1$

$$P^c_{N-1}(t,\,\mathbf{y}_2,\cdots,\mathbf{y}_N|\mathbf{y}_1)=\frac{P_N(t,\,\mathbf{y}_1,\,\mathbf{y}_2,\cdots,\mathbf{y}_N)}{P_1(t,\,\mathbf{y}_1)}.$$

Armed with these distribution functions, we can transform the ensemble average of a quantity f

$$\langle f(\mathbf{x},\,t)\rangle=\int_{\mathcal{D}}f(\mathbf{x},\,t|\mathcal{C}^N)P_N(t,\,\mathbf{y}_1,\,\mathbf{y}_2,\cdots,\mathbf{y}_N)\mathrm{d}\mathbf{y}_1\mathrm{d}\mathbf{y}_2\cdots\mathrm{d}\mathbf{y}_N$$

with the help of the conditional average of f

$$\langle f(\mathbf{x},\,t|\mathbf{y}_1)\rangle=\int_{\mathcal{D}^{N-1}}f(\mathbf{x},\,t|\mathcal{C}^N)P^c_{N-1}(t,\,\mathbf{y}_1,\,\mathbf{y}_2,\cdots,\mathbf{y}_N|\mathbf{y}_1)\mathrm{d}\mathbf{y}_2\cdots\mathrm{d}\mathbf{y}_N.$$

We obtain

$$\langle f(\mathbf{x},\,t)\rangle=\int_{\mathcal{D}}\langle f(\mathbf{x},\,t|\mathbf{y}_1)\rangle P_1(t,\,\mathbf{y}_1)\mathrm{d}\mathbf{y}_1.$$

The result can be extended to two particles or more

$$\langle f(\mathbf{x},\,t)\rangle=\int_{\mathcal{D}^2}\langle f(\mathbf{x},\,t|\mathbf{y}_1,\,\mathbf{y}_2)\rangle P_2(t,\,\mathbf{y}_1,\,\mathbf{y}_2)\mathrm{d}\mathbf{y}_1\mathrm{d}\mathbf{y}_2,$$

P_2 is *the pair distribution function* defined as the probability that simultaneously the centers of two spheres lie respectively in $\mathbf{y}_1$ and $\mathbf{y}_2$. The physical meaning of these equations is clear: we have to average a quantity f, which takes its values on both the solid and fluid phases and is influenced by the configuration $\mathcal{C}^N$ of the N spheres. The ensemble average of f is the mean value of f over all the possible configurations. By introducing conditional probabilities on one or more particle(s), we can focus our attention on a finite set of 'test' sphere(s). The notation $f(\mathbf{x},\, t|\mathbf{y}_1)$ reads "variation of $f(\mathbf{x},\, t)$ given that one particle is located at $\mathbf{y}_1$".

Further simplification is obtained by posing some assumptions on the configuration of the system. For instance, for a dilute suspension (ϕ small), the number of particles per unit volume is the density number n. Within a volume r^3, the number of particles is on average nr^3; if we assume that the distribution of the number of particles lying within a unit volume follows a Poisson distribution (an assumption that seems realistic for dilute suspensions), the probability $\mathcal{P}$ that k spheres are located at a distance lower than r from the test sphere is given by

$$\mathcal{P}(k) = e^{-nr^3}\frac{(nr^3)^k}{k!},$$

which shows that the probability of finding one particle around the test particle is of the order $\phi(r/a)^3$, thus is a small quantity. Likewise the probability of finding two spheres simultaneously is of the order $\phi^2(r/a)^6$ and so forth. If the function f is such that $f(\mathbf{x},\, t) \propto (a/x)^n$, with $n > 3$, then it decreases to zero more rapidly than $1/\mathcal{P}$, this means that the influence of other spheres can be neglected. In this case, in the definition of the conditional average

$$\langle f(\mathbf{x},\, t|\mathbf{y}_1,\, \mathbf{y}_2)\rangle = \int_{\mathcal{D}^{N-2}} f(\mathbf{x},\, t)P^c_{N-1}(t,\, \mathbf{y}_1,\, \mathbf{y}_2, \cdots, \mathbf{y}_N|\mathbf{y}_1,\, \mathbf{y}_2)\mathrm{d}\mathbf{y}_3\cdots\mathrm{d}\mathbf{y}_N,$$

we can consider that $f(\mathbf{x},\, t)$ is independent of the position of the $N-2$ remaining particles, which implies that we can extract $f(\mathbf{x},\, t)$ from the integrand. To order $O(\phi^2)$, we have

$$\langle f(\mathbf{x},\, t|\mathbf{y}_1,\, \mathbf{y}_2)\rangle = f(\mathbf{x},\, t|\mathcal{C}^N)\int_{\mathcal{D}^{N-2}} P^c_{N-1}(t,\, \mathbf{y}_1,\, \mathbf{y}_2, \cdots, \mathbf{y}_N|\mathbf{y}_1,\, \mathbf{y}_2)\mathrm{d}\mathbf{y}_3\cdots\mathrm{d}\mathbf{y}_N = f(\mathbf{x},\, t|\mathbf{y}_1,\, \mathbf{y}_2),$$

thus

$$\langle f(\mathbf{x},\, t)\rangle = \int_{\mathcal{D}^{N-2}} f(\mathbf{x},\, t|\mathbf{y}_1,\, \mathbf{y}_2)P_2(t,\, \mathbf{y}_1,\, \mathbf{y}_2)\mathrm{d}\mathbf{y}_1\mathrm{d}\mathbf{y}_2.$$

Furthermore, if we assume that there is no preferential direction for f (isotropy) and no explicit time dependence, then $P_2(t,\, \mathbf{y}_1,\, \mathbf{y}_2)$ reduces to the *radial distribution function* $g(r)$ with $r = |\mathbf{y}_1 - \mathbf{y}_2|$. In a number of kinetic theories or microstructural models, all the information on the microstructure is contained in the function $g(r)$.

In the developments above, emphasis has been given to defining the configuration of the system via the position of the N spheres. Obviously, we can extend the number of state parameters for refining the description, e.g., by including the velocity, the orientation, the spin, the acceleration, etc.

Boltzmann equation

One of the major achievements of microstructural theories was the kinetic theory for dilute gases proposed by Boltzmann in 1872. It took a long while to recognize that this theory was a decisive breakthrough in our way of thinking about the connection between molecules and bulk behavior of gases. One of the fundamental building block of this theory is the so-called *Boltzmann equation* that teaches us how the probability density function P describing the states of a system varies with time.

Let us consider particles that move at velocity $\mathbf{v}$ and experience forces $\mathbf{F}$. The governing equation is given by equation (3.3). The number of particles at time t within a small volume $\mathrm{d}\mathbf{r}$ around $\mathbf{r}$ and with velocities $\mathbf{v}$ is denoted by $f(\mathbf{x},\, \mathbf{v},\, t)$. The normalizing constraint is

$$\int_{\mathcal{D}}\mathrm{d}\mathbf{x}\int_{\mathbb{R}} f(\mathbf{x},\, \mathbf{v},\, t)\mathrm{d}\mathbf{v} = N$$

when there are N molecules in the domain $\mathcal{D}$. Differentiating with respect to time leads to

$$\int_{\mathcal{D}} \mathrm{d}\mathbf{x} \int_{\mathbb{R}^3} \left(\frac{\partial}{\partial t} f + \frac{\partial \mathbf{x}}{\partial t} \cdot \nabla_{\mathbf{x}} f + \frac{\partial \mathbf{v}}{\partial t} \cdot \nabla_{\mathbf{v}} f \right) \mathrm{d}\mathbf{v} = \int_{\mathcal{D}} \mathrm{d}\mathbf{x} \int_{\mathbb{R}^3} \left(\frac{\partial}{\partial t} f + \mathbf{v} \cdot \nabla_{\mathbf{x}} f + \frac{\mathbf{F}}{m_p} \cdot \nabla_{\mathbf{v}} f \right) = 0,$$

from which we deduce that if there is no jump in f, then

$$\frac{\partial}{\partial t} f + \mathbf{v} \cdot \nabla_{\mathbf{x}} f + \frac{\mathbf{F}}{m_p} \cdot \nabla_{\mathbf{v}} f = 0.$$

This derivation is valid solely for particles that do not interact. If particles interact (e;g., collision in a gas made up of molecules), then we have to take into account a source term due representing particle interactions. In kinetic theory, making allowance for particle interactions leads to an expression in the form

$$\frac{\partial}{\partial t} f + \mathbf{v} \cdot \nabla_{\mathbf{x}} f + \frac{\mathbf{F}}{m_p} \cdot \nabla_{\mathbf{v}} f = \left. \frac{\partial}{\partial t} f \right|_{collisions},$$

where the new contribution on the right-hand side indicates how collisions modify the time variations of the distribution function f. It can be shown (Chapman & Cowling, 1970; Drew & Passman, 1999)

$$\left. \frac{\partial}{\partial t} f \right|_{collisions} = \int \mathrm{d}\Omega \int_{\mathbb{R}^3} \mathrm{d}\mathbf{v}_1 |\mathbf{v} - \mathbf{v}_1| S_e(\Omega, |\mathbf{v} - \mathbf{v}_1| \left(f(\mathbf{r}, \mathbf{v}', t) f(\mathbf{r}, \mathbf{v}_1', t) - f(\mathbf{r}, \mathbf{v}, t) f(\mathbf{r}, \mathbf{v}_1, t) \right),$$

where Ω is the solid angle indicating the deflection of molecules after collision, the prime is used to refer to post-collision velocities, S_e is the efficient section ($IS_e(\Omega,|\mathbf{v})\mathrm{d}\Omega$ represents the number of molecules flying in the direction represented by the solid angle Ω where I is the number of particles per unit time crossing a unit surface normal to $\mathbf{u}$). The Boltzmann is the prototype of a kinetic equation describing the variations of the probability distribution f. Although it is one out of the simplest kinetic equations we can imagine, it is markedly difficult to solve because the equation is of integro-differential type. Usually, one restricts to steady or nearly steady flow conditions, which implies that

$$\left. \frac{\partial}{\partial t} f \right|_{collisions} \approx 0,$$

or more precisely $f(\mathbf{r}, \mathbf{v}', t) f(\mathbf{r}, \mathbf{v}_1', t) - f(\mathbf{r}, \mathbf{v}, t) f(\mathbf{r}, \mathbf{v}_1, t)$. Simple inspection the function f in a steady state must satisfy

$$\ln f = A e^{-B(\mathbf{v}-\mathbf{c})^2},$$

where A, B, and $\mathbf{c}$ are unknown quantities that can be determined using the normalizing constraint. By introducing the temperature T as

$$\frac{1}{2} m_p \int_{\mathbb{R}^3} \mathrm{d}\mathbf{v} |\mathbf{v}|^2 f(\mathbf{v}) = \frac{3}{2} \rho k_B T,$$

with ρ the gas density, k_B Boltzmann's constant, we deduce that the steady-state function is

$$f^{ss}(\mathbf{r}, \mathbf{v}, t) = \rho \left(\frac{m_p}{\rho k_B T} \right)^{3/2} e^{-\frac{1}{2} \frac{m_p |\mathbf{v}|^2}{k_B T}},$$

which is known as the *Maxwellian distribution of velocities* at temperature T

3.2 Dilute suspensions

After taking the volume average of the local conservation equations, the next step is to use ensemble averages instead of volume averages in the governing equations to transform the individual contributions (Batchelor, 1970; Hinch, 1977). The resulting averaged equations display terms that reflect what happens at the interface solid/fluid. We can show that these terms can be built as conditional averages of the stress state at the surface of a "target" particle when the position of the other particles is known; in so doing , we construct a hierarchy of equations that can be closed by assuming that the solid concentration is small (i.e., only pairs of particles are in hydrodynamic interaction).

Quite a similar approach can be developed at high Stokes numbers and when the particle Reynolds number is

- either small: $\mathrm{Re}_p \ll 1$ and $\mathrm{St} \gg 1$, which implies that the fluid phase can response instantaneously to any particle movement. This is typically the case of a suspension of particles within a gas. Kinetic theory can then be used (Sangani *et al.*, 1996; Kumaran & Koch, 1993);
- or very large: $\mathrm{Re}_p \gg 1$ and $\mathrm{St} \gg 1$, which implies that the fluid phase can be treated as an inviscid fluid. Some emulsions (e.g., flow of air bubble in water) belong to this category. Once again, kinetic theory can be used (Kang *et al.*, 1997).

We start with a short description of how this treatment is carried out for dilute suspensions at small Reynolds number, then we will explain the shortcomings of this approach as the solid concentration is increased. The next two subsections provide the reader with a more detailed description of the stress computations for dilute suspensions at low and large Reynolds numbers.

3.2.1 Dilute suspension in a Stokes regime: Stokesian theory

Multipole expansion

There are many ways of computing the velocity field of a fluid with inner boundaries (e.g., particle, bubble, etc.) and/or outer boundaries (e.g., solid wall or free surface) (Happel & Brenner, 1965; Kim & Karrila, 1991; Pozrikidis, 1992; Kohr & Pop, 2004). Here we will expound a method called the *multipole expansion*. This method relies on a close analogy with electrostatics, where elementary solutions to the Maxwell equations can be built by considering the field induced by one pole (with a given charge) or a combination of poles (and charges). The basic idea is to combine these elementary solutions to construct a solution that is consistent with the boundary conditions of the problem at hand (see § 2, Batchelor, 1967). This combination of "building blocks" is made possible here because of the linearity of the Stokes equation.

The use of multipole expansion has appeared very early in fluid mechanics, notably for treating potential flows. For instance, similarly to electrostatics, we can introduce a useful mathematical concept: the *source point*, i.e. a source of fluid that is localized in a point. If the source is located at $\mathbf{y}$ and by posing $\mathbf{x}' = \mathbf{x} - \mathbf{y}$, we arrive at the following definition of the potential and velocity fields (see §2.5, Batchelor, 1967):

$$\phi(\mathbf{x}) = -\frac{m}{4\pi x'} \text{ and } \mathbf{u}(\mathbf{x}) = \frac{m}{4\pi}\frac{\mathbf{x}'}{x'^3},$$

where $m > 0$ is called the source strength; the sink point has the same expression except that its strength is negative. The flow rate through a closed surface that encloses $\mathbf{y}$ is m. We can imagine another singularity by placing a source point of strength m at $\mathbf{y} + \boldsymbol{\xi}/2$ and a sink point of strength $-m$ at $\mathbf{y} - \boldsymbol{\xi}/2$. The separation $\boldsymbol{\xi}$ is allowed to approach zero and the strength to approach infinity such that their product $\boldsymbol{\lambda} = \lim_{\xi\to 0}(\boldsymbol{\xi} m)$ tends to a finite value. The resulting singularity is called a *potential dipole* or *source doublet* of strength $\boldsymbol{\lambda}$. The resulting fields are

$$\phi_D(\mathbf{x}) = -\frac{\boldsymbol{\lambda}}{4\pi}\cdot\nabla_{\mathbf{x}'}\frac{1}{x'} = \frac{\boldsymbol{\lambda}}{4\pi}\cdot\frac{\mathbf{x}'}{x'^3} \text{ and } \mathbf{u}_D(\mathbf{x}) = \frac{1}{4\pi}\boldsymbol{\lambda}\cdot\nabla\frac{\mathbf{x}'}{x'^3} = \frac{1}{4\pi x'^3}\left(-\mathbf{1}+3\frac{\mathbf{x}'\mathbf{x}'}{x'^2}\right)\cdot\boldsymbol{\lambda}. \quad (3.21)$$

For future use, the tensor $\frac{1}{4\pi x'^3}\left(-\mathbf{1}+3\frac{\mathbf{x}'\mathbf{x}'}{x'^2}\right)$ is denoted by $\mathbf{D}$. The flow rate through a closed surface that encloses the source doublet is 0.

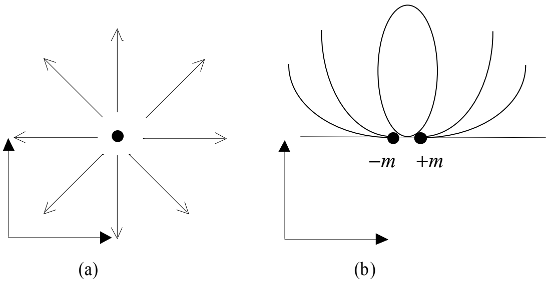

Figure 3.4 *(a) streamlines around a source point, (b) streamlines around a source dipole.*

In repeating the procedure we can obtain other singularities such as the potential quadruple (two symmetric source doublets). The concept of line/surface source can also be developed to determine the potential field due to a source distribution along a line or surface. For instance, the velocity field induced by a potential *quadrupole* is $\mathbf{u}_Q(\mathbf{x}) = \mathbf{Q} : \boldsymbol{\Lambda}$, where $\boldsymbol{\Lambda}$ is the tensor representing the two doublets and $\mathbf{Q}$ is a third-order tensor called the potential quadrupole tensor

$$\mathbf{Q} = -\frac{3}{x^5}(\mathbf{x1}+\mathbf{1x}+\mathbf{x1}) + 15\frac{\mathbf{xxx}}{x^7},$$

that is readily obtained by taking the gradient of the velocity field (3.21) due to a potential dipole.

The multipole expansion for Stokes flows is close to the treatment used for potential flows. There are plenty of expositions of the multipole expansion method. Here we will follow the presentation given by Pozrikidis (1992). In § 3.1.1, we have seen that the velocity disturbance caused by a sphere can be computed by considering that the surface of this sphere is a distribution of point forces, which leads to[8]

$$\mathbf{u}'(\mathbf{x}) = -\int_S \mathbf{I}(\mathbf{x},\,\mathbf{x}')\cdot\mathbf{f}(\mathbf{x}')\mathrm{d}\mathbf{x}',$$

where $\mathbf{I} = (8\pi\mu x)^{-1}(\mathbf{1}+\mathbf{xx}/x^2)$ is the *Oseen tensor* introduced earlier (see § 3.1.1); here $\mathbf{I}(\mathbf{x},\,\mathbf{x}')$ means $\mathbf{I}(\mathbf{x}-\mathbf{x}')$. It is possible to obtain an asymptotic expansion of this disturbance by expanding the Oseen tensor into a Taylor series with respect to $\mathbf{x}'$ about a point $\mathbf{y}$, which is assumed to be inside the particle:

$$\mathbf{I}(\mathbf{x},\mathbf{x}') = \mathbf{I}(\mathbf{x},\,\mathbf{y}) + ((\mathbf{x}'-\mathbf{y})\cdot\nabla_{\mathbf{x}'})\mathbf{I} + \frac{1}{2}((\mathbf{x}'-\mathbf{y})\cdot\nabla_{\mathbf{x}'})^2\mathbf{I} + \cdots .$$

We then obtain

$$\mathbf{u}'(\mathbf{x}) = -\mathbf{I}(\mathbf{x},\,\mathbf{y})\cdot\int_S \mathbf{f}(\mathbf{x}')\mathrm{d}\mathbf{x}' - \nabla_{\mathbf{x}'}\mathbf{I}(\mathbf{x},\,\mathbf{y}) : \int_S (\mathbf{x}'-\mathbf{y})\mathbf{f}(\mathbf{x}')\mathrm{d}\mathbf{x}' + \cdots . \quad (3.22)$$

---

[8] Note the minus sign that appears in the following equation compared to the relation used in § 3.1.1 because here $\mathbf{f}$ is assumed to the be the force exerted by the particle on the fluid (by the virtue of the principle of action/reaction).

This asymptotic expansion can be very useful when one is interested in determining the bulk properties of the flow without dwelling on the details. We can comment on the different terms that appear in this expansion:

- The first integral on the right-hand side is simply the net force **F** exerted on the particle. It is equivalent to the velocity field induced by a point force $\mathbf{f} = -\mathbf{F}/(4\pi a^2)$. When this net force is zero, the particle is said to be *force free.* Recall (see § 3.1.1) that if a point force **f** is added at $\mathbf{x} = 0$ within a fluid velocity field, this field is distorted and the governing equations are given by equation (3.8). The solution to this equation is called the *Stokeslet* and takes the form
$$\mathbf{u}^{(0)}(\mathbf{x}) = \mathbf{I}(\mathbf{x})\cdot\mathbf{f} \text{ and } p(\mathbf{x}) = \frac{1}{4\pi x^3}\mathbf{x}\cdot\mathbf{f},$$
where $x = |\mathbf{x}|$. This velocity and pressure perturbations induce a slight disturbance in the stress field $\boldsymbol{\sigma} = \mathbf{T}\cdot\mathbf{f}$, where $\mathbf{T}^{(0)}$ is a third-order tensor
$$\mathbf{T}^{(0)} = -\frac{3}{4\pi}\frac{\mathbf{xxx}}{x^5}.$$
- The second term on the right-hand side of equation (3.22) is related to the first moment of the surface force exerted on the particle. It also represents the velocity field induced by a *doublet* of point forces. Indeed, in a way similar to the treatment done above for a potential dipole, let us consider a *dipole* or Stokeslet *doublet*, i.e., the association of two Stokeslet, very close each to other, but with opposite strength: we place another force point at finite and very small distance $-\boldsymbol{\beta}$ from the first one; this new Stokeslet is associated with an opposite strength $-\boldsymbol{\alpha}$. The velocity field is merely the superposition of the two elementary solutions
$$\mathbf{u}'^{(1)} = \mathbf{u}_1 + \mathbf{u}_2 = (\mathbf{I}(\mathbf{x}) - \mathbf{I}(\mathbf{x}-\boldsymbol{\beta}))\cdot\boldsymbol{\alpha} = [(\boldsymbol{\beta}\cdot\nabla)\mathbf{I}(\mathbf{x})]\cdot\boldsymbol{\alpha} + \cdots = (\boldsymbol{\beta}\boldsymbol{\alpha}) : \nabla\mathbf{I} + \cdots,$$
which is structurally similar to the second term on the right-hand side of equation (3.22). To go farther in the interpretation, we split the first moment into three components
$$\mathbf{M} = \boldsymbol{\beta}\boldsymbol{\alpha} = \int_S (\mathbf{x}' - \mathbf{y}) f(\mathbf{x}')\mathrm{d}\mathbf{x}' = s\mathbf{1} + \mathbf{S} + \mathbf{R},$$
where
  - the first term is an isotropic part $s = \frac{1}{3}\mathrm{tr}\,\mathbf{M}$. If $\boldsymbol{\alpha}$ and $\boldsymbol{\beta}$ are orthogonal, then we have $s = 0$. This isotropic plays no role since $s\mathbf{1} : \nabla\mathbf{I} = s\nabla\cdot\mathbf{I} = 0$.
  - the second component is a symmetric part
$$\mathbf{S} = \frac{1}{2}\left(\mathbf{M} + \mathbf{M}^T - 2s\mathbf{1}\right),$$
which is called the *stresslet* tensor; by construction **S** is traceless. When $s = 0$, the stresslet is directly the symmetric part of $\mathbf{M} = \boldsymbol{\beta}\boldsymbol{\alpha}$. Note that we can also express **S** in the integral form
$$\mathbf{S} = \int_S \left((\boldsymbol{\sigma}\cdot\mathbf{k})\cdot\mathbf{x} + \mathbf{x}\cdot(\boldsymbol{\sigma}\cdot\mathbf{k}) - \frac{1}{3}(\boldsymbol{\sigma} : \mathbf{kx})\mathbf{1}\right)\mathrm{d}S.$$
  - the third component is an antisymmetric term
$$\mathbf{R} = \frac{1}{2}\left(\mathbf{M} - \mathbf{M}^T\right),$$
which is related to the torque **L** exerted on the particle with respect to **y**
$$\mathbf{L} = \int_S \mathbf{z}\times\mathbf{f}\mathrm{d}S,$$
with $\mathbf{z} = \mathbf{x}' - \mathbf{y}$. For any vector **n**, we have $\mathbf{R}\cdot\mathbf{n} = \frac{1}{2}\mathbf{L}\times\mathbf{n}$.

The gradient of **I** can also be broken down into a symmetric and an antisymmetric parts. In so doing, we can transform the second term on the right-hand of equation (3.22) into[9]

$$\nabla_{\mathbf{x}'}\mathbf{I}(\mathbf{x},\,\mathbf{y}) : \int_S (\mathbf{x}'-\mathbf{y}) f(\mathbf{x}')\mathrm{d}\mathbf{x}' = (\boldsymbol{\beta}\mathbf{f}) : \nabla\mathbf{I} = \frac{1}{2}\left(\nabla\mathbf{I}+(\nabla\mathbf{I})^T\right) : \mathbf{S} + \frac{1}{2}\left(\nabla\mathbf{I}-(\nabla\mathbf{I})^T\right) : \mathbf{R}. \tag{3.23}$$

The first term on the right-hand side of (3.23) represents the flow due to a symmetric pair of point-force doublets and therefore is called a *quadrupole*. The second term represents the rotational flow due to a *couplet* or *rotlet*.

In short, we have

$$\mathbf{u}'(\mathbf{x}) = -\underbrace{\mathbf{I}(\mathbf{x})\cdot\mathbf{f}}_{\text{0th-order contribution}} - \underbrace{\frac{1}{2}\left(\nabla\mathbf{I}+(\nabla\mathbf{I})^T\right) : \mathbf{S}}_{\text{symmetric 1th-order contribution}} - \underbrace{\frac{1}{2}\left(\nabla\mathbf{I}-(\nabla\mathbf{I})^T\right) : \mathbf{R}}_{\text{antisymmetric 1th-order contribution}} + \cdots .$$

We can go further in the interpretation of the first-order contribution by replacing the Oseen tensor by its expression. It can be shown (Chwang & Wu, 1975) that the first-order expression of the velocity is

$$\mathbf{u}'^{(1)} = \underbrace{\frac{(\boldsymbol{\beta}\times\boldsymbol{\alpha})\times\mathbf{x}}{x^3}}_{\text{antisymmetric part}} \underbrace{-\frac{(\boldsymbol{\alpha}\cdot\boldsymbol{\beta})\mathbf{x}}{x^3} + 3\frac{(\boldsymbol{\alpha}\cdot\mathbf{x})(\boldsymbol{\beta}\cdot\mathbf{x})\mathbf{x}}{x^5}}_{\text{symmetric part}}.$$

The first term on the right-hand side member is clearly antisymmetric. The last two terms form the following expression, which is symmetric (with respect to interchange of the $\boldsymbol{\alpha}$ and $\boldsymbol{\beta}$):

$$\mathbf{u}_S'^{(1)} = -\frac{(\boldsymbol{\alpha}\cdot\boldsymbol{\beta})\mathbf{x}}{x^3} + 3\frac{(\boldsymbol{\alpha}\cdot\mathbf{x})(\boldsymbol{\beta}\cdot\mathbf{x})\mathbf{x}}{x^5} = \left[\frac{1}{x^2}\left(-\frac{\mathbf{1}}{x} + 3\frac{\mathbf{x}\mathbf{x}}{x^3}\right)\mathbf{x}\right] : (\boldsymbol{\alpha}\boldsymbol{\beta}),$$

which also takes the following form when $s = 0$

$$\mathbf{u}_S'^{(1)} = \frac{1}{x^3}\mathbf{S} : \mathbf{1}\mathbf{x} - \frac{3}{x^5}\mathbf{x}\cdot\mathbf{S}\cdot\mathbf{x}\mathbf{x}.$$

Physically, this stresslet can be interpreted as a straining motion of the fluid symmetric about the plane $(\boldsymbol{\alpha},\,\boldsymbol{\beta})$; the principal axes of strain lie in the $\boldsymbol{\alpha}+\boldsymbol{\beta}$, $\boldsymbol{\alpha}-\boldsymbol{\beta}$, and $\boldsymbol{\alpha}\times\boldsymbol{\beta}$ directions.

Note that there is a correspondence between potential and force fields since we have the relation (Chwang & Wu, 1975)

$$\mathbf{u}_D(\mathbf{x},\,\boldsymbol{\delta}) = -\frac{1}{2}\nabla^2\mathbf{u}^{(0)}(\mathbf{x},\,\boldsymbol{\delta})$$

where $\mathbf{u}_D$ is the velocity due to a potential doublet defined in equation (3.21) and $\mathbf{u}^{(0)}$ is the Stokeslet. This means that the Stokeslet quadrupole can be related to the potential doublet, which turns out to be helpful in building the solutions when high-orders terms in the expansion (3.22) are needed.

Some of the salient features and the physical role played by the terms in the solution have been summarized in table 3.1. Essentially, we can use the following rules (Chwang & Wu, 1975):

- a Stokeslet is required when the primary-flow velocity has a non-zero average over the body surface;
- a stresslet can be used when the the primary flow has a non-zero velocity gradient on average over the body surface;
- associating a quadrupole and stresslet makes it possible to have the same dependence on the base vectors.

---

[9] Recall that tr $\mathbf{A}\cdot\mathbf{S} = 0$ if $\mathbf{S}$ is symmetric and $\mathbf{A}$ is antisymmetric. Moreover, the transpose of a third-order tensor is defined as $M^T_{ijk} = M_{ikj}$.

Table 3.1 *Construction of the solution to specific boundary-value problems from the singular solutions. After (Chwang & Wu, 1975).*

Primary flow	Singularities
uniform flow	Stokeslet + potential dipole
shear flow	Stokeslet dipole + potential quadrupole
extensional flow	stresslet + quadrupole

Application to the multipole expansion

Example 1: According to table 3.1, the disturbance induced by a translating rigid (solid) sphere (with no spin) in a quiescent fluid is a combination of a Stokeslet and a potential doublet

$$\mathbf{u}' = \hat{\mathbf{I}} \cdot \hat{\mathbf{f}} + \hat{\mathbf{D}} \cdot \hat{\boldsymbol{\lambda}}$$

where $\hat{\mathbf{I}}$ is reduced the Oseen tensor[10], $\hat{\mathbf{D}}$ is the potential-doublet tensor introduced in equation (3.21), and $\hat{\boldsymbol{\lambda}}$ and $\hat{\mathbf{f}}$ are two unknown vectors to be determined. These vectors are determined by imposing that the velocity at the particle surface equals the particle velocity $\mathbf{v}_p$ at $x = a$. Since

$$\mathbf{u}' = \left(\frac{1}{x}\mathbf{1} + \frac{\mathbf{xx}}{x^3}\right) \cdot \hat{\mathbf{f}} + \left(-\frac{1}{x^3}\mathbf{1} + 3\frac{\mathbf{xx}}{x^5}\right) \cdot \hat{\boldsymbol{\lambda}}$$

$\hat{\boldsymbol{\lambda}}$ and $\hat{\mathbf{f}}$ must be collinear with $\mathbf{v}_p$. Solving the system we find:

$$\hat{\mathbf{f}} = \frac{3}{4}a\mathbf{v}_p \text{ and } \hat{\boldsymbol{\lambda}} = -\frac{1}{4}a^3\mathbf{v}_p.$$

Since the net force due to a potential dipole is zero, we retrieve the Stokes force

$$\mathbf{F} = \int_S \mathbf{f}\mathrm{d}S = -8\pi\mu\hat{\mathbf{f}} = -6\pi\mu a\mathbf{v}_p.$$

Example 2: According to table 3.1, the disturbance induced by a linear flow $\mathbf{u}_\infty = \mathbf{G} \cdot \mathbf{x}$ past a rigid (solid) sphere (with no spin) is given by a combination of a potential quadrupole and a Stokes doublet. We assume that this flow at infinity is irrotational, implying that $\mathbf{G}$ is symmetric and traceless (because of the continuity equation). Thus we write

$$\mathbf{u}'(\mathbf{x}) = \hat{\mathbf{Q}} : \boldsymbol{\Lambda} + \nabla\hat{\mathbf{I}} : \mathbf{M}.$$

The boundary condition is $\mathbf{u}' = -\mathbf{G} \cdot \mathbf{x}$ when $x = a$. We obtain

$$\mathbf{M} = -\frac{5}{a^2}\boldsymbol{\Lambda},$$

and after a few computations, we find

$$\boldsymbol{\Lambda} = \frac{a^5}{6}\mathbf{G} \text{ and } \mathbf{M} = -\frac{5}{6}a^3\mathbf{G}.$$

The stresslet $\mathbf{S}$ is $\mathbf{M}$ to within the multiplicative factor $-(8\pi\mu)^{-1}$

$$\mathbf{S} = \frac{20}{3}\pi\mu a^3\mathbf{G}. \tag{3.24}$$

Making allowance of the relation between the potential quadrupole velocity disturbance can be written

---

[10] Here, to simplify the computations, we get rid of the multiplier $(4\pi\mu)^{-1}$ and $(8\pi\mu)^{-1}$ that can be embodied in the unknown vectors, e.g., we simply pose $\hat{\mathbf{I}} = (8\pi\mu)\mathbf{I}$ and $\hat{\mathbf{D}} = (4\pi\mu)\mathbf{D}$.

3.2.2 Computations of the constitutive equation

We consider a dilute suspension of rigid spherical solid particles within a Newtonian fluid. We assume that the particles are force-free and torque-free, i.e., in a Stokesian regime St → 0, the solid phase is the slave of the fluid phase. We have shown in § 3.1.3 that the bulk stress tensor $\bar{\boldsymbol{\sigma}}$ can be broken into a fluid and solid contributions

$$\bar{\boldsymbol{\sigma}} = \bar{\boldsymbol{\sigma}}^{(f)} = +\bar{\boldsymbol{\sigma}}^{(p)},$$

where the solid contribution is given by equation (3.18) while the fluid contribution is given by equation (3.17). Neglecting the Reynolds stress tensor, we have

$$\bar{\boldsymbol{\sigma}}^{(p)} = \frac{1}{V}\int_S \boldsymbol{\sigma}\cdot\mathbf{x}\mathbf{k}\mathrm{d}S \text{ and } \bar{\boldsymbol{\sigma}}^{(f)} = -\bar{p}\mathbf{1} + 2\mu\bar{\mathbf{d}}.$$

In the solid contribution, the integral term is nothing but the first moment of the stresses exerted on the particle surface, which corresponds to the stresslet in the case of force-free and torque-free particles. This result holds because we neglect pairwise interactions between particles in the low-concentration limit. Since in the volume V, the number of particles is $\phi V[(4\pi a^3/3)]^{-1}$

$$\bar{\boldsymbol{\sigma}}^{(p)} = \frac{1}{V}\int_S \boldsymbol{\sigma}\cdot\mathbf{x}\mathbf{k}\mathrm{d}S = \phi\frac{3}{4\pi a^3}\mathbf{S},$$

and making use of equation (3.24) with $\mathbf{G} = \bar{\mathbf{d}}$, we arrive at the following constitutive equation

$$\bar{\boldsymbol{\sigma}} = -\bar{p}\mathbf{1} + 2\mu\left(1+\frac{5}{2}\phi\right)\bar{\mathbf{d}}.$$

3.3 Concentrated suspensions

However, except for these limiting cases, averaging raises several theoretical issues

- if fluid inertia cannot be neglected, we are faced with a major issue :
  - averaging (3.1) produced a term in the form $\nabla \cdot \langle \mathbf{uu} \rangle$, which cannot be expressed easily as a function of **u** since the Reynolds decomposition leads to an expression in the form $\nabla \cdot \langle \mathbf{u} \rangle \langle \mathbf{u} \rangle + \nabla \cdot \langle \mathbf{u}'\mathbf{u}' \rangle$, where a kinetic term (Reynolds tensor) appears.
  - averaging (3.1) also produces $\langle \partial \mathbf{u}/\partial t \rangle$, which implies that the history of the configuration must be taken into account, notably particle acceleration must be included in the state space.
  - note that the Stokes equation becomes nonlinear, which precludes from using the superposition principle.
- for sufficiently high solid concentration, interactions between particles are increasingly important in the suspension dynamics. The close equations and approximations previously used are no longer valid because three-particle interactions are possible;
- When the Stokes number is intermediate ($\mathrm{St} = \mathcal{O}(1)$), the phase interplay becomes more complex, which is reflected at the bulk scale by the failure of the one-phase approximation;
- as shown later, when the solid concentration comes close to the maximum random concentration, a network of particles in contact forms. Contacts between particles are dissipative, especially when particles rotate and slip. Further equations are needed to take this network into account.

To overcome these issues, scientists use more or less sophisticated methods such as

- to introduce additional closure equations, *ad hoc* or inferred from numerical simulations;
- to increase the dimension of the state space;
- to replace a few complicated terms complexes with stochastic process (e.g., Brownian motion).

3.3.1 Constitutive equations for concentrated suspensions

Here we are speaking of very concentrated suspensions to refer to systems of particles, the solid concentration of which is very close to the maximum solid concentration ϕ_m. This imparts very specific properties to the system, properties that we can review quickly

- a network of particles in contact (the word *contact* is used in a loose sense) ;
- this network can transmit forces over large distances quite instantaneously ;
- this network can be responsible for significant loads on particles ;
- the geometric constraints related to this network when the latter is flowing lead to phenomena such as dilatancy (volume variation of the suspension when shearing) and jamming (arching effects leading to flow cessation) ;
- as the suspension is close the maximum solid concentration, fluid/solid transitions are possible;
- arches in the network give rise to bounded zones, where the stress level can be significantly lower;
- heterogeneities in stress distributions are associated with local variations in the solid concentration.

As an example, figure 3.5 shows a typical network obtained by Prochnow and Chevoir using a Contact-Dynamics numerical model. At the base of the flow, it can be seen that there is a significant increase in the normal force experienced by particles belonging to the network while, for particle clusters surrounding the percolating network, the force chains are much weaker (vault

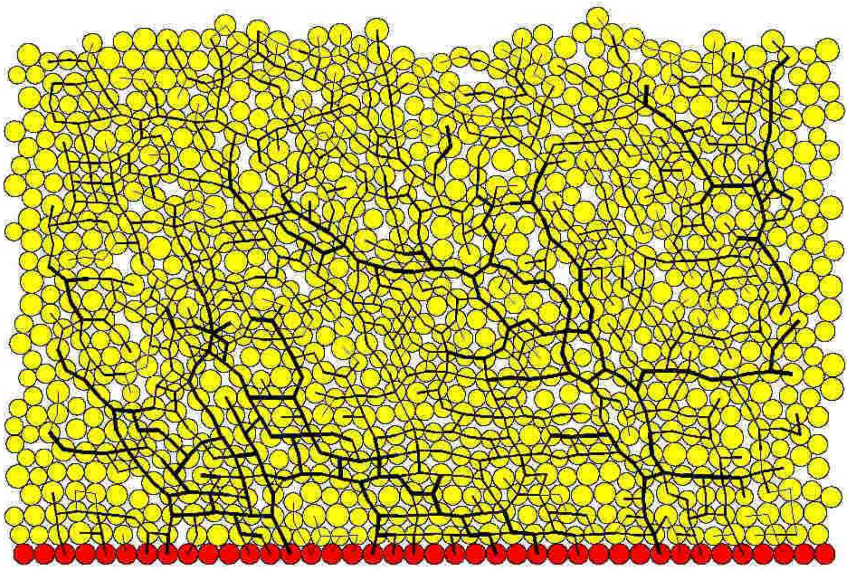

Figure 3.5 *Simulation of force network within a granular flow. Lines represent the normal forces transmitted by the network of particles (cylinder of various size); the line thickness is related to the force strength. The channel slope is* 18° *(Prochnow* et al.*, 2000).*

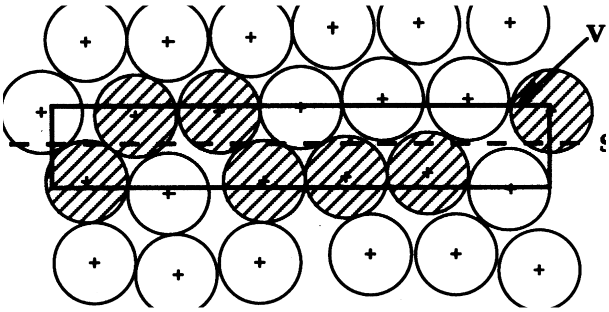

Figure 3.6 *Volume control*

effect). This statistically heterogenous distribution of forces implies that very different types of particle interaction can occur, depending on whether the particles belong to a percolating network or not (Ancey & Evesque, 2000; Ancey, 2002)

The most important is the first term on the right-hand side, which can be cast in the following form: $na < \mathbf{fk} >$, which is obtained by specifying that at the particle surface, the stress balance leads to $\mathbf{f} = \boldsymbol{\sigma}_p \cdot \mathbf{k} d\mathcal{A} = (\boldsymbol{\sigma}_f - \mathbf{1}) \cdot \mathbf{k} d\mathcal{A} + \mathbf{f}_c$, where $\mathbf{f}$ denotes the surface forces acting on a particle and $\mathbf{f}_c$ the contact action when two particles get in touch. Assuming that the system is ergodic, we have replaced volume averages with ensemble averages. This result is well known from the soil-mechanician community and more generally in homogenization (Christoffersen *et al.*, 1981; Cambou *et al.*, 1995, 2000; Cambou & Jean, 2001; Vardoulakis & Sulem, 1995). This relation makes it possible to establish a direct connection between force networks $\mathbf{f}$ and bulk stresses.

For simple shear flows, the idea is to take a thin band, as shown in figure 3.6. Note that $\mathcal{V}$ does not necessarily include entire volumes of particle, as depicted in figure 3.6. To overcome this problem, we replace this volume with the material volume $\mathcal{V}'$ including all the particles, the center of which lies within $\mathcal{V}$ (i.e., excluding those, the center of which lies outside of $\mathcal{V}$), which is licit here because of the shape of $\mathcal{V}$ and our assumption on suspension homogeneity (Ancey *et al.*, 1999).

From this discussion, we must keep in mind that

- when the one-phase flow approximation (at the bulk scale) holds, the governing equation is (3.15). The mass and volume density coincide. The bulk extra-stress tensor is given by equation (3.16) and results from a fluid and a solid contributions;
- in the converse case, the mixture behaves as a two-phase material on a bulk scale. Each phase must be characterized and described using specific equations (3.13–3.14). The two equations are coupled by a coupling term that reflects stress equilibrium at the interface.

3.3.2 Regime diagram and computation of individual contributions

The volume-averaging operator has been so far used to establish the link between micro- and macro-structure. However, we must assume ergodicity, which makes it possible to replace volume averages with ensemble averages[11]. Usually, we try to simplify the problem by neglecting contributions to the bulk stress tensor that have minor effects. Using dimensionless numbers makes it possible to to evaluate, even grossly, the magnitude of an interaction. For an interaction to prevail, it must have time to occur and its magnitude must be high compared to the other interactions. In practice, most dimensionless numbers can be interpreted in terms of force ratios or characteristic-time ratios. An example is the Stokes number, which is the ratio of the relaxation times (particle/ fluid) and ratio of forces (particles' inertia/viscous forces).

Let us consider the example of figure 3.5, representing a dry granular flow. Particles networks form when the material is sheared. At any time, branches are created, while others are destroyed. Let us take a particle within a force network, hence experiencing frictional forces. At depth h, the magnitude of the normal stress σ_n is $\rho_p g h$. The characteristic time t_p is estimated from the equation of motion for this particle: $m\dot{v} \approx -\lambda \sigma_n a^2$, where λ denotes the friction coefficient. We deduce that the characteristic time (defined as the time required for the particle to travel a distance a) is $t_p \propto \sqrt{\rho_p a^2/\sigma_n}$. This time can be compared to the typical lifetime of the network t_n. For simple shear flows, after $t_n \approx \dot{\gamma}^{-1}$, two particles initially in contact are then separate. We define the Coulomb dimensionless number:

$$Co = \left(\frac{t_p}{t_n}\right)^2 = \frac{\rho_p a^2 \dot{\gamma}^2}{\sigma_n}$$

ratio that can be also interpreted as the ratio of a collisional force and frictional force. This entails the following partitioning

- if $Co \ll 1$, this means that (i) the particle has time to adapt to the variations in bulk stresses during the lifetime of the network to which it belongs (ii) inertial effects are negligible, (iii) the contact network has time to transmit forces from upper to lower layers (iv) a particle in the network undergoes forces created at a finite correlation length (non-local effects). Frictional forces are expected to play the key role in the bulk dynamics. We refer to this regime as the *frictional* regime.
- on the opposite, if $Co \gg 1$, this means that (i) the network lifetime is too short for the force transmission to occur, (ii) inertial effects become predominant, (iii) particle motion is influenced by neighboring particles (behavior similar to a dense gas). We call *collisional regime* this flow regime.

Using dimensionless numbers leads to plotting a simplified diagram of interaction predominance (Coussot & Ancey, 1999*b*,*a*; Ancey *et al.*, 1999). Figure 3.7 provides such a diagram for simple shear flows of suspensions. The two key bulk variables are assumed to be the solid concentration

---

[11] Zhang & Prosperetti (1994, 1997) started directly with an ensemble averaging of the local equations, which produces little differences with our results

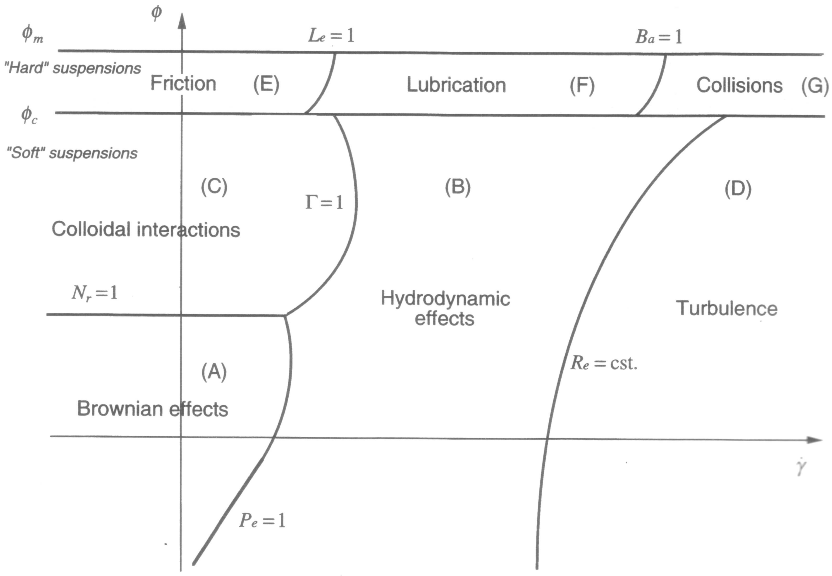

Figure 3.7 *Simplified diagram of flow regimes. The transitions between regimes are described using dimensionless numbers: The Péclet* Pe $= 6\pi\mu a^3\dot\gamma/(kT)$ *(T the temperature, k the Boltzmann constant) for the transition between Brownian (thermal agitation of particles) and viscous regimes; the repulsion number* Nr $= \Psi/(kT)$ *(with Ψ the van der Waals interaction potential) for the transition between the colloidal and Brownian regimes;* $\Gamma = 6\pi\mu a^3\dot\gamma/\Psi$ *is a number reflecting the ratio between viscous and colloidal interactions; the particle or flow Reynolds number is used for the transition towards turbulence; the Leighton number* Le $= \mu\dot\gamma a/(\epsilon\sigma_n)$ *(with ϵa the mean distance between the surfaces of two close particles) for the transition between the viscous and frictional regimes; the Bagnold number* Ba $= \rho_p\dot\gamma\epsilon a/\mu$ *is used for the transition between the viscous and collisional regimes. ϕ_m denotes the maximum random solid concentration ($\phi_m \approx$* 0.635 *for spherical particles of equal size) and ϕ_c is the minimum concentration for a network of particles in close contact to form ($\phi_c \approx$* 0.5 *for spherical particles of equal size).*

ϕ and the shear rate $\dot{\gamma}$. For dilute and moderately concentrated suspensions, the flow regimes are usually well established (Russel *et al.*, 1995). However, at high solid concentrations, the determination of the constitutive equation is much more difficult. We can cite:

- for the regime dominated by colloidal interactions (regime C on the diagram) the works by Kapur *et al.* (1997); Scales *et al.* (1998) and Zhou *et al.* (1999).
- for the regime dominated by lubricated-contact interactions, the work by van der Brule & Jongshaap (1991).
- for the collisional regime, an abundant literature can be found on the application of kinetic theory to dry granular flows (Savage & Jeffrey, 1981; Savage, 1984; Campbell, 1990; Jenkins & Savage, 1983). For wetted materials, less works are available Jenkins & Hanes (1998) ;
- for the frictional regime, the papers by Cambou & Jean (2001); Cambou *et al.* (1995, 2000).

References

Abramovich, F. & Silverman, B. 1998 Wavelet decomposition approaches to statistical inverse problems. *Biometrika* **85**, 115–129.

Ancey, C. 2002 Dry granular flow down an inclined channel: Experimental investigations on the frictional-collisional regime. *Phys. Rev. E* **65**, 11304.

Ancey, C. 2005 Solving the Couette inverse problem by using a wavelet-vaguelette decomposition. *J. Rheol.* **49**, 441–460.

Ancey, C., Coussot, P. & Evesque, P. 1996 Examination of the possibility of a fluid-mechanics treatment for dense granular flows. *Mech. Cohesive-Frict. Mater.* **1**, 385–403.

Ancey, C., Coussot, P. & Evesque, P. 1999 A theoretical framework for very concentrated granular suspensions in a steady simple shear flow. *J. Rheol.* **43**, 1673–1699.

Ancey, C. & Evesque, P. 2000 Frictional-collisional regime for granular suspension flows down an inclined channel. *Phys. Rev. E* **62**, 8349–8360.

Astarita, G. 1990 The engineering reality of the yield stress. *J. Rheol.* **34**, 275–277.

Auton, T., Hunt, J. & Prud'homme, M. 1988 The force exerted on a body in inviscid unsteady non-uniform flow rotational flow. *J. Fluid Mech.* **197**, 241–257.

Barnes, H. 1995 A review of the slip (wall depletion) of polymer solutions, emulsions and particle suspensions in viscometers: its cause, character, and cure. *J. Non-Newtonian Fluid Mech.* **56**, 221–251.

Barnes, H. 1997 Thixotropy - a review. *J. Non-Newtonian Fluid Mech.* **70**, 1–33.

Barnes, H. 1999 The yield stress –a review or '$\pi\alpha\nu\tau\alpha\ \rho\epsilon\iota$' – everything flows? *J. Non-Newtonian Fluid Mech.* **81**, 213–217.

Barnes, H. 2000 *A Handbook of Elementary Rheology*. Aberystwyth: University of Wales.

Barnes, H. & Carnali, J. 1990 The vane-in-cup as a novel rheometer geometry for shear thinning and thixotropic materials. *J. Rheol.* **34**, 851–866.

Barnes, H. & Nguyen, Q. 2001 Rotating vane rheometry - a review. *J. Non-Newtonian Fluid Mech.* **98**, 1–14.

Batchelor, G. 1967 *An introduction to fluid dynamics*. Cambridge University Press.

Batchelor, G. 1970 The stress system in a suspension of free-forces particles. *J. Fluid Mech.* **41**, 545–570.

Batchelor, G. 1972 Sedimentation in a dilute dispersion of spheres. *J. Fluid Mech.* **52**, 245–268.

Baudez, J., Rodts, S., Chateau, X. & Coussot, P. 2004 New technique for reconstructing instantaneous profiles from viscometric tests: application to pasty materials. *J. Rheol.* **48**, 69–82.

Bedford, A. & Dumheller, D. 1983 Theories of immiscible and structured mixtures. *Int. J. Eng. Sci.* **21**, 863–960.

Bertero, M., De Mol, C. & Pike, E. 1985 Linear inverse problems with discrete data. I: General formulation and singular system analysis. *Inverse Prob.* **1**, 301–330.

Bertero, M., De Mol, C. & Pike, E. 1988 Linear inverse problems with discrete data. II: Stability and regularization. *Inverse Prob.* **4**, 573–594.

Bird, R., Armstrong, R. & Hassager, O. 1987 *Dynamics of Polymeric Liquids*. New York: John Wiley & Sons.

Bird, R., Dai, G. & Yarusso, B. 1983 The rheology and flow of viscoplastic materials. *Rev. Chem. Eng.* **1**, 1–70.

Boehler, J., ed. 1987 *Applications of tensor functions in solid mechanics*, *International Centre for Mechanical Sciences, Courses and Lectures*, vol. 292. New York: Springer Verlag.

Boger, D. & Walters, K. 1993 *Rheological Phenomena in Focus*. Amsterdam: Elsevier.

Borgia, A. & Spera, F. 1990 Error analysis for reducing noisy wide-gap concentric cylinder rheometric data for nonlinear fluids: theory and applications. *J. Rheol.* **34**, 117–135.

Brady, J. & Bossis, G. 1988 Stokesian dynamics. *Annu. Rev. Fluid Mech.* **20**, 111–157.

Brady, J. & Morris, J. 1997 Microstructure of strongly sheared suspensions and its impact on rheology and diffusion. *J. Fluid Mech.* **348**, 103–139.

van der Brule, B. & Jongshaap, R. 1991 Modeling of concentrated suspensions. *J. Stat. Phys.* **62**, 1225–1237.

Cai, T. 1999 Adaptative wavelet estimation: a block thresholding and oracle inequality approach. *Ann. Stat.* **27**, 898–924.

Cai, T. 2002 On adaptive wavelet estimation of a derivative and other related linear inverse problems. *J. Stat. Planning Infer.* **108**, 329–349.

Cambou, B., Chaze, M. & Dedecker, F. 2000 Change of scale in granular materials. *Eur. J. Mech. A* **19** (6), 999–1014, tY - JOUR.

Cambou, B., Dubujet, P., Emeriault, F. & Sidoroff, F. 1995 Homogenization for granular materials. *Eur. J. Mech. A* **14**, 255–276.

Cambou, B. & Jean, M., ed. 2001 *Micromécanique des matériaux granulaires*. Paris: Hermès Science, tY - JOUR.

Campbell, C. 1990 Rapid granular flows. *Annu. Rev. Fluid Mech.* **22**, 57–92.

Chapman, S. & Cowling, T. 1970 *The mathematical theory of non-uniform gases*, 3rd edn. Cambrige: Cambrige University Press.

Christoffersen, J., Mehrabadi, M. & Nemat-Nasser, S. 1981 A micromechanical description of granular behavior. *J. Appl. Mech.* **48**, 339–344.

Chwang, A. & Wu, T. Y.-T. 1975 Hydrodynamics of low-Reynolds-number flow. Part 2. Singularity method for Stokes flow. *J. Fluid Mech.* **67**, 787–815.

Coimbra, C. & Rangel, R. 1998 General solution of the particle momentum equation in unsteady Stokes flows. *J. Fluid Mech.* **370**, 53–72.

Coleman, B., Markowitz, H. & Noll, W. 1966 *Viscometric flows of non-Newtonian fluids*, *Springer Tracts in natural philosophy*, vol. 5. Berlin: Springer-Verlag.

Courant, R. & Friedrich, K. 1948 *Supersonic Flow and Shock Waves*. New York: Intersciences Publishers.

Coussot, P. & Ancey, C. 1999*a* Rheophysical classification of concentrated suspensions and granular pastes. *Phys. Rev. E* **59**, 4445–4457.

Coussot, P. & Ancey, C. 1999*b* *Rhéophysique des pâtes et des suspensions*. Les Ulis: EDP Sciences.

Coussot, P., Proust, S. & Ancey, C. 1996 Rheological interpretation of deposits of yield stress fluids. *J. Non-Newtonian Fluid Mech.* **66**, 55–70.

Darby, R. 1985 Couette viscometer data reduction for materials with a yield stress. *J. Rheol.* **29**, 369–378.

Dicken, V. & Maass, P. 1996 Wavelet-Galerkin methods for ill-posed problems. *J. Inv. Ill-Posed Problems* **4**, 203–221.

DONOHO, D. 1995 Nonlinear solution of linear inverse problems by wavelet-vaguelette decomposition. *Appl. Comp. Harmonic Anal.* **2**, 101–126.

DONOHO, D. & JOHNSTONE, I. 1995 Wavelet shrinkage: asymptotia? *J. Royal. Stat. Soc. B* **57**, 301–369.

DORAISWAMY, D., MUJUMDAR, A., TASO, I., BERIS, A., DANFORTH, S. & METZNER, A. 1991 The Cox-Merz rule extended: a rheological model for concentrated suspensions and other materials with a yield stress. *J. Rheol.* **35**, 647–685.

DREW, D. & PASSMAN, S. 1999 *Theory of Multicomponent Fluids*. New York: Springer.

EINSTEIN, A. 1911 Berichtigung zu meiner Arbeit "Eine neue Bestimmung der Moleküldimensionen". *Annalen der Physik* **34**, 591–592.

EVANS, I. 1992 On the nature of the yield stress. *J. Rheol.* **36**, 131–1318.

FRANKEL, N. & ACRIVOS, A. 1967 On the viscosity of a concentrated suspension of solid spheres. *Chemical Engineering Science* **22**, 847–853.

FRIEDRICH, C., HONERKAMP, J. & WEESE, J. 1996 New ill-posed problems in rheology. *Rheol. Acta* **35**, 186–193.

GAMBOA, F. & GASSIAT, E. 1997 Bayesian methods and maximum entropy for ill-posed inverse problems. *Ann. Stat.* **25**, 328–350.

GARABEDIAN, P. 1966 Free boundary flows of a viscous liquid. *Comm. Pure Appl. Math.* **19**, 421–434.

GEISSLE, W. & HOCHSTEIN, B. 2003 Validity of the Cox-Merz rule for concentrated suspensions. *J. Rheol.* **47**, 897–910.

GERMAIN, P. 1973*a* La méthode des puissances virtuelles en mécanique des milieux continus. *Journal de Mécanique* **12**, 235–274.

GERMAIN, P. 1973*b* The method of virtual power in continuum mechanics, Part 2: Microstructure. *SIAM J. Appl. Math.* **25** (3), 556–575.

GOLBERG, M. 1979 A method of adjoints for solving some ill-posed equations of the first kind. *Appl. Math. Comput.* **5**, 123–130.

HAPPEL, J. & BRENNER, H. 1965 *Low Reynolds number hydrodynamics*. Englewood Cliffs: Prentice Hall.

HARNETT, J. & HU, R. 1989 The yield stress-An engineering reality. *J. Rheol.* **33**, 671–679.

HART, J. 1999 *Nonparametric Smoothing and Lack-of-Fit Tests*. New York: Springer.

HINCH, E. 1977 An averaged-equation approach to particle interactions in a fluid suspension. *J. Fluid Mech.* **83**, 695–720.

HOWE, M., LAUCHKE, G. & WANG, J. 2001 Aerodynamic lift and drag fluctuations of a sphere. *J. Fluid Mech.* **436**, 41–57.

HUTTER, K. & JÖHNK, K. 2004 *Continuum Methods of Physical Modeling*. Berlin: Springer.

HUTTER, K., LALOUI, L. & VULLIET, L. 1999 Thermodynamically based mixture models of saturated and unsaturated soils. *Mech. Cohesive-Frict. Mater.* **4**, 295–338.

JENKINS, J. & HANES, H. 1998 Collisional sheet flows of sediment driven by a turbulent fluid. *J. Fluid Mech.* **370**, 29–52.

JENKINS, J. & SAVAGE, S. 1983 A theory for the rapid flow identical, smooth, nearly elastic, spherical particles. *J. Fluid Mech.* **130**, 187–202.

JONGSCHAAP, R. & DOEKSEN, D. 1983 The average stress tensor in systems with interacting particles. *Rheol. Acta* **22**, 4–11.

KANG, S., SANGANI, A., TSAO, H. & KOCH, D. 1997 Rheology of dense bubble suspensions. *Phys. Fluids* **9**, 1540–1561.

KAPUR, P., SCALES, P., BOGER, B. & HEALY, T. . 1997 A theoretical framework for the yield stress of suspensions loaded with size distributed particles. *AIChE J.* **43**, 1171–1179.

DE KEE, D. & CHAN MAN FONG, C. 1993 A true yield stress? *J. Rheol.* **37**, 775–776.

Kim, S. & Karrila, S. 1991 *Microhydrodynamics: Principles and Selected Applications*. Stoneham: Butterworth-Heinemann.

Kohr, M. & Pop, I. 2004 *Viscous incompressible flow for low Reynolds numbers*. Southampton: WIT press.

Kovac, A. 1998 Wavelet Thresholding for Unequally Spaced Data. Phd thesis, University of Bristol.

Krieger, I. 1968 Shear rate in the Couette viscometer. *Trans. Soc. Rheol.* **12**, 5–11.

Krieger, I. & Elrod, H. 1953 Direct determination of the flow curves of non-Newtonian fluids. II Shearing rate in the concentric cylinder viscometer. *J. Appl. Phys.* **24**, 134–136.

Krieger, I. & Maron, S. 1952 Direct determination of the flow curves of non-Newtonian fluids. *J. Appl. Phys.* **23**, 147–149.

Kumaran, V. & Koch, D. 1993 Properties of a bidisperse particle-gas suspension. Part 2. Viscous relaxation time small compared with collision time. *J. Fluid Mech.* **247**, 643–660.

Lamb, H. 1932 *Hydrodynamics*. Cambridge: Cambridge University Press.

Landau, L. & Lifschitz, E. 1987 *Fluid Mechanics*. London: Pergamon.

Leong, Y. & Yeow, Y. 2003 Obtaining the shear stress shear rate relationship and yield of liquid foods from Couette viscometry data. *Rheol. Acta* **42**, 365–371.

Lhuillier, D. 1982*a* Forces d'inertie sur une bulle en expansion se déplac,ant dans un fluide. *Comptes Rendus de l'Académie des Sciences, série II* **295**, 95–98.

Lhuillier, D. 1982*b* On the equation of motion of a rigid sphere in a non uniform and accelerated inviscid fluid. Incidence on two-phase flow equations. *Mechanics Research Communications* **9**, 295–299.

Louis, A. 1999 A unified approach to regularization methods for linear and ill-posed problems. *Inverse Prob.* **15**, 489–498.

Louis, A., Maass, P. & Rieder, A. 1997 *Wavelets, Theory and Applications*. Chichester: John Wiley & Sons.

Lundgren, T. 1972 Slow flow through stationary random beads and suspensions of spheres. *J. Fluid Mech.* **51**, 273–299.

Macsporran, W. 1989 Direct numerical evaluation of shear rates in concentric cylinder viscometry using least-squares cubic splines. *J. Rheol.* **33**, 745–755.

Magnin, A. & Piau, J. 1987 Shear rheometry of fluids with a yield stress. *J. Non-Newtonian Fluid Mech.* **23**, 91–106.

Magnin, A. & Piau, J. 1990 Cone-and-plate rheometry of yield stress fluids. Study of an aqueous gel. *J. Non-Newtonian Fluid Mech.* **36**, 85–108.

Mazur, P. & Bedeaux, D. 1974 A generalization of Faxén's theorem to nonsteady motion of a sphere through an incompressible fluid in arbitrary flow. *Physica* **76**, 235–246.

McKarthy, K. & Seymour, J. 1994 Gravity current analysis of the Bostwick consistometer for power-law foods. *Journal of Texture Studies* **25**, 207–220.

Mendes, P. & Dutra, E. 2004 Viscosity function for yield-stress liquids. *Applied Rheology* **14**, 296–302.

Middleton, G. & Wilcock, P. 1994 *Mechanics in the Earth and Environmental Sciences*. Cambridge: Cambridge University Press.

Minier, J.-P. & Peirano, E. 2001 The pdf approach to turbulent polydispersed two-phase flows. *Physics Reports* **352** (1-3), 1–214.

Mooney, M. 1931 Explicit formulas for slip and fluidity. *J. Rheol.* **2**, 210–222.

Morrison, F. 2001 *Understanding Rheology*. New York: Oxford University Press.

Mosegaard, K. & Sambridge, M. 2002 Monte Carlo analysis of inverse problems. *Inverse Prob.* **18**, R29–R54.

Murdoch, A. & Bedeaux, D. 1994 Continuum equations of balance via weighted averages of microscopic quantities. *Proc. Roy. Soc. London* **445**, 157–179.

Nguyen, Q. & Boger, D. 1992 Measuring the flow properties of yield stress fluids. *Annu. Rev. Fluid Mech.* **24**, 47–88.

Oldroyd, J. 1950 On the formulation of rheological equations of state. *Proc. Roy. Soc. London A* **200**, 523–541.

O'Sullivan, F. 1986 A statistical perpective on ill-posed inverse problems. *Stat. Sci.* **1**, 502–527.

Pashias, N. & Boger, D. 1996 A fifty cent rheometer for yield stress measurement. *J. Rheol.* **40**, 1179–1189.

Piau, J.-M. & Debiane, K. 2005 Consistometers rheometry of power-law viscous fluids. *J. Non-Newtonian Fluid Mech.* **127**, 213–224.

Pope, S. 2000 *Turbulent Flows*. Cambridge: Cambridge University Press.

Pozrikidis, C. 1992 *Boundary Integral and Singularity Methods for Linearized Viscous Flows*. Cambridge: Cambridge University Press.

Prochnow, M., Chevoir, F., Mills, P. & Jenkins, J. 2000 Ecoulements granulaires denses sur un plan incliné : microstructure et loi de comportement. In *Physique et Mecanique des Materiaux Granulaires* (ed. F. Chevoir), p. 425. Champ-sur-Marne: Presses du LCPC, Paris.

Prosperetti, A. 2004 The average stress in incompressible disperse flow. *Int. J. Multiphase Flow* **30**, 1011–1036.

Rieder, A. 1997 A wavelet multilevel method for ill-posed problems stabilized by Tikhonov regularization. *Numer. Math* **75**, 501–522.

Roberts, G. & Barnes, H. 2001 New measurements of the flow-curves for Carbopol dispersions without slip artefacts. *Rheol. Acta* **40**, 499–503.

Russel, W., Saville, D. & Schowalter, W. 1995 *Colloidal dispersions*. Cambridge: Cambridge University Press.

Sangani, A., Mo, G., Tsao, H. & Koch, D. 1996 Simple shear flows of dense gas-solid suspensions at finite Stokes numbers. *J. Fluid Mech.* **313**, 309–341.

Savage, S. 1984 The mechanics of rapid granular flows. *Adv. Appl. Mech.* **24**, 289–366.

Savage, S. 1989 Flow of granular materials. In *Theoretical and Applied Mechanics* (ed. P. Germain, J.-M. Piau & D. Caillerie), pp. 241–266. Amsterdam: Elsevier.

Savage, S. 1994 Marginal ice zone dynamics modelled by computer simulations involving floe collisions. In *Mobile particulate systems* (ed. E. Guazelli & L. Oger), pp. 305–330. Carghese: Kluwer Academic Publishers.

Savage, S. & Jeffrey, D. 1981 The stress tensor in a granular flow at high shear stress rates. *J. Fluid Mech.* **110**, 255–272.

Scales, P., Kapur, P., Johnson, S. & Healy, T. 1998 The shear yield stress of partially flocculated colloidal suspensions. *AIChE J.* **44**, 538–544.

Schowalter, W. & Christensen, G. 1999 Toward a rationalization of the slump test for fresh concrete: comparisons of calculations and experiments. *J. Rheol.* **42**, 865–870.

Shaqfeh, E. 1996 Purely elastic instabilities in viscometric flows. *Annu. Rev. Fluid Mech.* **28**, 129–185.

Spaans, R. & Williams, M. 1995 At last, a true liquid-phase yield stress. *J. Rheol.* **39**, 241–246.

Steffe, J. 1996 *Rheological methods in food process engineering*, 2nd edn. East Langing, USA: Freeman Press.

Tanner, R. 1988 *Engineering Rheology*. Oxford: Clarendon Press.

Tanner, R. & Williams, G. 1970 Iterative numerical methods for some integral equations arising in rheology. *Trans. Soc. Rheol.* **14**, 19–38.

Tenorio, L. 2001 Statistical regularization of inverse problems. *SIAM Rev.* **43**, 347–366.

Truesdell, C. 1966 *Six Lectures on Modern Natural Philosophy*. New York: Springer Verlag.

Truesdell, C. 1974 The meaning of viscometry in fluid dynamics. *Annu. Rev. Fluid Mech.* **6**, 111–147.

Vardoulakis, I. & Sulem, J. 1995 *Bifurcation Analysis in Geomechanics*. Glasgow: Blackie Academic & Professional.

Wahba, G. 1990 *Spline Models for Observational Data*. Philadelphia: Society for Industrial and Applied Mathematics.

Walters, K. 1975 *Rheometry*. London: Chapman and Hall.

Wang, Y. & Hutter, K. 1999 A constitutive model of multiphase mixtures and its application in shearing flows of saturated solid-fluid mixtures. *Granul. Matter* **1**, 163–181.

Werman, M. & Keren, D. 2001 A Bayesian method for fitting parametric and nonparametric models to noisy data. *IEEE Transactions on Pattern Analysis and Machine Intelligence* **23**, 528–534.

Wieghardt, K. 1975 Experiments in granular flow. *Annu. Rev. Fluid Mech.* **7**, 89–114.

Yang, T. & Krieger, I. 1978 Comparison of methods for calculating shear rates in coaxial viscometers. *J. Rheol.* **22**, 413–421.

Yeow, Y., Ko, W. & Tang, P. 2000 Solving the inverse problem of Couette viscometry by Tikhonov regularization. *J. Rheol.* **44**, 1335–1351.

Zarraga, I., Hill, D. & Leighton, D. 2000 The characterization of the total stress of concentrated suspensions of noncolloidal spheres in Newtonian fluids. *J. Rheol.* **44**, 185–221.

Zdunkowski, W. & Bott, A. 2003 *Dynamics of the Atmosphere*. Cambridge: Cambridge University Press.

Zhang, D. & Prosperetti, A. 1994 Averaged equations for inviscid disperse two-phase flow. *J. Fluid Mech.* **267**, 185–219.

Zhang, D. & Prosperetti, A. 1997 Momentum and energy equations for disperse two-phase flows and their closure for dilute suspensions. *Int. J. Multiphase Flow* **23**, 425–453.

Zheng, Q.-S. 1994 Theory of representations for tensor functions- A unified invariant approach to constitutive equation. *Appl. Mech. Rev.* **47**, 545–586.

Zhou, Z., Solomon, M., Scales, P. & Boger, D. 1999 The yield stress of concentrated flocculated suspensions of size distributed particles. *J. Rheol.* **43**, 651–671.

Index

adherence, 51
average
    ensemble, 90, 91, 99
    volume, 91, 92, 99

biharmonic, 11

compliance, 41
creep, 41
cross-over frequency, 44
curl, 11

density number, 92
depletion, 51
description
    Eulerian, 63
    Lagrangian, 63
Dirac, 11
divergence, 11
doublet, 102

effect
    added mass, 87
    die-swell, 33
    end, 51
    wall, 51
    Weissenberg, 33, 53
energy
    free, 68
    kinetic, 75, 76
    total, 76
energy dissipation rate, 75, 76, 79
equation
    Basset-Boussinesq-Oseen, 90
    Bernoulli, 75
    Boltzmann, 97
    conservative, 78
    constitutive, 22, 68
    continuity, 73
    Faxén, 90
    Navier-Stokes, 61, 84
    non-conservative, 78
    Stokes, 87
    topological, 93

fading memory, 41, 70
flow curve, 37
fluid
    inviscid, 75
    Newtonian, 29, 34, 36, 43, 60, 68, 79
    polymeric, 34
    power-law, 29
    simple, 22, 23, 28, 53, 61, 68
Fourier transform, 11
function
    characteristic, 92, 96
    Maxwellian (velocity distribution), 98
    pair distribution, 97
    radial distribution, 97

gradient, 11

harmonic, 11
heat, 76

incompressible, 74
invariant, 70, 71
irrotational, 11
isochoric, 74

jump, 78

Laplacian, 11
law
    thermodynamics, 76

material
    homogeneous, 70
    isotropic, 70
model
    Bingham, 38, 79
    Burgers, 40
    Carreau, 37
    Casson, 38
    Cross, 37
    Herschel-Bulkley, 38
    Kelvin-Voight, 40

    Maxwell, 40, 81
    power-law, 37
    Sisko, 37
modulus
    complex, 43
    elastic, 40
    loss, 43
    relaxation, 41
    storage, 43
multipole expansion, 90

number
    Coulomb, 107
    Deborah, 39
    Reynolds, 84
    Stokes, 84

overshoot, 36, 48

point
    force, 88, 100
    source, 99
    source doublet, 99
pressure, 61, 68
    generalized, 75
    hydrostatic, 68
    mean, 68
    thermodynamic, 68

realization, 90
rheometer, 18, 21, 51
rheometry, 7, 17, 22
rotlet, 102
rule
    Cox-Merz, 44
    Gauss, 90
    Laun, 44
    Leibnitz, 90
    plastic, 80
    Reynolds, 90

shear localization, 53
shear thickening, 37
shear thinning, 37, 46
shock, 74
slipping, 48, 51, 53
solid concentration, 92
Stokeslet, 88, 99, 100
stresslet, 102
symmetry, 70

tensor
    bulk extra-stress, 94
    Cauchy-Green, 64
    deviatoric strain, 71
    deviatoric stress, 61, 68, 71
    extra-stress, 61, 68
    gradient, 63
    Green-Lagrange, 64
    Oseen, 99
    Reynolds, 105
    strain, 71
    strain rate, 66
    stress, 67, 71
    stretch, 64
    velocity gradient, 66
test
    Bostwick, 57
    constrained recoil, 34
    creep, 34
    Pashias, 57
    recovery, 34
    slump, 56
    stress growth, 34
    stress relaxation, 34
theorem
    Cayley-Hamilton, 70
    Green-Ostrogradski, 11
    kinetic energy, 75
    Leibnitz, 72
    representation, 79
    Reynolds, 73
    transport, 72
thixotropy, 46, 48

viscoelasticity, 40
viscometers, 51
viscometric treatment, 51
viscometry, 22
viscoplastic, 79
viscosity
    complex, 43
    dynamic, 60
    Newtonian, 60, 61
    Trouton, 60
volume
    control, 73
    material, 73
von Mises criterion, 80

yield stress, 31, 38, 79